Supporting Information

Accurate Construction of Monolayer, Bilayer, Sandwich Bilayer, Four-layer, Multi-layer and Chiral Bilayer 2D Pillararene-Type Supramolecular Networks

Table of contents

Experimental Methods 3
Characterization data of metal-organic coordination polymers 8
Crystal data and structure refinement 65
^{1}H-NMR and ^{13}C-NMR spectrum 70

Experimental Methods

All reagents were obtained from commercial suppliers and used without further purification unless otherwise noted. ^{1}H, ^{13}C NMR, 2D NOESY and COSY spectra spectra were recorded on 400 MHz, 500 MHz and 600 MHz spectrometers in the indicated solvents at room temperature (298 K). UV-Vis absorption spectrum was performed on a UV-2600i UV-Vis spectrophotometer. X-ray diffraction (XRD) measurements were carried out using a PANalytical X'Pert PRO powder diffractometer. Fluorescence spectra were recorded on an RF-6000 (Excitation slit = 5 nm, Emission slit = 5 nm). Liquid phase circular dichroism (CD) spectra were recorded on a Chirascan Circular Dichroism Chiroptical spectrometer in chloroform and solid phase circular dichroism (CD) spectra were recorded on a JASCO J-810 Circular Dichroism Chiroptical spectrometer. Transmission electron micrographs (TEM) were recorded on FEI Tecnai G2 F20S-TWINTMP. Atomic Force Microscopy (AFM) measurement was performed in tapping mode on a Shimadzu spm9700. The thickness difference in the acquired AFM images was analyzed by drawing line sections that are perpendicular to the scanning direction in the AFM tapping mode. The resolution of racemic-P6 was performed by Daicel Chiral Technologies (China) Co., Ltd. on chiral HPLC equipment Shimadzu LC-20AT (CP-HPLC-06) with a CHIRALPAK IC(IC00CD-NA012) preparation column using methanol/dichloromethane/diethanol amine (MeOH/DCM/DEA) = 40/60/0.1(V/V/V) as the mobile phase.

The X-ray crystallographic data of **P5PhPy2**, **P5PhPy4**, **P6PhPy4**, **P5PhPy2Cu-1**, **P5PhPy2Cu-3** was obtained on Bruker D8 VENTURE diffractometer with a CCD diffractometer using graphite-monochromated MoKα radiation (λ= 0.71073Å) at 300k for **P5PhPy2**, 292 K for **P5PhPy4** and **P5PhPy2Cu-1**, 296 K for **P6PhPy4** and 150 K for **P5PhPy2Cu-3**. The absolute configuration of **P5PhPy2Cu-4** was determined by single crystal X-ray diffraction analysis on Rigaku XtaLAB PRO MM003-DS dual system with a Cu micro-focus source (λ = 1.5418 Å) at 173.00 K. The X-ray diffraction data of **bl-2D-P5MOCN**, **fl-2D-P6MOCN**, **R-bl-2D-P6MOCN**, **S-bl-2D-P6MOCN** was collected on a Bruker D8 VENTURE diffractometer outfitted with a PHOTON-100 CMOS detector using Turbo X-ray Source (TXS) rotating anode MoKα radiation (λ= 0.71073 Å) at 193 K by chilled nitrogen flow controlled by a KRYOFLEX II low-temperature attachment. The X-ray diffraction data of **P5PhPy2Cu-2**, **P5PhPy2Co-1**, **ml-2D-P5MOCN**, **sbl-2D-P6MOCN-2** and **mtl-2D-P6MOCN** was collected on a Bruker D8 VENTURE diffractometer equipped with an Excillum METALJET Ga-Kα radiation (λ=1.34139 Å) and a PHOTON II CMOS detector with a Helios Multi-layer Optic monochromator at 193 K using an Oxford Cryosystems Cryostream 800 cryostat. The X-ray diffraction data of **bl-2D-P6MOCN**, **sbl-2D-P6MOCN**, $I_2 \subset$ **mtl-2D-P6MOCN** was collected on a Bruker D8 VENTURE dual-wavelength Mo/Cu diffractometer equipped with INCOATEC I\mS DIAMOND CuKα radiation (λ=1.54178 Å) and a PHOTON II CMOS detector with a Helios Multi-layer Optic monochromator at 193K temperature

using an Oxford Cryosystems Cryostream 800 cryostat. Deposition numbers 2244320 (for **P5PhPy4**), 2244321 (for **P5PhPy2**), 2244322 (for **P5PhPy2Cu-1**), 2244323 (for **P5PhPy2Cu-2**), 2244324 (for **P5PhPy2Cu-3**), 2244325 (for **P5PhPy2Cu-5**), 2244326 (for **P5PhPy2Co-1**), 2244327 (for **ml-2D-P5MOCN**), 2244328 (for **bl-2D-P5MOCN**), 2326170 (for **P6PhPy4**), 2326171 (for **bl-2D-P6MOCN**), 2342430 (for **sbl-2D-P6MOCN**), 2326172 (for **sbl-2D-P6MOCN**), 2326174 (for **fl-2D-P6MOCN**), 2326175 (for **mtl-2D-P6MOCN**), 2326165 (for I_2@**mtl-2D-P6MOCN**), 2326166 (for **R-bl-2D-P6MOCN**), and 2326167 (for **S-bl-2D-P6MOCN**) contain the supplementary crystallographic data for this paper. These data are provided free of charge by the joint Cambridge Crystallographic Data Centre via www.ccdc.cam.ac.uk/ data_request/cif. All data integration and empirical absorption correction were carried out using the SAINT program. Using Olex2 and SHELXTL, the structure was solved by direct method and refined matrix least-squares on F2 with anisotropic displacement. Non-hydrogen atoms were refined anisotropically, hydrogen atoms were constrained to ideal geometries.

Compounds **1**, **2**, **4** and **P5PhPy2** were prepared according to the reported method.[1-5]

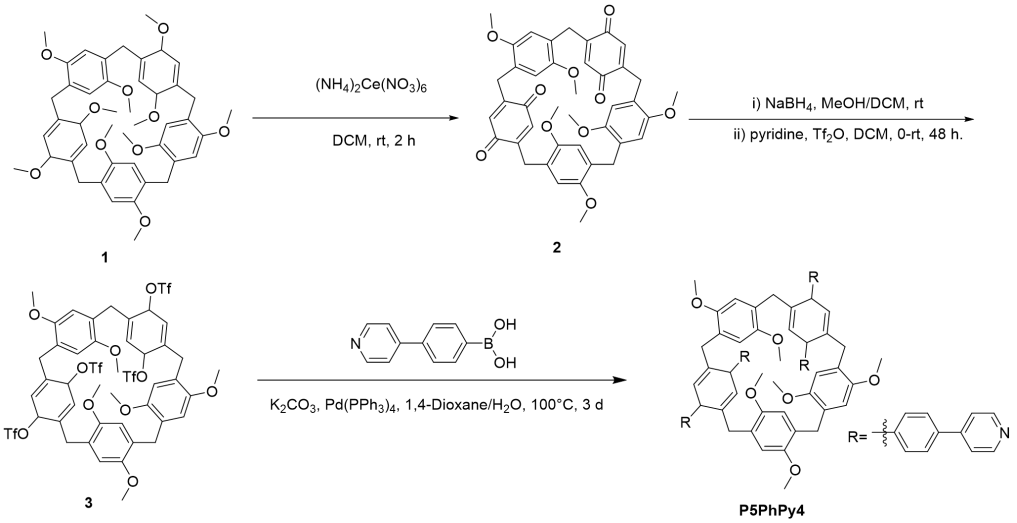

Compound **3**: $NaBH_4$ (402 mg, 10.6 mmol) was added to a solution of compound **2** (1.63 g, 2.36 mmol) in CH_2Cl_2/MeOH (5:1, 60 mL) at room temperature. The mixture was stirred until it turned colourless at room temperature, washed with aqueous HCl solution (1.0 M), and concentrated to give white solid, then added white solid and pyridine (1.2 mL, 14.16 mmol) in CH_2Cl_2 (90 mL) was added triflic anhydride (1.7 mL, 9.9 mmol) at 0 °C, which resulted in a mixture that was stirred at room temperature for 2 d, washed with aqueous HCl solution (1.0 M), and concentrated. The residue was purified by column chromatography (petroleum ether/dichloromethane = 4:1, v/v) to afford compound **3** (1.5 g, 51%) as a white solid. M.p. > 82 °C (decomp). ^{1}H NMR (400 MHz, $CDCl_3$) δ 7.33 (s, 2H), 7.30 (s, 2H), 6.84 (s, 2H), 6.74 (d, J = 3.7 Hz, 4H), 3.88 (s, 8H), 3.84 (s, 2H), 3.76 (s, 6H), 3.70 (s, 6H) 3.67 (s, 6H). ^{13}C NMR (101 MHz, $CDCl_3$) δ 150.58, 150.52, 150.47, 146.23, 146.18,

133.96, 133.56, 129.44, 125.62, 124.60, 124.54, 124.29, 120.11, 120.09, 116.92, 113.97, 113.50, 113.19, 55.73, 55.16, 55.03, 30.68, 30.37, 29.37. $[M+H]^+$ calcd for $C_{45}H_{38}N_4F_{12}O_{10}S_4$, 1223.0822; found, 1223.0859.

Compound **P5PhPy4**: A mixture of compound **3** (1 g, 0.81 mmol), K_2CO_3 (338 mg, 2.4 mmol), $Pd(PPh_3)_4$ (217 mg), and 4-(4-pyridyl)phenylboric acid (1.3 g, 6.52 mmol) in the mixed solution of 1,4-Dioxane/water (3:1, 80 mL) was heated to 100 °C under nitrogen for 3 d. After falling to room temperature, 1,4-dioxane and water were removed by rotary evaporation. Water (160 mL) was added to the reaction mixture after it was cooled down to room temperature. The resulting mixture was filtered to afford a solid which was purified by column (dichloromethane/methanol = 50:1, v/v) to obtain white solid compound **P5PhPy4** (490 mg, 48%). M.p. > 212 °C (decomp). ^{1}H NMR (400 MHz, $CDCl_3$) δ 8.66 (dd, J = 9.2 Hz, 5.6 Hz, 8H), 7.41(dt, J = 18.4 Hz, 6.8 Hz, 16H), 7.17 (s, 2H), 7.11 (t, J = 8.4 Hz, 8H), 6.89 (s, 2H), 6.76 (s, 2H), 5.98 (s, 2H), 5.93 (s, 2H), 3.90-3.99 (m, 6H), 3.67-3.80 (m, 4H), 3.49 (s, 6H), 3.33 (s, 6H) 3.16 (s, 6H). ^{13}C NMR (101 MHz, $CDCl_3$) δ 151.01, 150.87, 150.65, 150.31, 147.85, 147.79, 143.00, 142.53, 140.32, 140.29, 136.87, 136.67, 136.26, 136.19, 132.47, 131.61, 130.04, 130.01, 128.59, 128.46, 128.17, 126.59, 126.38, 121.34, 114.86, 114.03, 113.56, 56.16, 55.51, 55.37, 33.73, 33.48. $[M+H]^+$ calcd for $C_{85}H_{70}N_4O_6$, 1243.5368; found, 1243.5374.

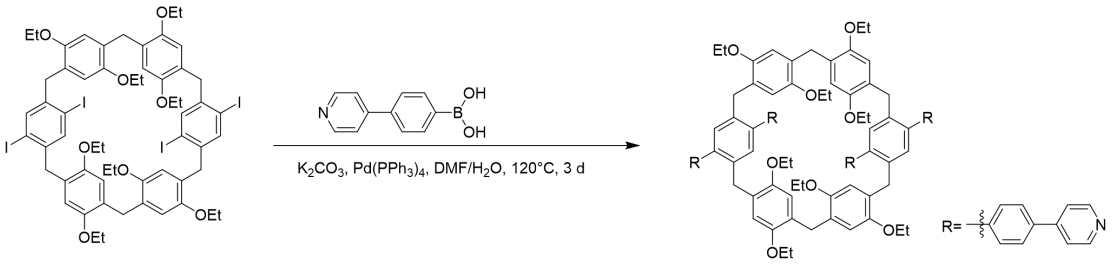

Compound **P6PhPy4**: A mixture of compound **4** (1 g, 0.72 mmol), K_2CO_3 (178.2 mg, 1.3 mmol), $Pd(PPh_3)_4$ (190 mg), and 4-(4-pyridyl)phenylboric acid (712 mg, 3.6 mmol) in the mixed solution of DMF/water (3:1, 12 mL) was heated to 120 °C under nitrogen for 3 d. After falling to room temperature, DMF and water were removed by rotary evaporation. Water (160 mL) was added to the reaction mixture after it was cooled down to room temperature. The resulting mixture was filtered to afford a solid which was purified by column (dichloromethane/methanol = 50:1, v/v) to obtain white solid compound **P6PhPy4** (400 mg, 40%). M.p. > 261 °C (decomp). ^{1}H NMR (600 MHz, DMF-d_7) δ 8.73 – 8.67 (m, 8H), 7.63 – 7.57 (m, 16H), 7.24 (d, J = 8.2 Hz, 8H), 7.14 (s, 4H), 6.76 (s, 4H), 6.24 (s, 4H), 4.05 (d, J = 15.1 Hz, 4H), 3.88 (d, J = 15.2 Hz, 4H), 3.80 (dq, J = 9.1, 7.0 Hz, 4H), 3.73 – 3.67 (m, 8H), 3.64 – 3.54 (m, 8H), 1.14 (dt, J = 18.7, 7.0 Hz, 24H). ^{13}C NMR (126 MHz, CD_2Cl_2) δ 151.52, 151.25, 151.21, 148.62, 143.74, 141.39, 137.49, 136.98, 132.56, 130.84, 129.45, 128.55, 127.25, 122.29, 116.39, 115.37, 65.01, 64.69, 34.99, 15.90, 15.86. ^{1}H NMR (500 MHz, Methylene Chloride-d_2) δ 8.61 (s, 8H), 7.33 (s, 16H), 7.13 (s, 8H), 7.02 (s, 4H),

6.74 (s, 4H), 6.09 (s, 4H), 3.96 (d, J = 14.8 Hz, 4H), 3.79 (t, J = 12.7 Hz, 8H), 3.66 (d, J = 14.5 Hz, 8H), 3.57 – 3.46 (m, 8H), 1.20 – 1.09 (m, 24H).

P5PhPy2: **P5PhPy2** (5 mg, 0.005 mmol), and 500 μL DMF were added in a 4 mL vial. Slow evaporation of the solvent in the air over 2 days at room temperature, and then a single-crystal product suitable for electron diffraction (clear crystal) was obtained.

P5PhPy2Cu-1: **P5PhPy2** (5.0 mg, 0.005 mmol), $Cu(AC)_2$ (2.0 mg, 0.01 mmol) and 500 μL DMF were added in a 4 mL vial. Slow evaporation of the solvent in the air over about 4 days at room temperature, and then a single-crystal product suitable for x-ray single-crystal diffraction analysis (green crystal) was obtained.

P5PhPy2Cu-2: **P5PhPy2** (5.0 mg, 0.005 mmol), $Cu(AC)_2$ (2.0 mg, 0.01 mmol), 500 μL DMF and 50 μL CH_3COOH were added to a 4 mL vial. Over about 4 days at room temperature under airtight conditions, and then a single-crystal product suitable for x-ray single-crystal diffraction analysis (green crystal) was obtained.

P5PhPy2Cu-3 and **P5PhPy2Cu-4**: **P5PhPy2** (5.0 mg, 0.005 mmol), $Cu(NO_3)_2•3H_2O$ (2.4 mg, 0.01 mmol), 1.0 mL DMF and 100 μL CH_3COOH were added a 4 mL vial. The mixture was heated at 80 ℃ for 10 days under airtight conditions and then cooled to room temperature, two types of single-crystal products suitable for x-ray single-crystal diffraction analysis (blue and green crystal) were obtained.

P5PhPy2Co-1: **P5PhPy2** (5.0 mg, 0.005 mmol), $Co(NO_3)_2•6H_2O$ (3.0 mg, 0.01 mmol), 500 μL DMF and 50 μL CH_3COOH were added a 4 mL vial. The mixture was heated at 80 ℃ for 10 days under airtight conditions and then cooled to room temperature, a single-crystal product suitable for x-ray single-crystal diffraction analysis (pink crystal) was obtained.

P5PhPy4: **P5PhPy4** (3.3 mg, 0.0025 mmol), 500 μL CH_2Cl_2 and 250 μL C_2H_5OH was added to a 4 mL vial. Slow evaporation of the solvent in the air over about 2 days at room temperature, then a single-crystal product suitable for x-ray single-crystal diffraction analysis (colourless crystal) was obtained.

ml-2D-P5MOCN: **P5PhPy4** (3.3 mg, 0.0025 mmol), 1.0 mL DMF, 100 μl H_2O, $Co(NO_3)_2•6H_2O$ (3 mg, 0.01 mmol), and 100 μL CH_3COOH vial was added a 4 mL vial. The mixture was heated at 80 ℃ for 2 days under airtight conditions, and then a single-crystal product suitable for electron diffraction (pink crystal) was obtained.

bl-2D-P5MOCN: **P5PhPy4** (3.3 mg, 0.0025 mmol), 1.0 mL DMF, $Co(NO_3)_2•6H_2O$ (3 mg, 0.01 mmol) and 100 μL CH_3COOH were added to a 4 mL vial. The mixture was stood for 4 weeks at room temperature, and then a single-crystal product suitable for electron diffraction (pink crystal) was obtained.

P6PhPy4: **P6PhPy4** (3.0 mg, 0.0019 mmol), 500 μL CH_2Cl_2 and 250 μL MeOH were added to a 4 mL vial. Slow evaporation of the solvent in the air throughout about 24 h at room temperature, then a single-crystal product suitable for x-ray single-crystal diffraction analysis (colourless crystal) was obtained.

mtl-2D-P6MOCN: **P6PhPy4** (3.0 mg, 0.0019 mmol), 0.5 mL DMF, 50 μl H_2O, $Cu(NO_3)_2$•$3H_2O$ (1.9 mg, 0.008 mmol), and 50 μL CH_3COOH vial was added a 4 mL vial. The mixture was heated at 80 ℃ for 24 h under airtight conditions, then a single-crystal product suitable for electron diffraction (blue crystal) was obtained.

fl-2D-P6MOCN: **P6PhPy4** (3.0 mg, 0.0019 mmol), 0.5 mL DMF, 50 μl H_2O, $Cu(NO_3)_2$•$3H_2O$ (1.9 mg, 0.008 mmol), and 50 μL CH_3COOH vial was added a 4 mL vial. The mixture was heated at 80 ℃ for 2 weeks under airtight conditions, and then a single-crystal product suitable for electron diffraction (green crystal) was obtained.

bl-2D-P6MOCN: The crystals of **mtl-2D-P6MOCN/fl--2D-P6MOCN** were redissolved at 120 ℃ and then heated at 80 ℃ for 72 h under airtight conditions, and then a single-crystal product suitable for electron diffraction (green crystal) was obtained.

sbl-2D-P6MOCN/sbl-2D-P6MOCN-2: **P6PhPy4** (3.0 mg, 0.0019 mmol), 0.5 mL DMF, 50 μl H_2O, $Cu(NO_3)_2$•$3H_2O$ (1.9 mg, 0.008 mmol), 5 μL adiponitrile and 50 μL CH_3COOH vial was added a 4 mL vial. The mixture was heated at 80 ℃ for 3 days or 10 days under airtight conditions, then a single-crystal product suitable for electron diffraction (blue crystal) was obtained.

***R*-bl-2D-P6MOCN**: ***R*-P6PhPy4** (3.0 mg, 0.0019 mmol), 0.5 mL DMF, 50 μl H_2O, $Cu(NO_3)_2$•$3H_2O$ (1.9 mg, 0.008 mmol), and 50 μL CH_3COOH vial was added a 4 mL vial. The mixture was heated at 80 ℃ for 24 h under airtight conditions, and then a single-crystal product suitable for electron diffraction (blue crystal) was obtained.

***S*-bl-2D-P6MOCN**: ***S*-P6PhPy4** (3.0 mg, 0.0019 mmol), 0.5 mL DMF, 50 μl H_2O, $Cu(NO_3)_2$•$3H_2O$ (1.9 mg, 0.008 mmol), and 50 μL CH_3COOH vial were added a 4 mL vial. The mixture was heated at 80 ℃ for 24 h under airtight conditions, and then a single-crystal product suitable for electron diffraction (blue crystal) was obtained.

I2@mtl-2D-P6MOCN: **mtl-2D-P6MOCN** (1.0 mg) and the aqueous solution of I_2 (1.0 mM, 2.5 mL) were added to a 4 mL vial. The mixture was allowed to stand for 10 h, and the aqueous solution of I_2 (1.0 mM, 2.5 mL) changed from yellowish brown to colourless transparent, and the crystals of **mtl-2D-P6MOCN** changed from blue to reddish-brown.

Characterization data of metal-organic coordination polymers

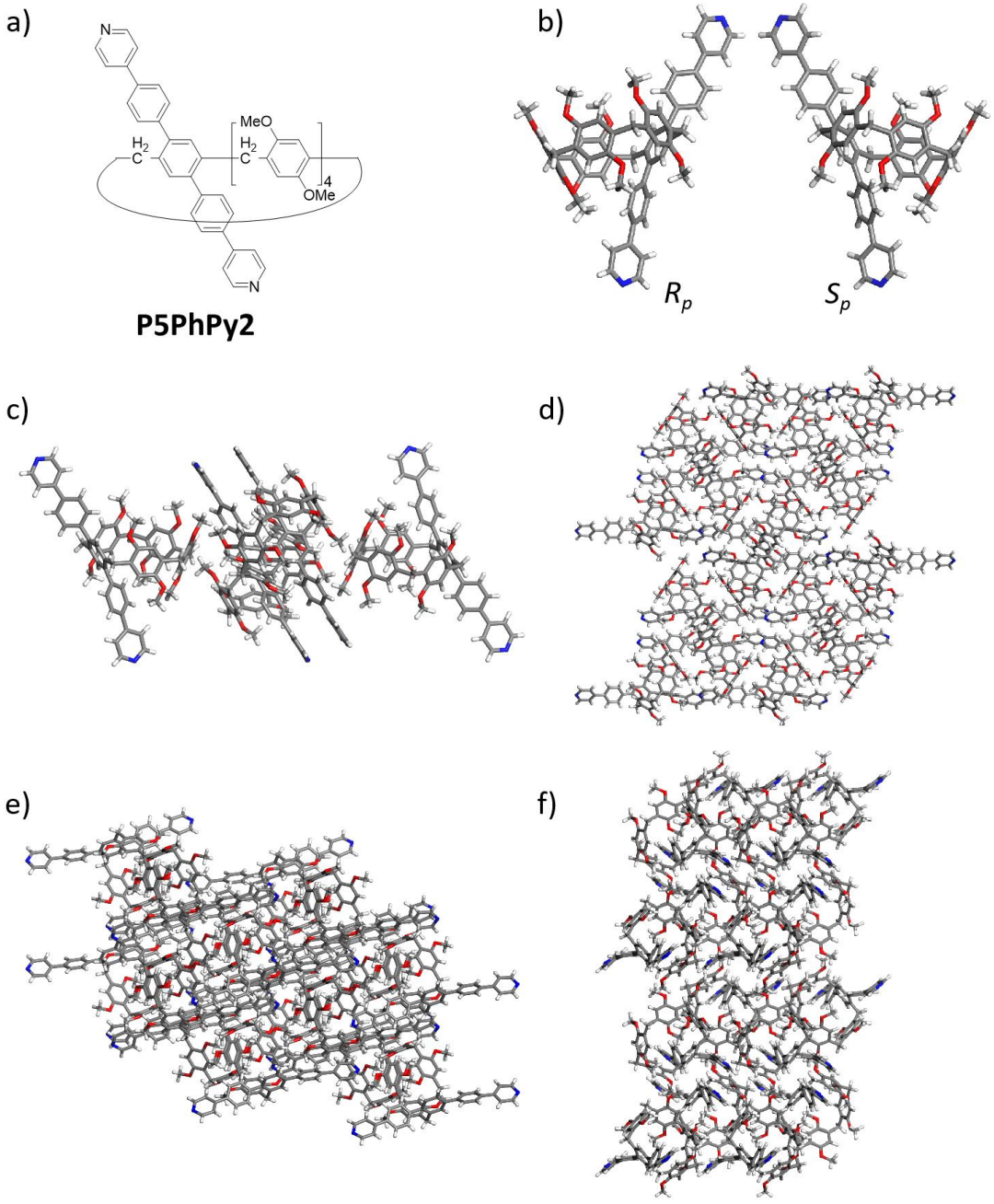

Figure S1. Compounds **P5PhPy2** (a) and the crystal structure of **P5PhPy2** (Rp, Sp) (b-c) and the top view demonstrating a compact packing manner in the (1,0,0), (0,1,0) and (0,0,1) direction (d-f).

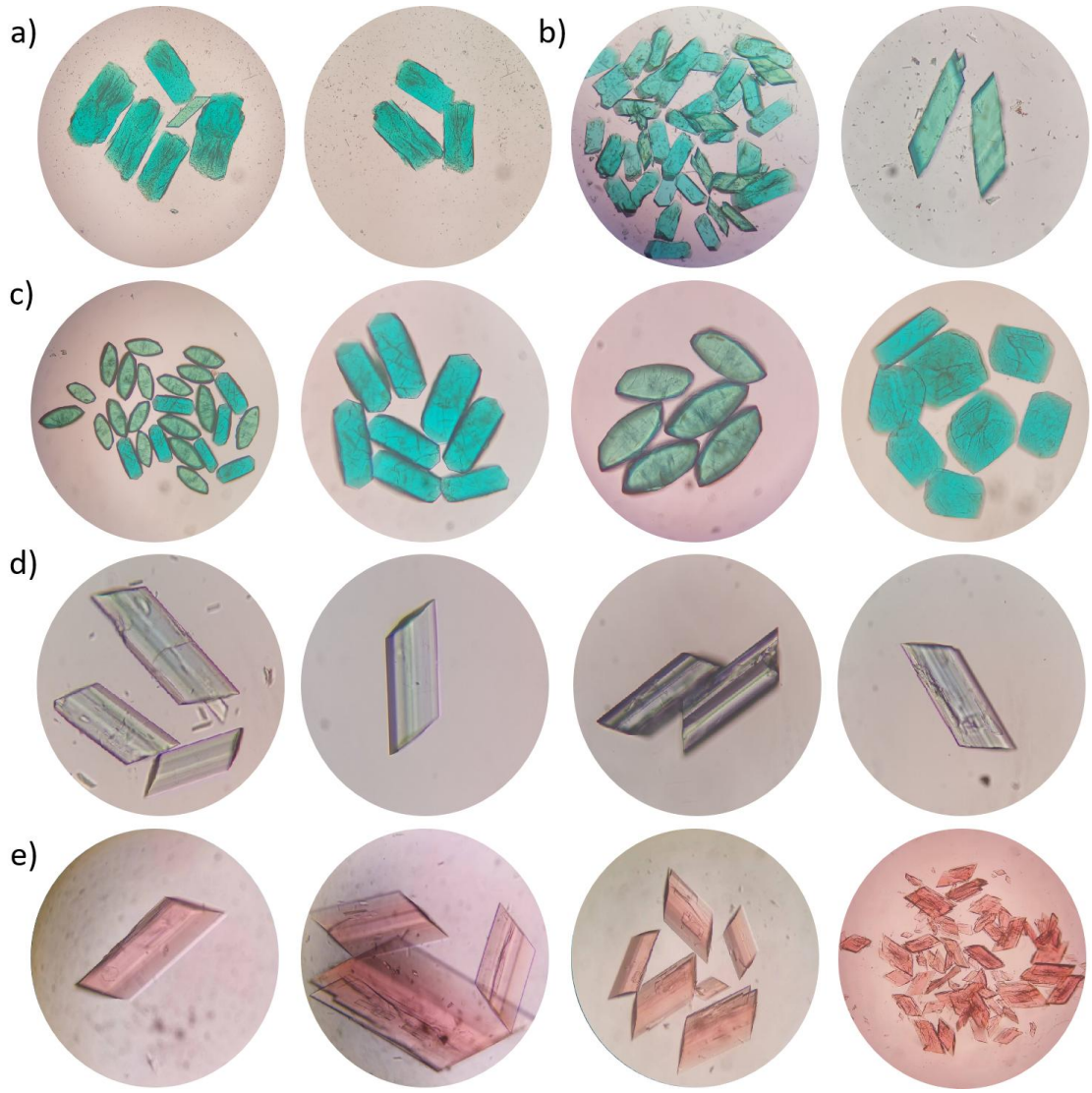

Figure S2. Microscope images of **P5PhPy2Cu-1** (a), **P5PhPy2Cu-2** (b), **P5PhPy2Cu-3** (c), **P5PhPy2Cu-4** (d) and **P5PhPy2Co-1** (e).

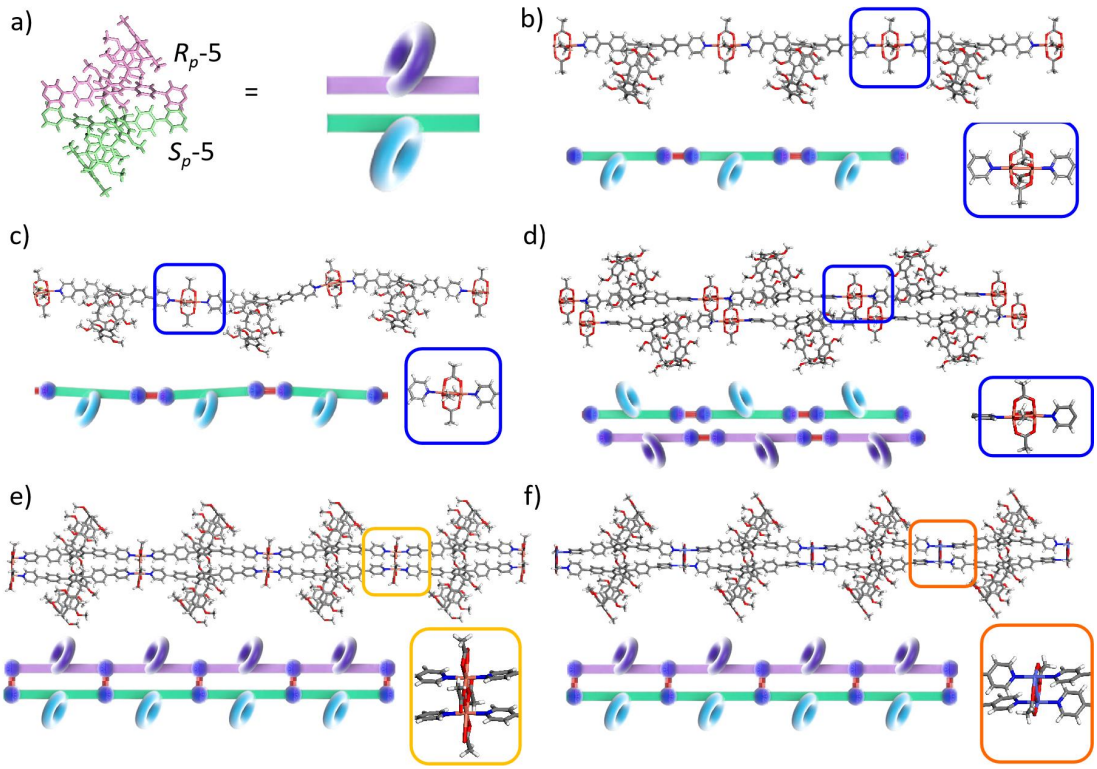

Figure S3. The crystal structure and diagram of **P5PhPy2** (Rp, Sp), 1D coordination of the polymer **P5PhPy2Cu-1** and **P5PhPy2Cu-2** (b and c), parallel 1D coordinations of the polymer **P5PhPy2Cu-3** (d), ladder-like 1D coordination polymer **P5PhPy2Cu-4** and **P5PhPy2Co-1** (e and f). Noncoordinated solvent molecules are omitted.

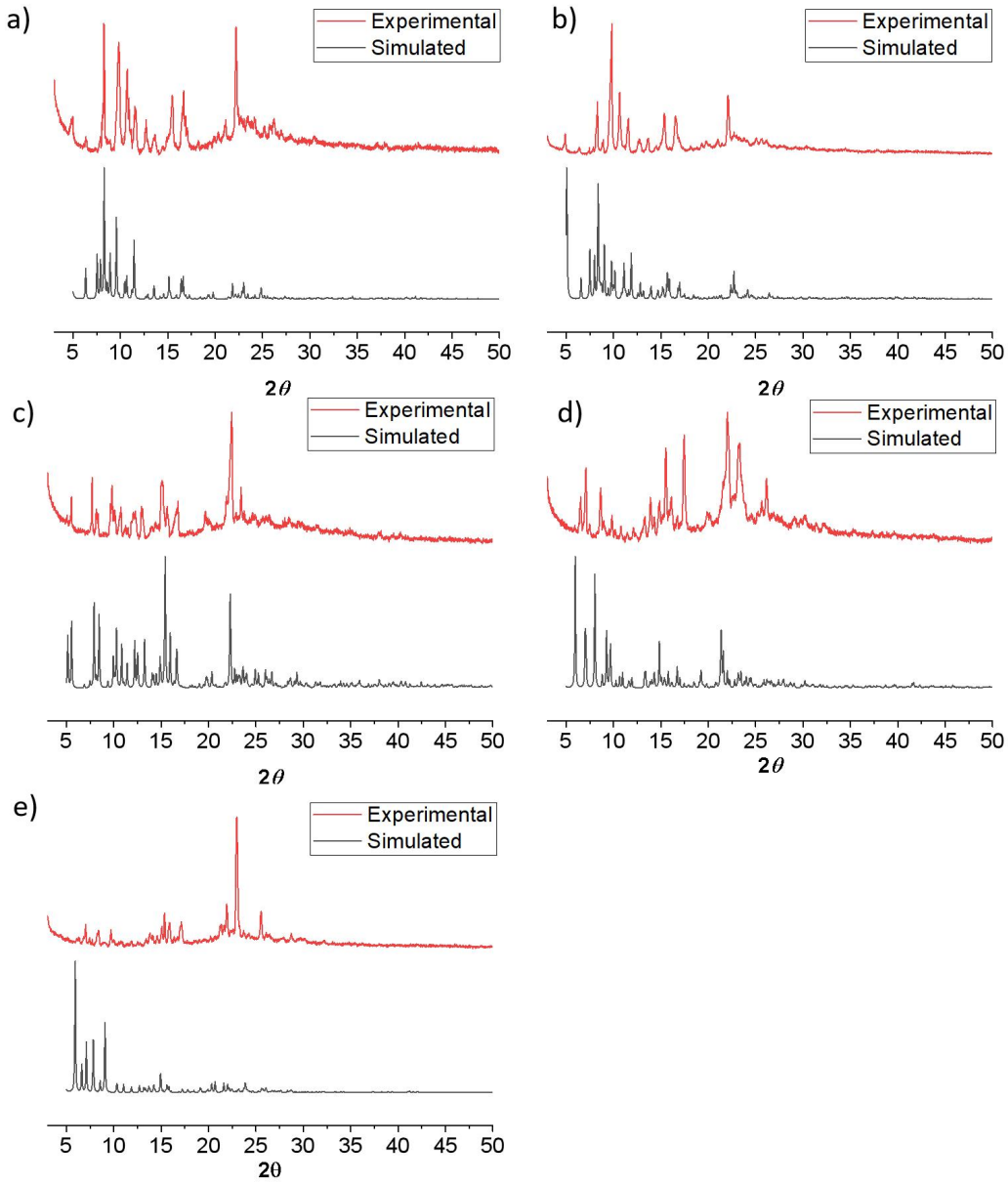

Figure S4. Experimental (red) and simulated (black) PXRD patterns of **P5PhPy4Cu-1** (a), **P5PhPy4Cu-2** (b), **P5PhPy4Cu-3** (c), **P5PhPy4Cu-4** (d) and **P5PhPy4Co-1** (e).

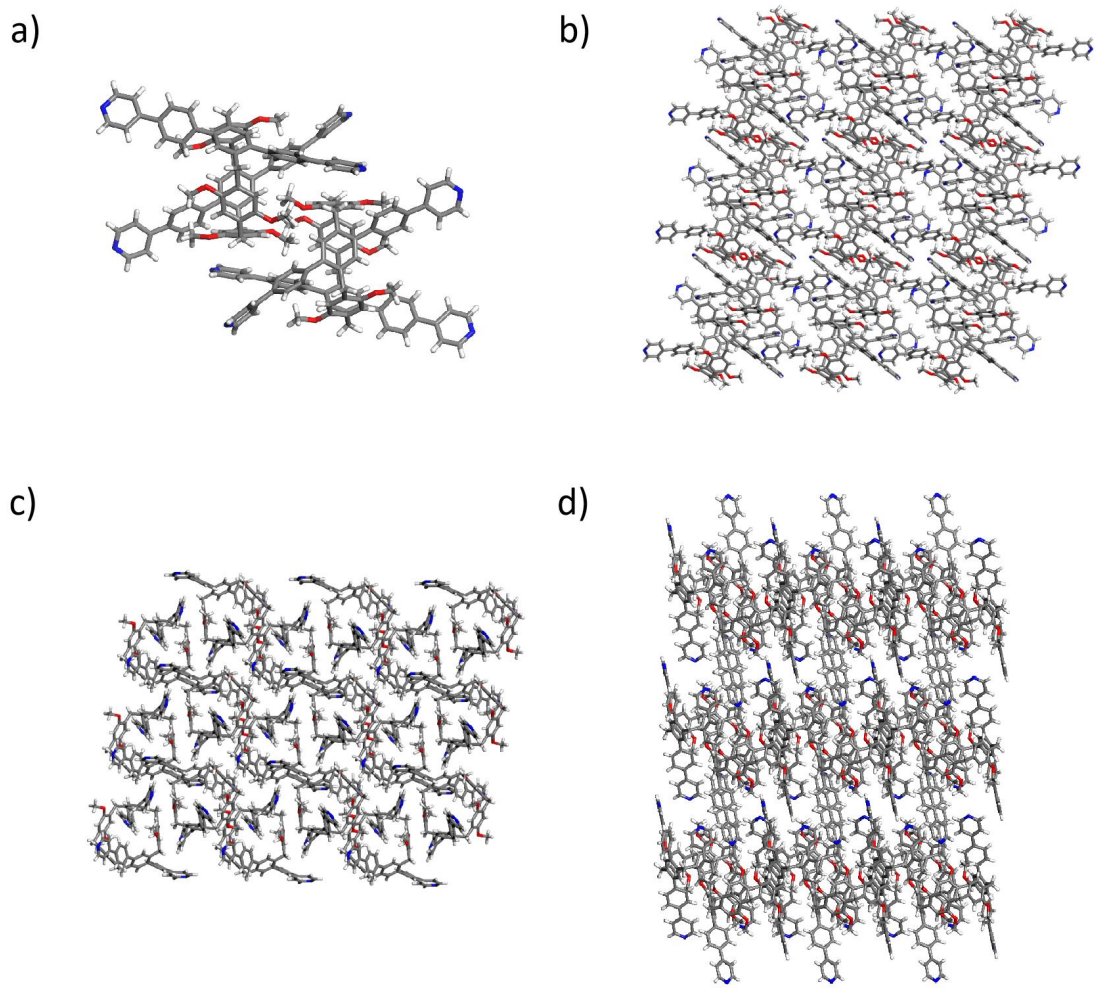

Figure S5. The crystal structure of **P5PhPy4** (a), and the top view demonstrating a compact packing manner in the (1,0,0), (0,1,0) and (0,0,1) direction (b-d).

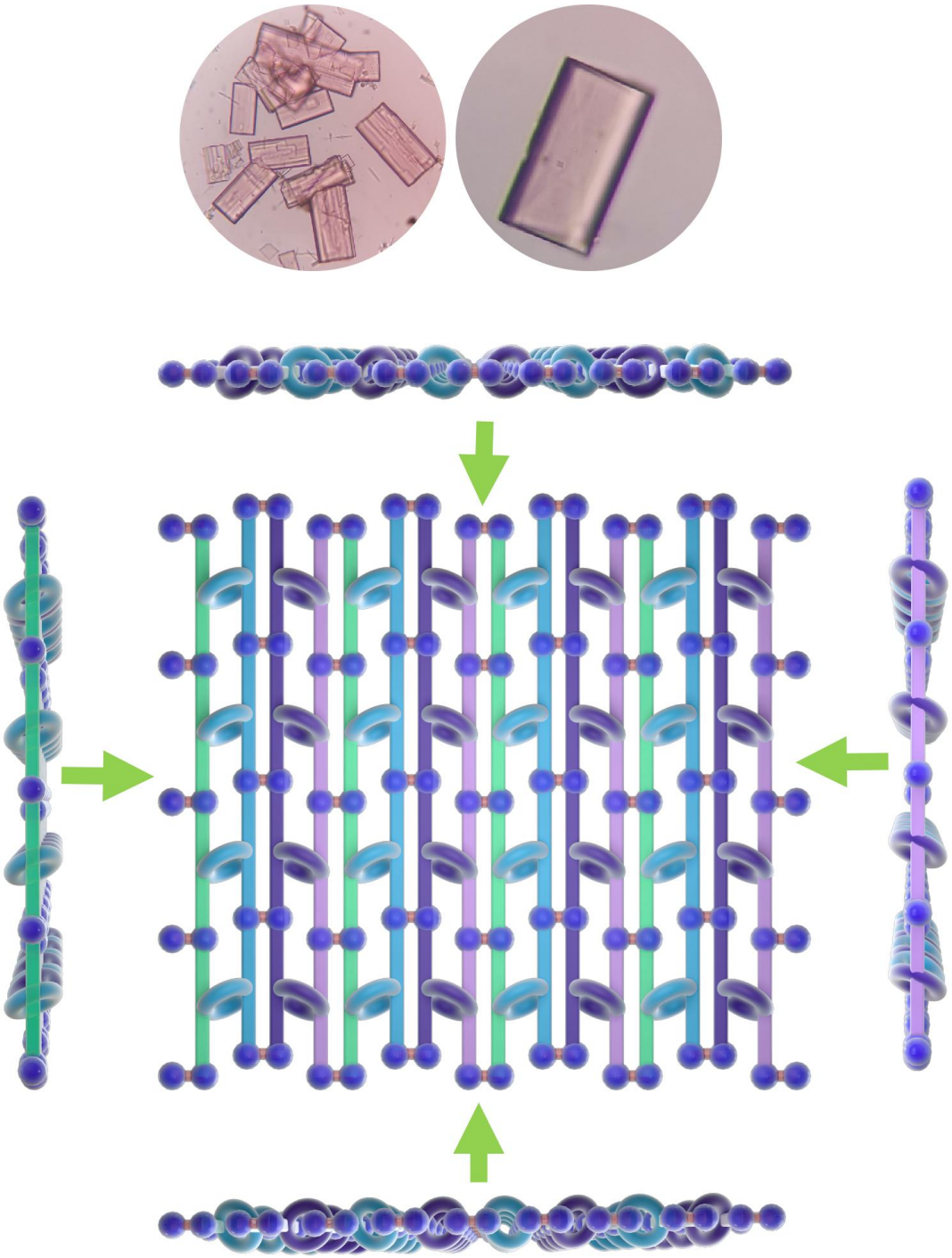

Figure S6. Microscope images of **ml-2D-P5MOCN** and the side and top cartoon view of a single layer 2D coordination the polymer **ml-2D-P5MOCN**.

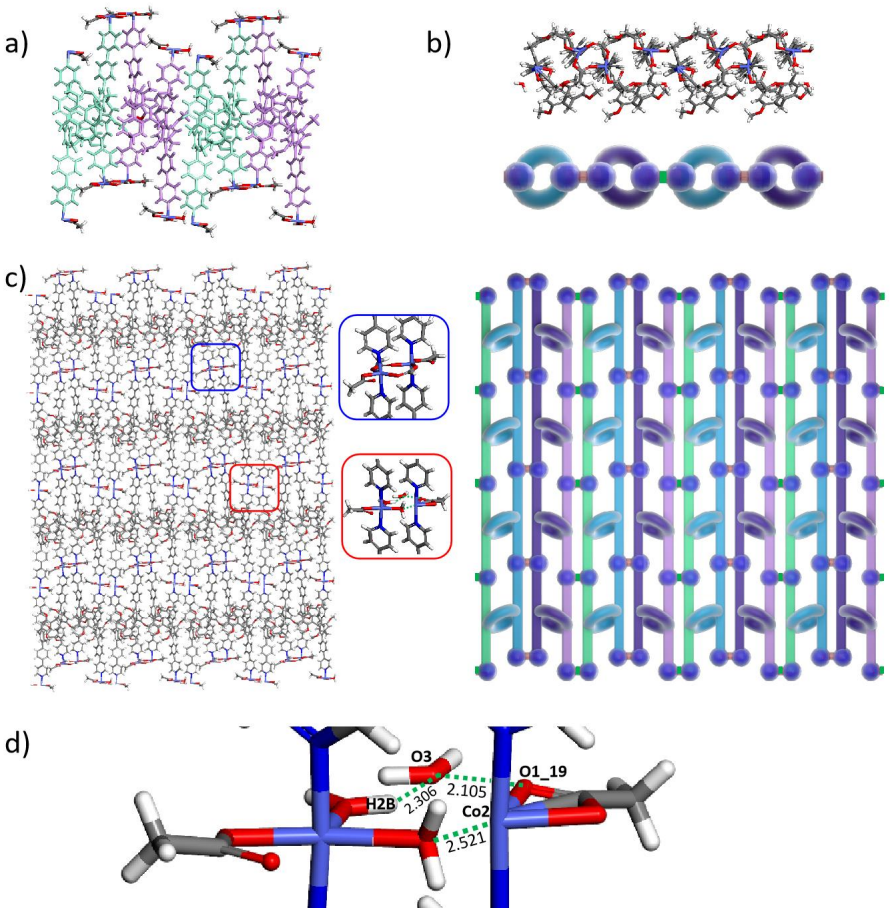

Figure S7. a) The crystal structure and diagram of the coordination between **P5PhPy4** (Rp-5 and Sp-5) and Co(II). b) The side view of a single layer 2D coordination the polymer **ml-2D-P5MOCN**. c) The top view of a single layer 2D coordination the polymer **ml-2D-P5MOCN**. d) The hydrogen bond in 2D coordination the polymer **ml-2D-P5MOCN**.

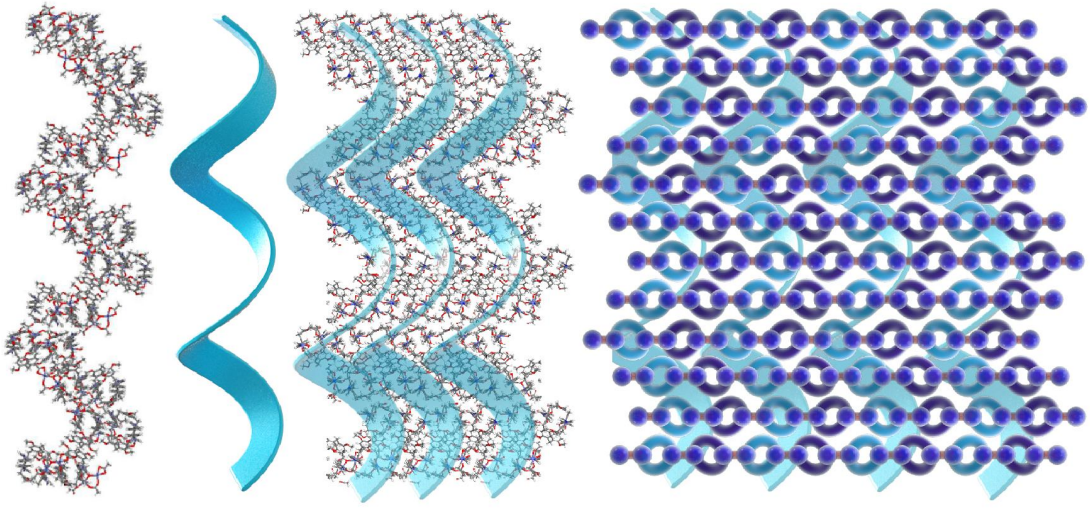

Figure S8. The lateral side view shows that the pillar[5]arene units in the laminated structure are arranged in a microhelix-like S-shaped curve .

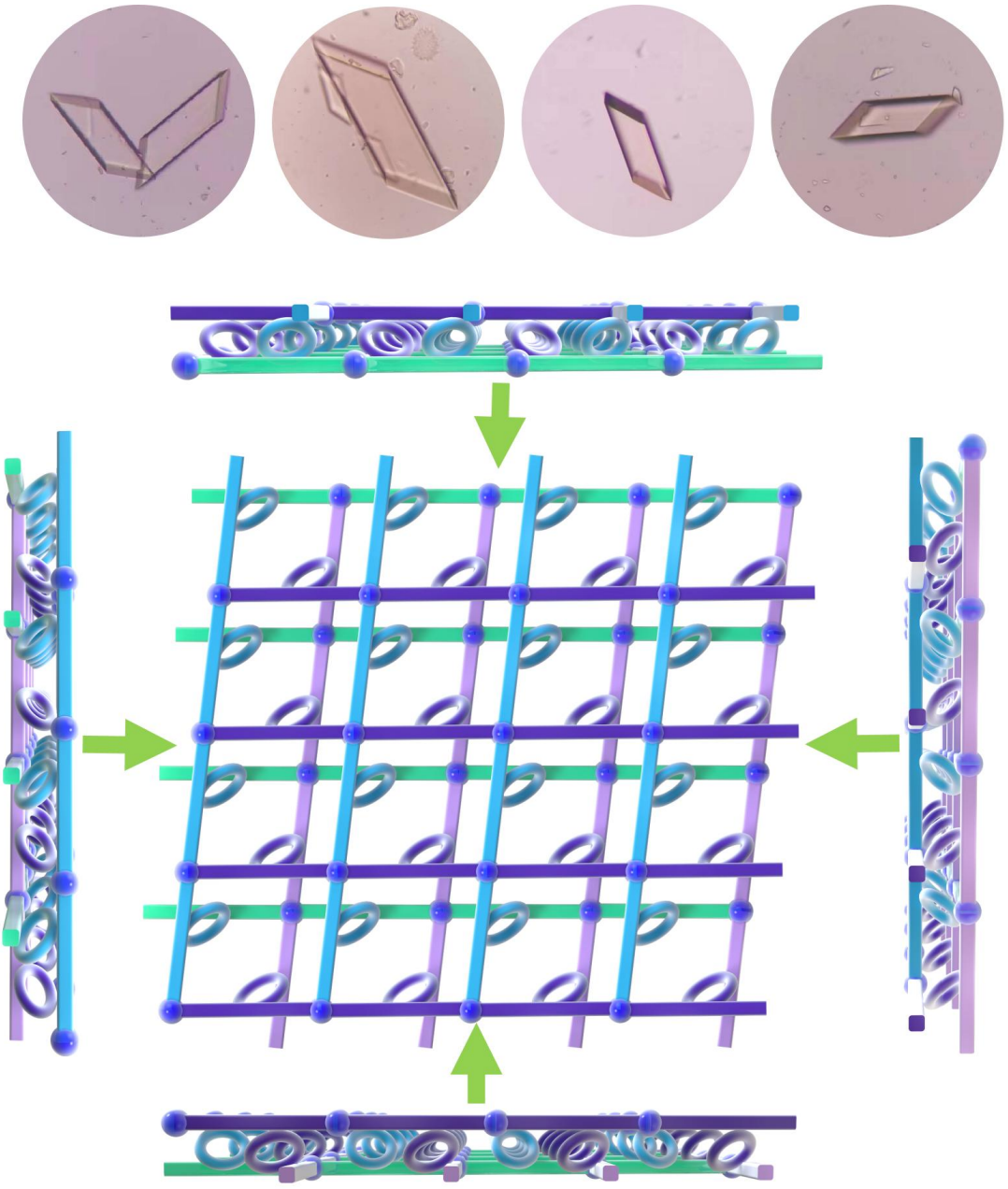

Figure S9. Microscope images of **bl-2D-P5MOCN** and the side and top cartoon view of a single layer 2D coordination the polymer **bl-2D-P5MOCN**.

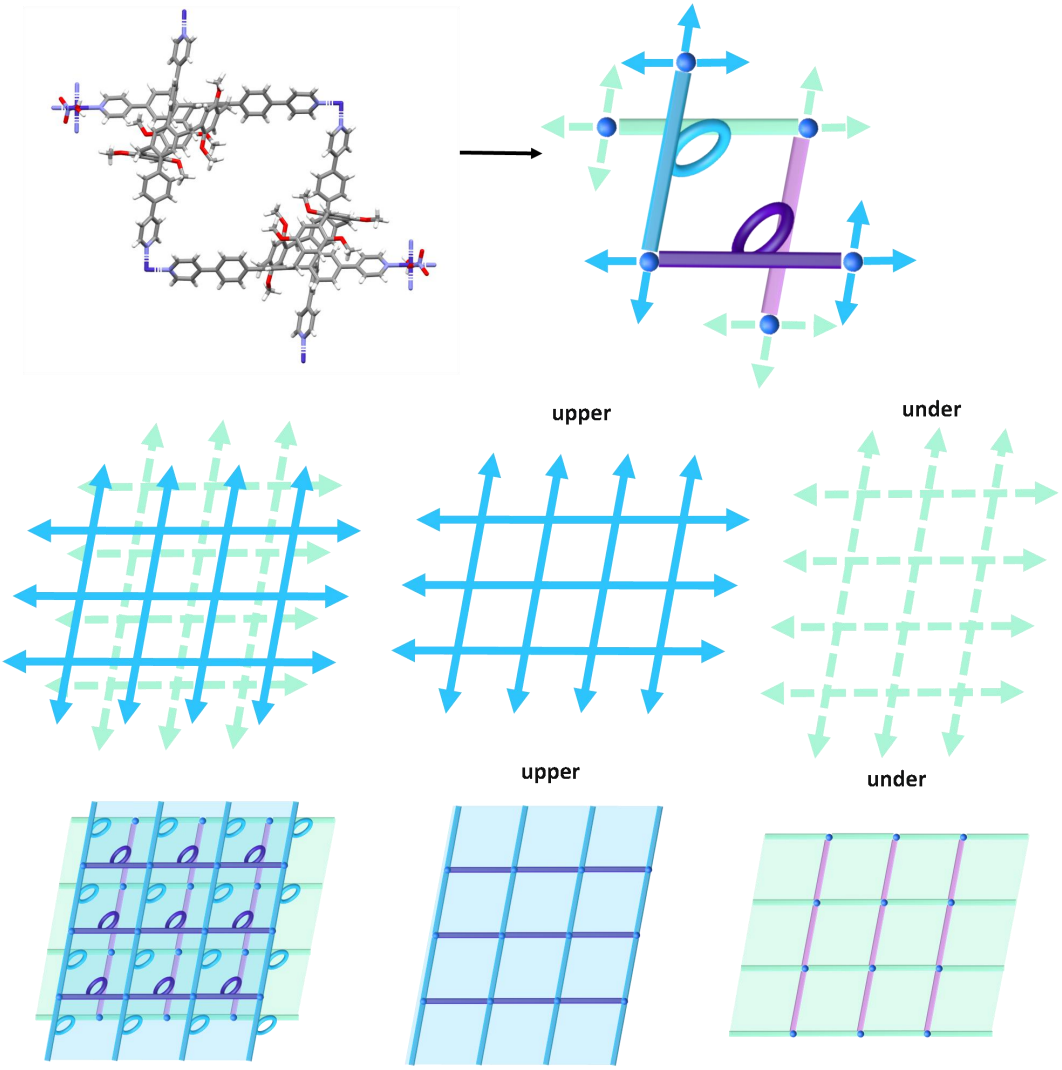

Figure S10. The crystal structure and diagram of the coordination between **P5PhPy4** and Co(II).

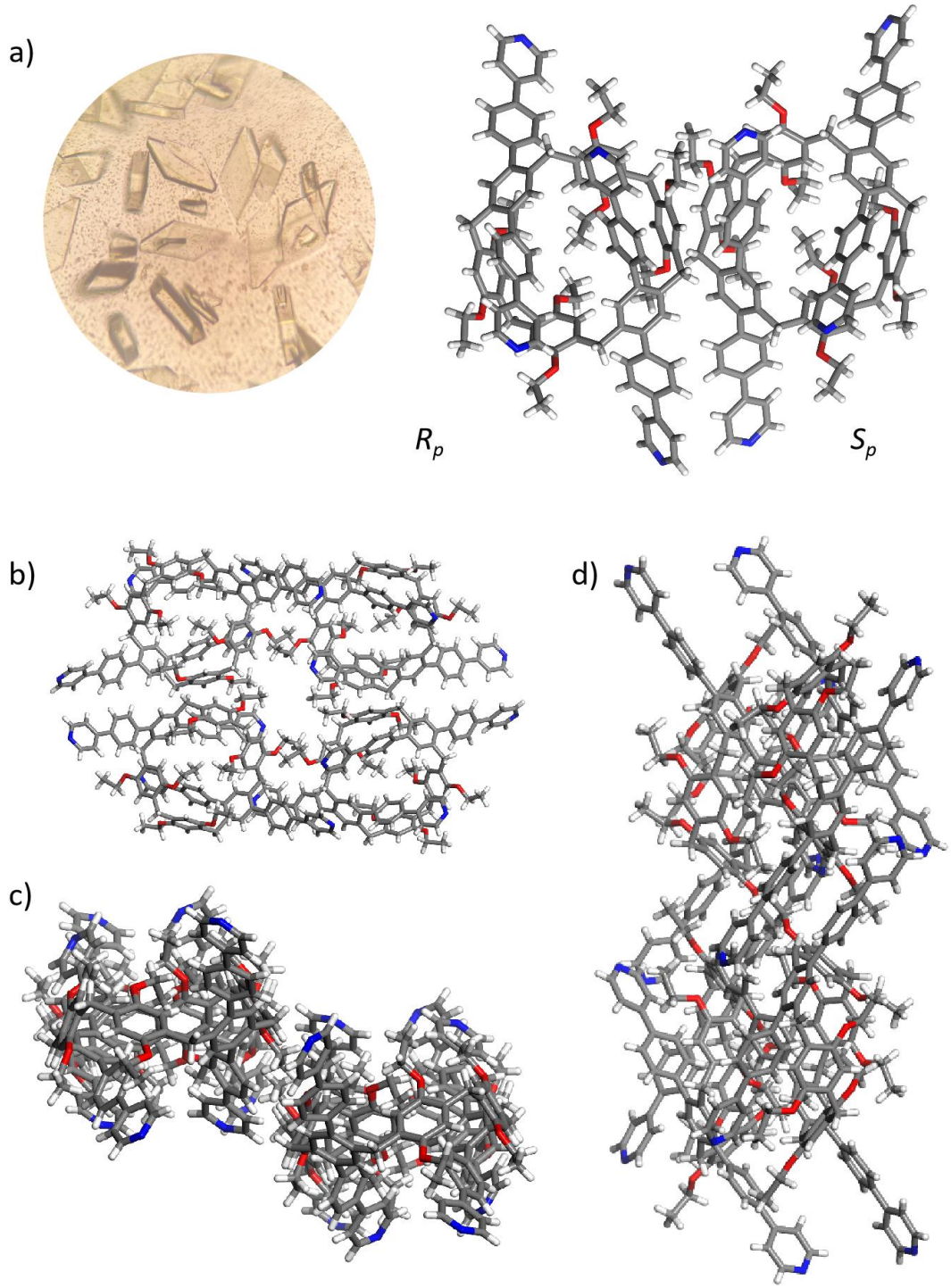

Figure S11. The microscope images and crystal structure of **P6PhPy4** (a) and the top view demonstrating a compact packing manner in the (1,0,0), (0,1,0) and (0,0,1) direction (b-d).

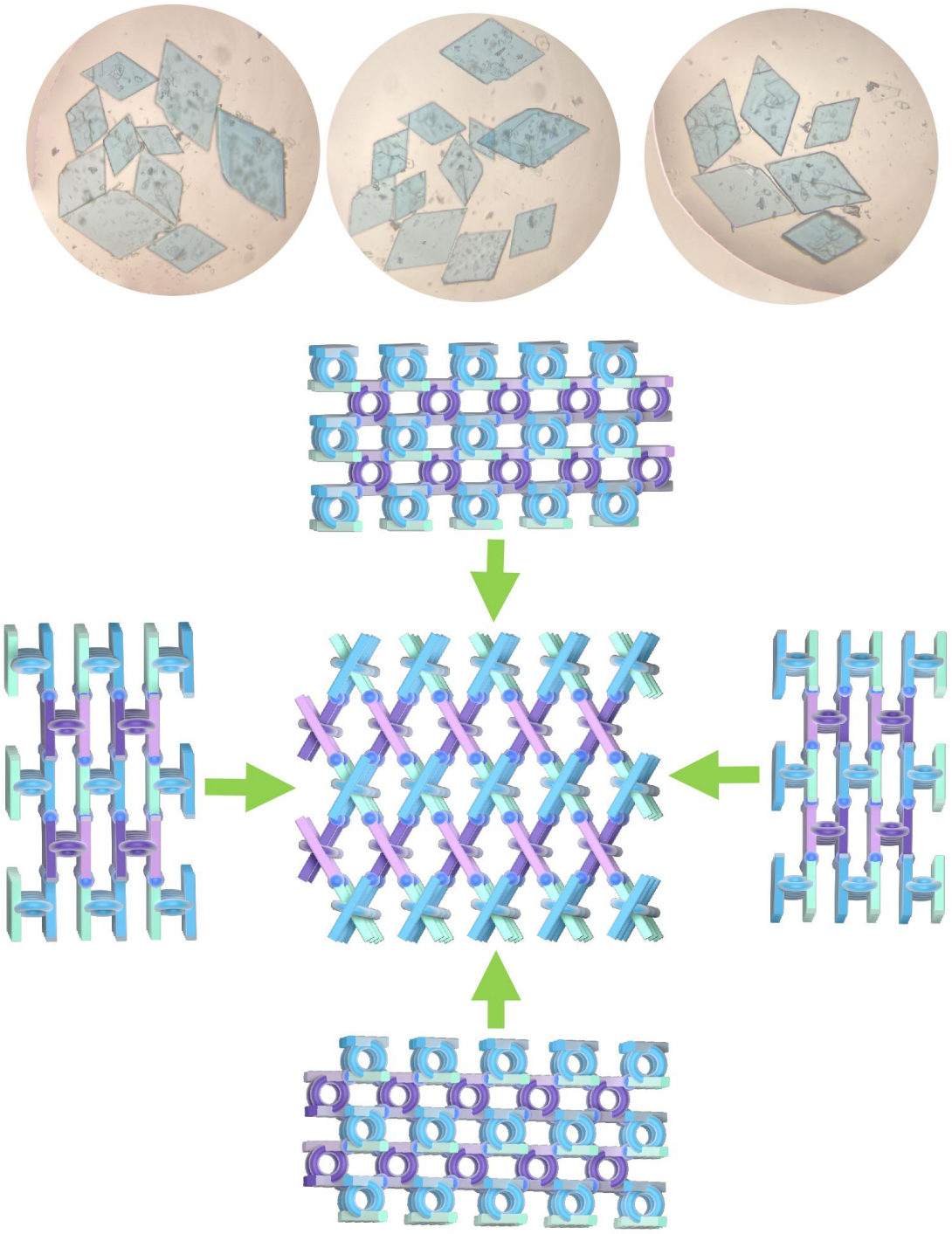

Figure S12. Microscope images of **mtl-2D-P6MOCN** and the top and side carton view of a single layer 2D coordination the polymer **mtl-2D-P6MOCN**.

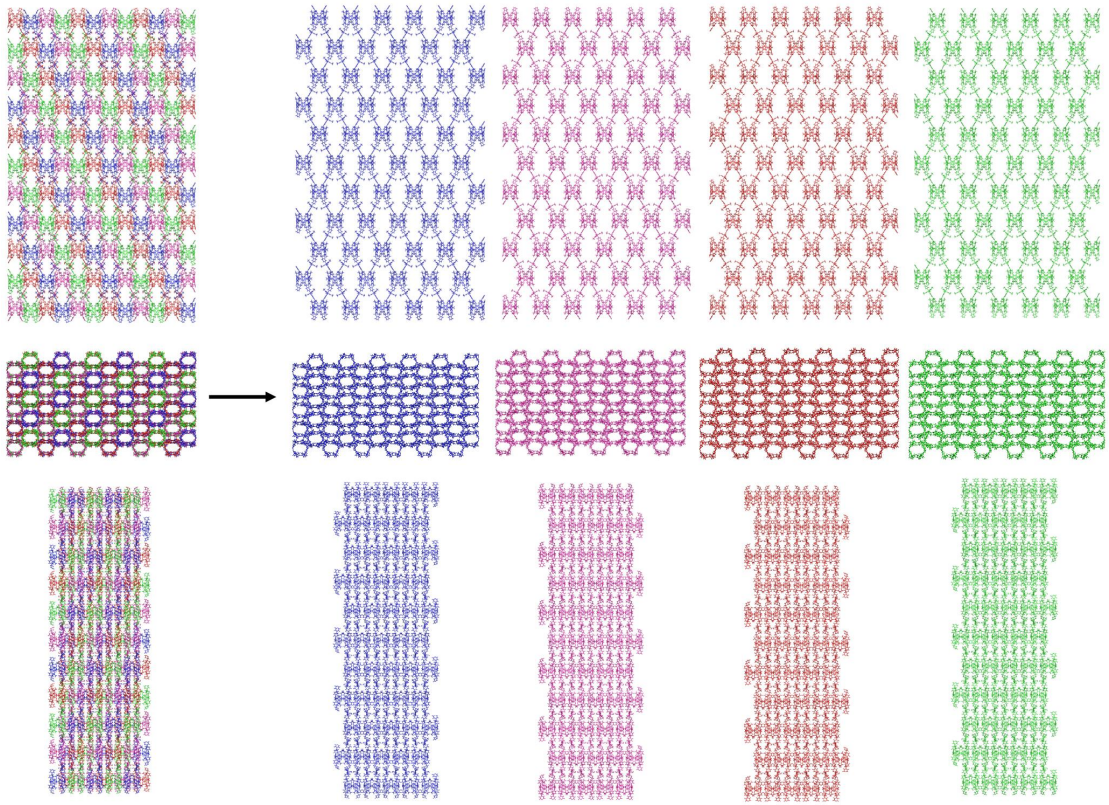

Figure S13. The four-fold interpenetrating structure of **mtl-2D-P6MOCN**.

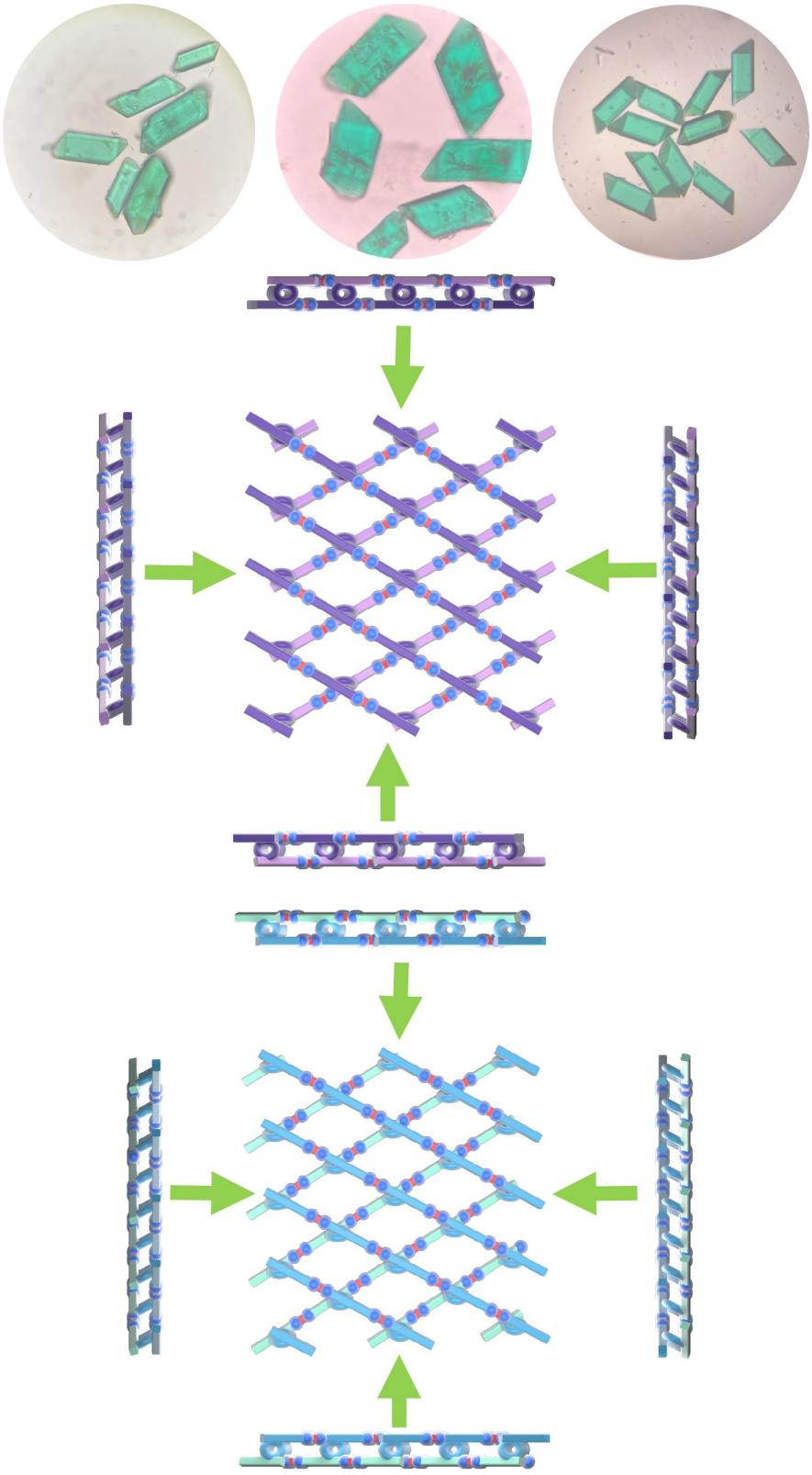

Figure S14. Microscope images of **bl-2D-P6MOCN** and the top and side carton view of a single layer 2D coordination the polymer **bl-2D-P6MOCN** (R and S).

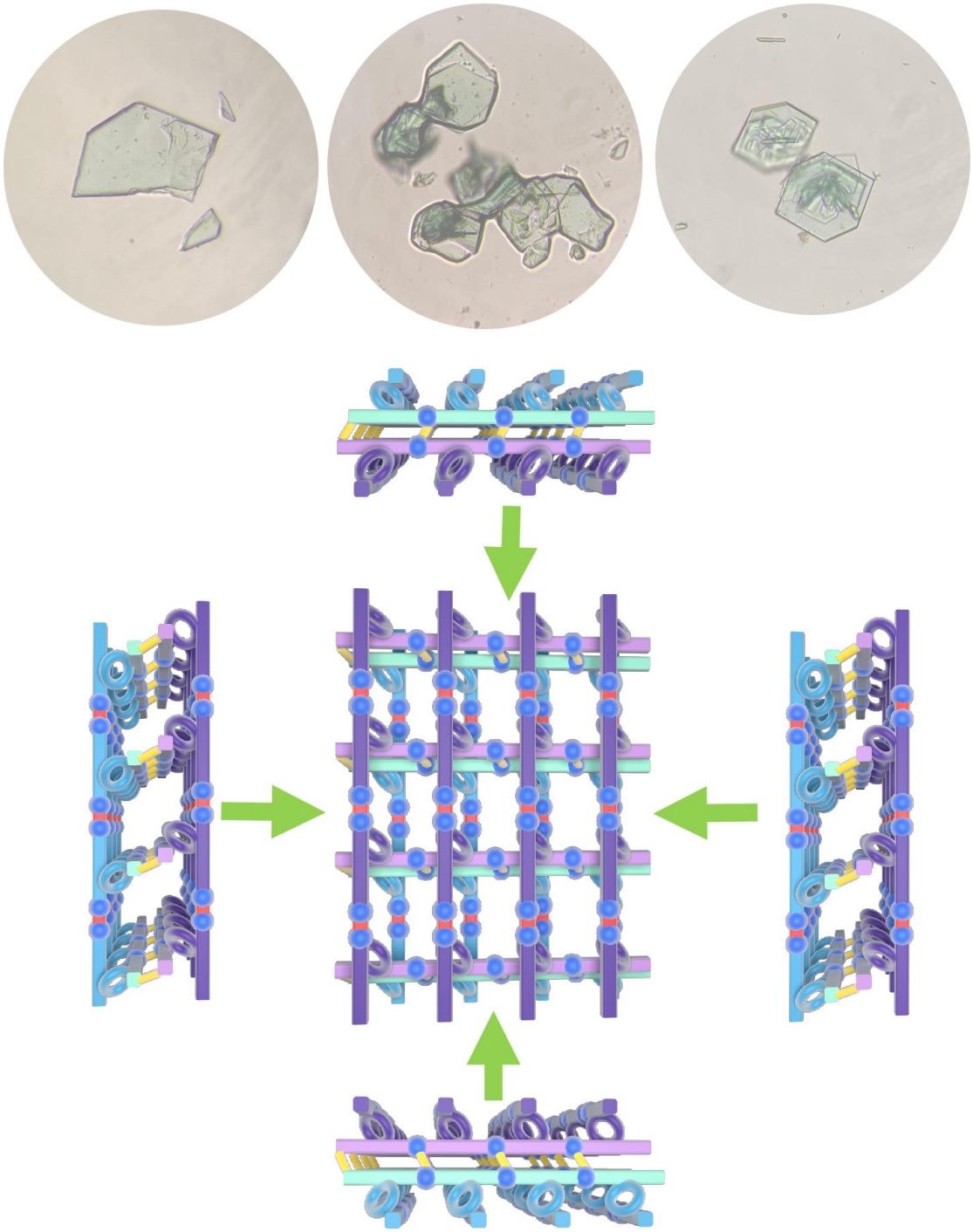

Figure S15. Microscope images of **fl-2D-P6MOCN** and the top and side carton view of a single layer 2D coordination the polymer **fl-2D-P6MOCN**.

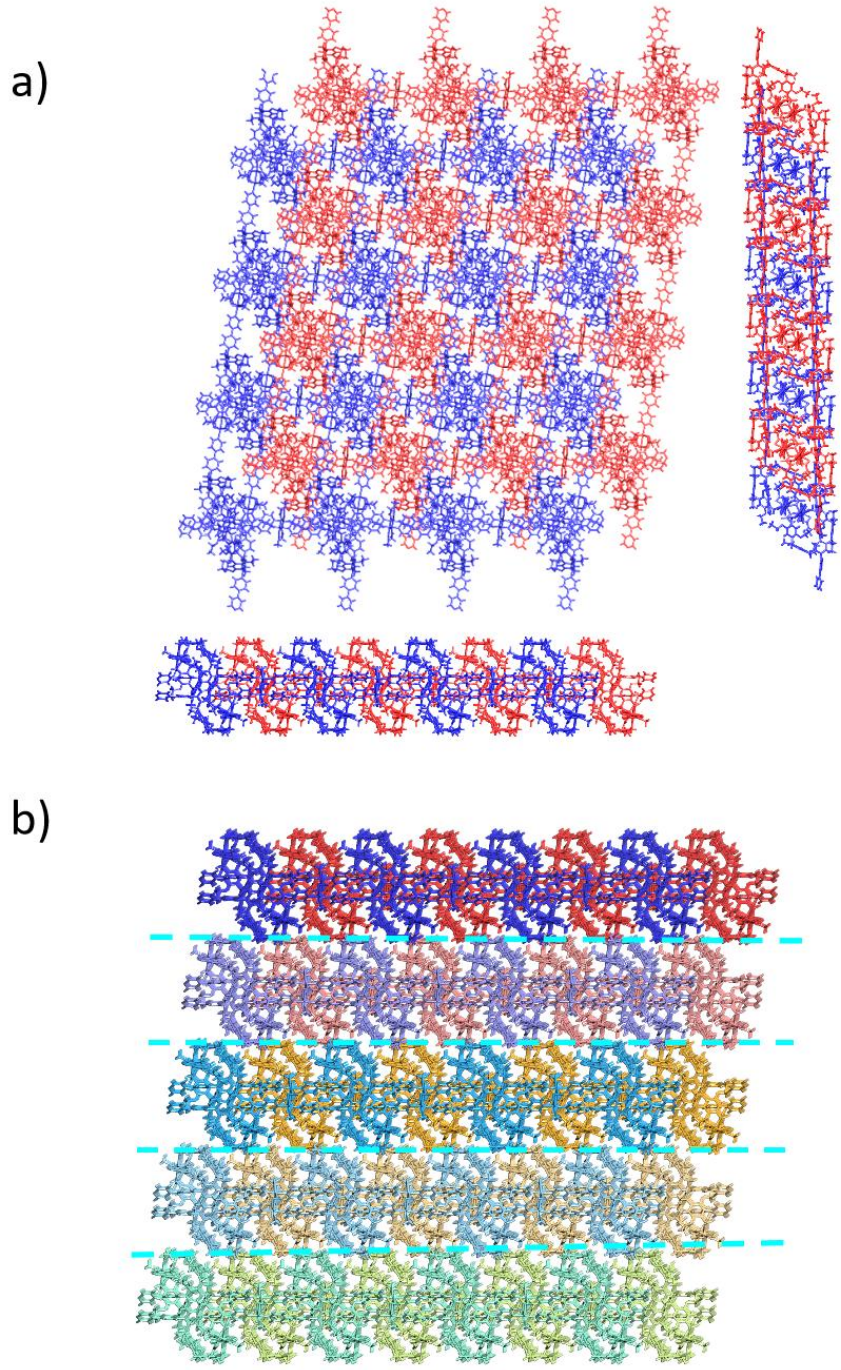

Figure S16. The two-fold interpenetrating structure of **fl-2D-P6MOCN** (a) and layer upon layer form of **fl-2D-P6MOCN** (b).

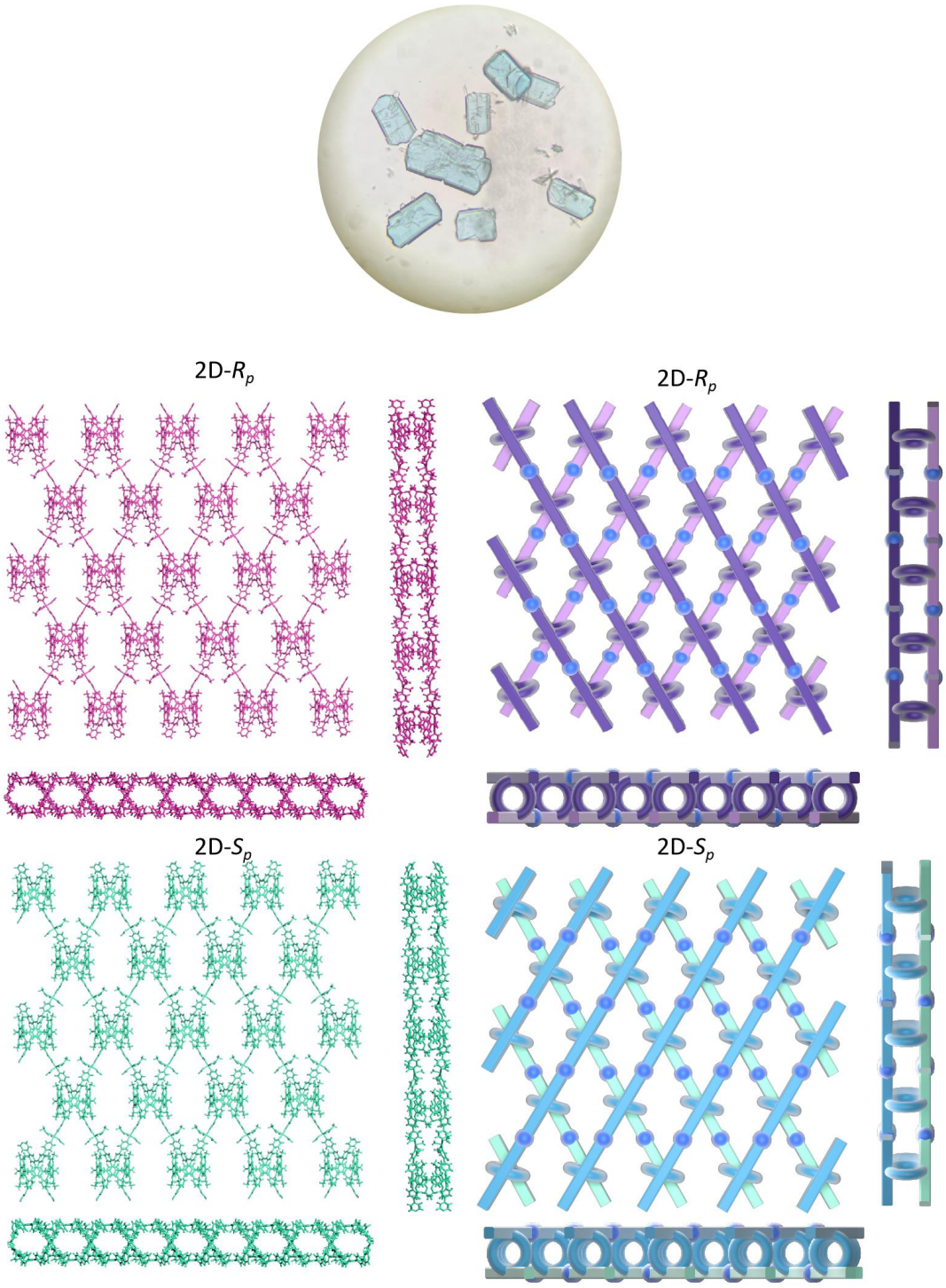

Figure S17. Microscope images of **sbl-2D-P6MOCN** and the top and side carton view of the polymer **sbl-2D-P6MOCN**.

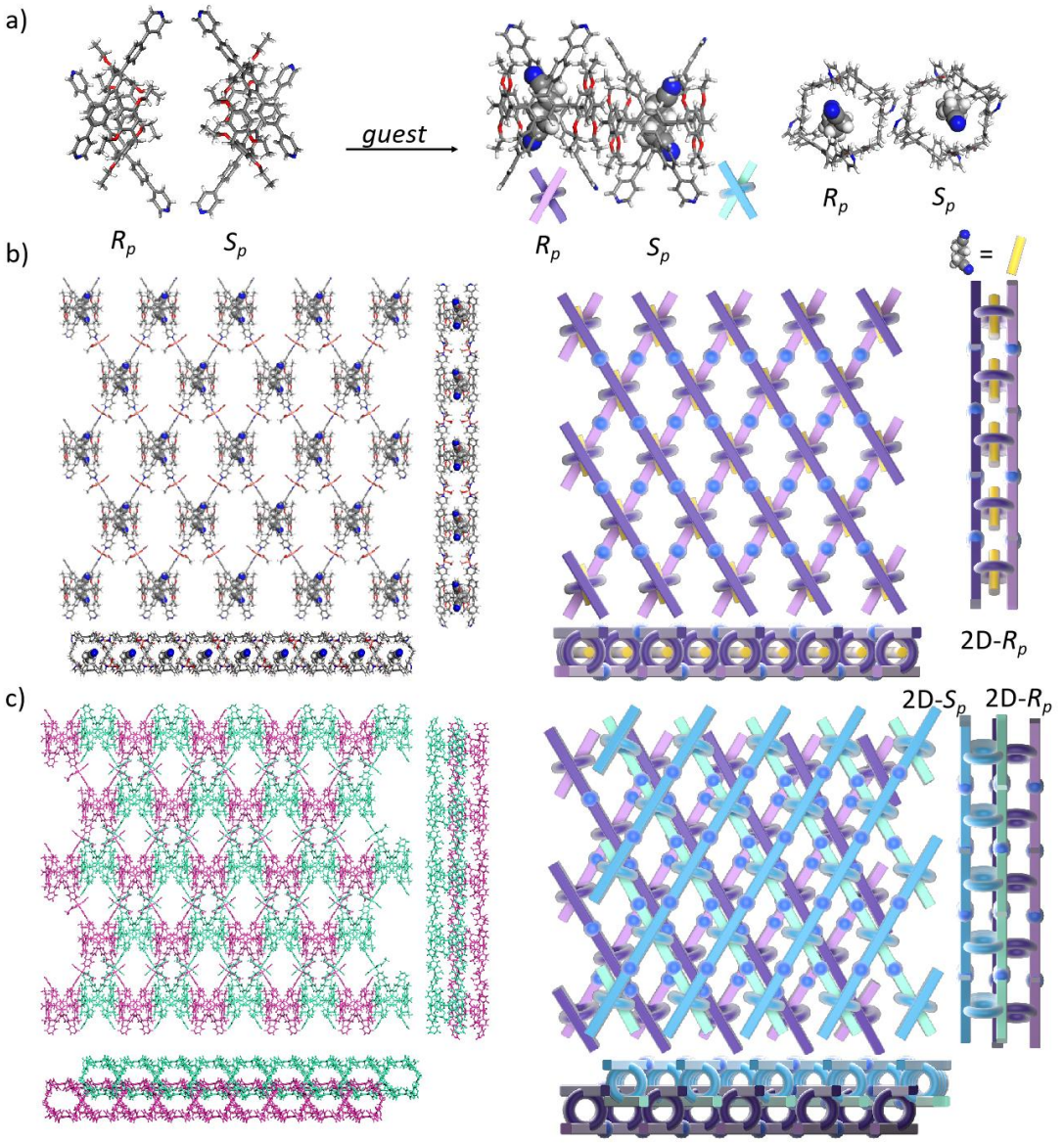

Figure S18. The top and side view of **sbl-2D-P6MOCN** (3 days).

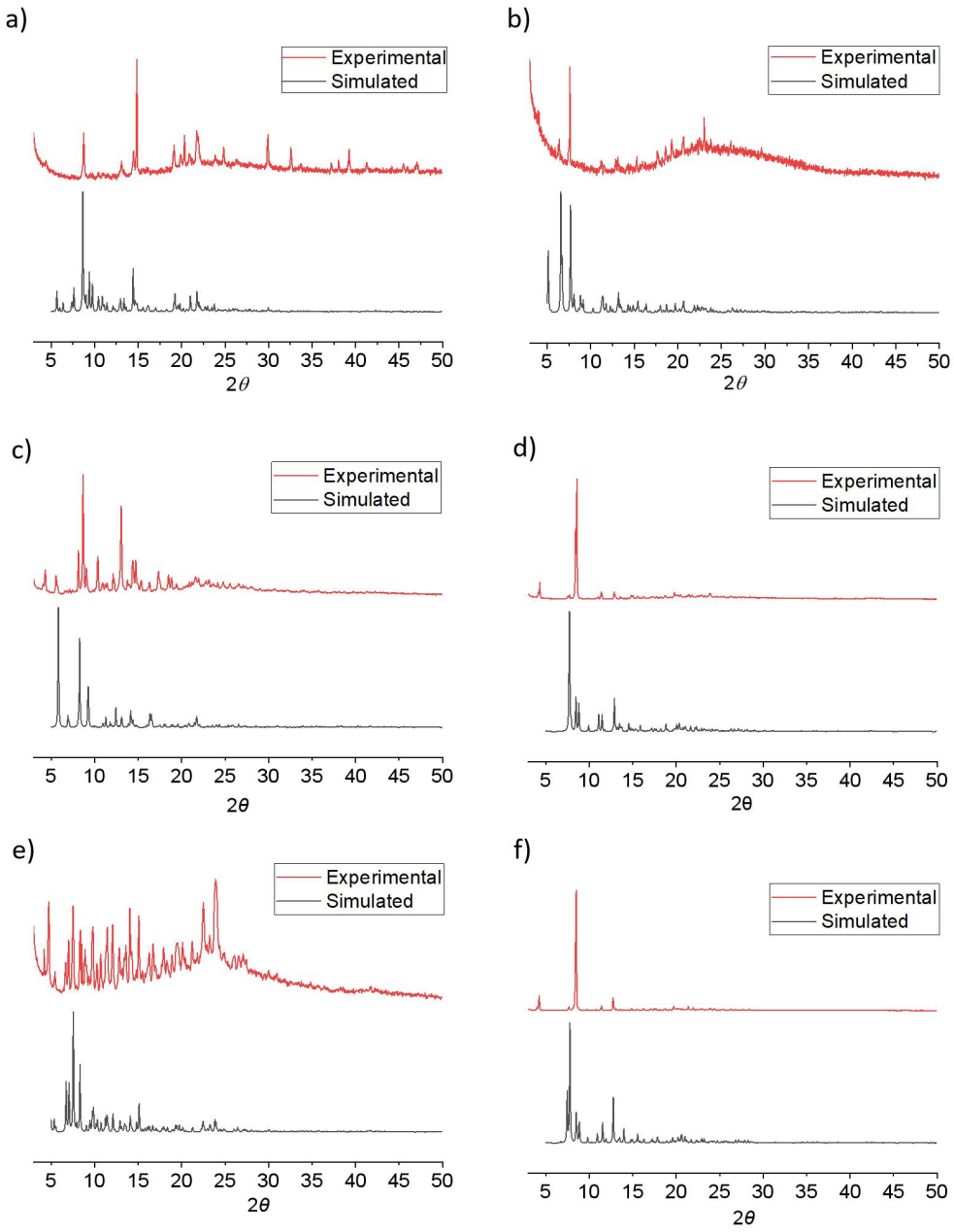

Figure S19. Experimental (red) and simulated (black) PXRD patterns of **ml-2D-P5MOCN** (a), **bl-2D-P5MOCN** (b), **bl-2D-P6MOCN** (c), **sbl-2D-P6MOCN** (d), **fl-2D-P6MOCN** (e) and **mtl-2D-P6MOCN** (f).

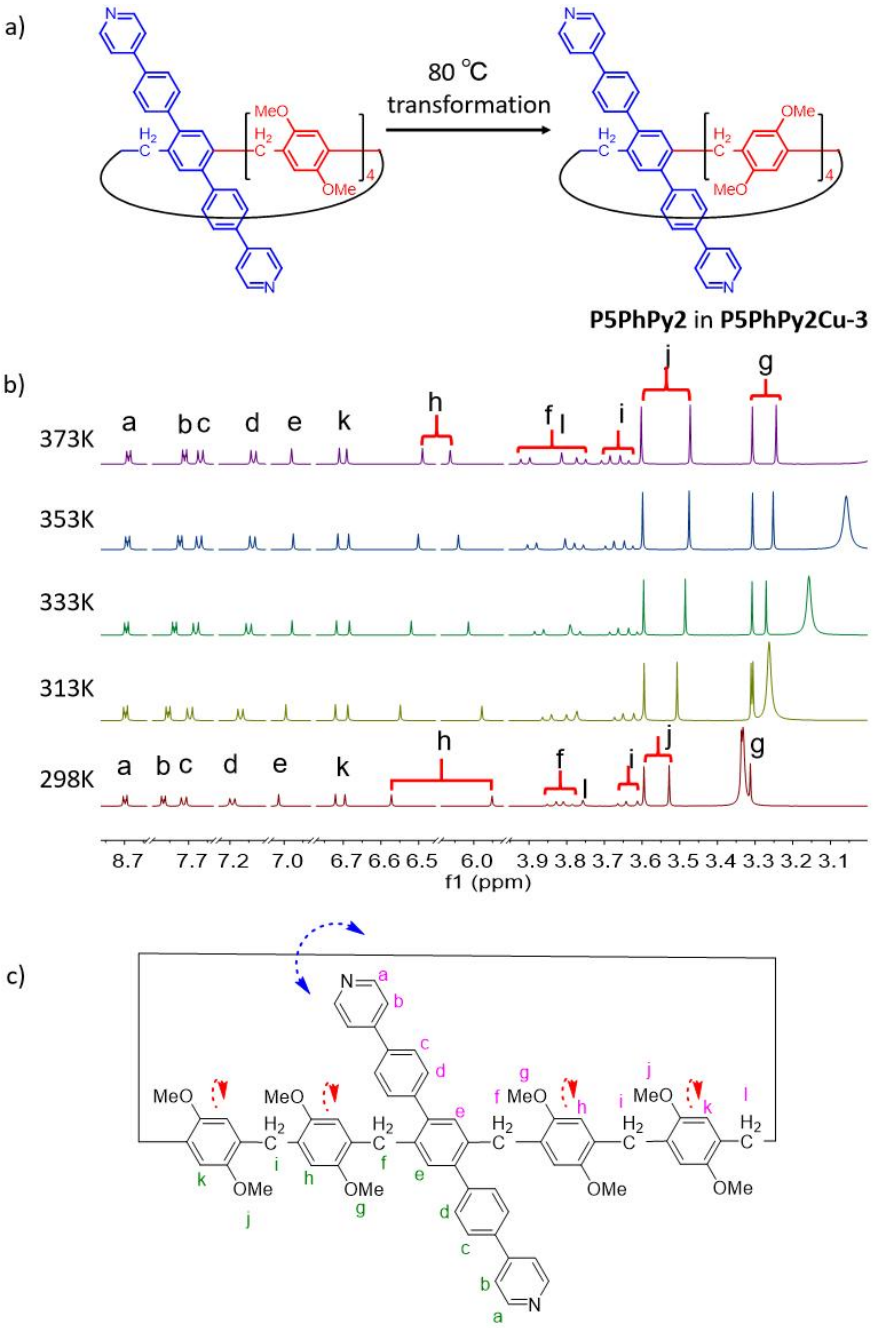

Figure S20. The transformation of **P5PhPy2** in crystal **P5PhPy2Cu-3** (a). The variable-temperature experiment of **P5PhPy2** in DMSO-D6 (600 MHz, from 298K to 373K) and the diagrammatic drawing of **P5PhPy2** (b-c).

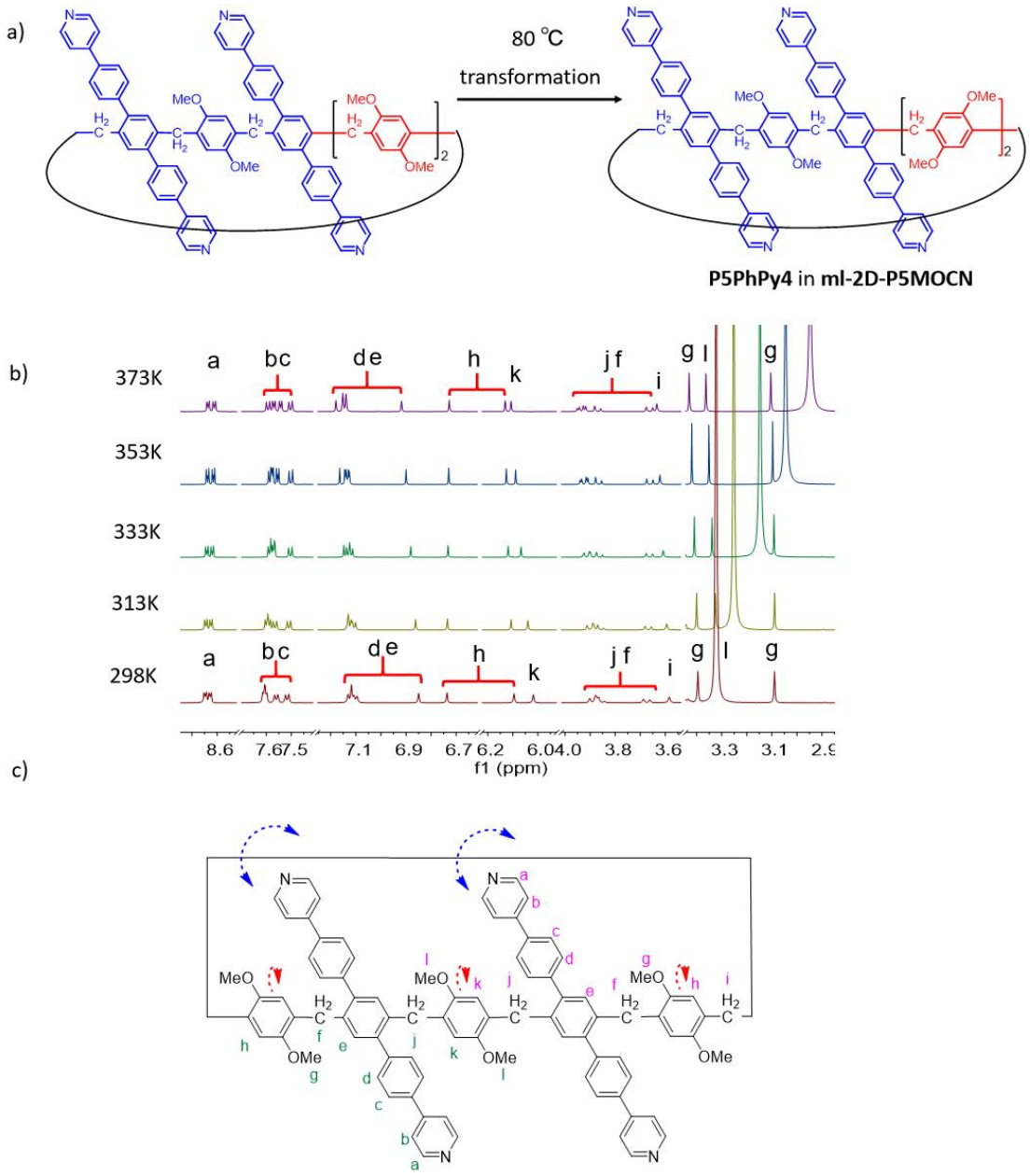

Figure S21. The transformation of **P5PhPy4** in crystal **ml-2D-P5MOCN** (a). The variable-temperature experiment of **P5PhPy4** in DMSO-D6 (600 MHz, from 298K to 373K) and the diagrammatic drawing of **P5PhPy4** (b-c).

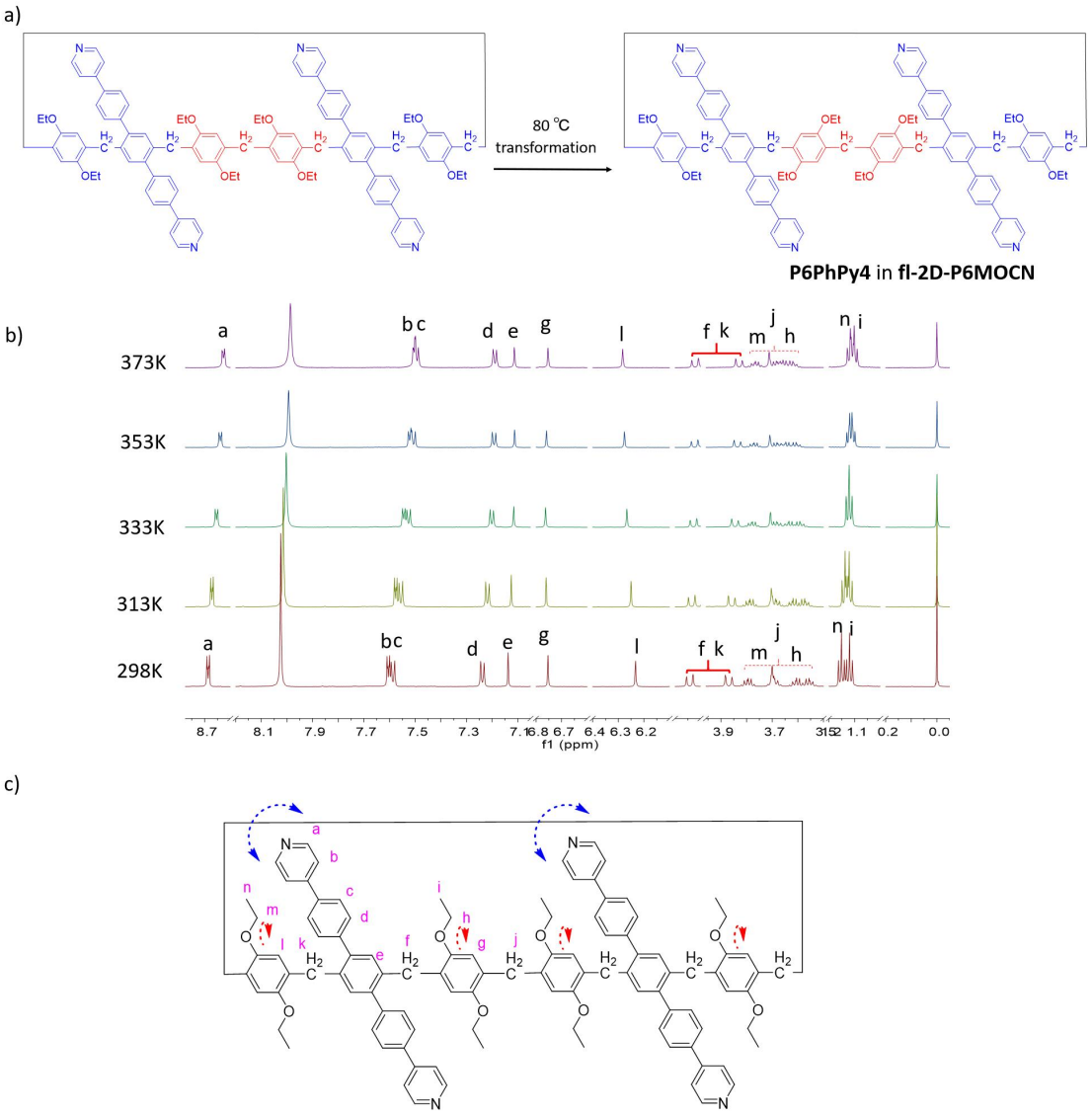

Figure S22. The transformation of **P6PhPy4** in crystal **fl-2D-P6MOCN** (a). The variable-temperature experiment of **P6PhPy4** in DMF-D7 (from 600 MHz, 298K to 373K) and the diagrammatic drawing of **P6PhPy4** (b-c).

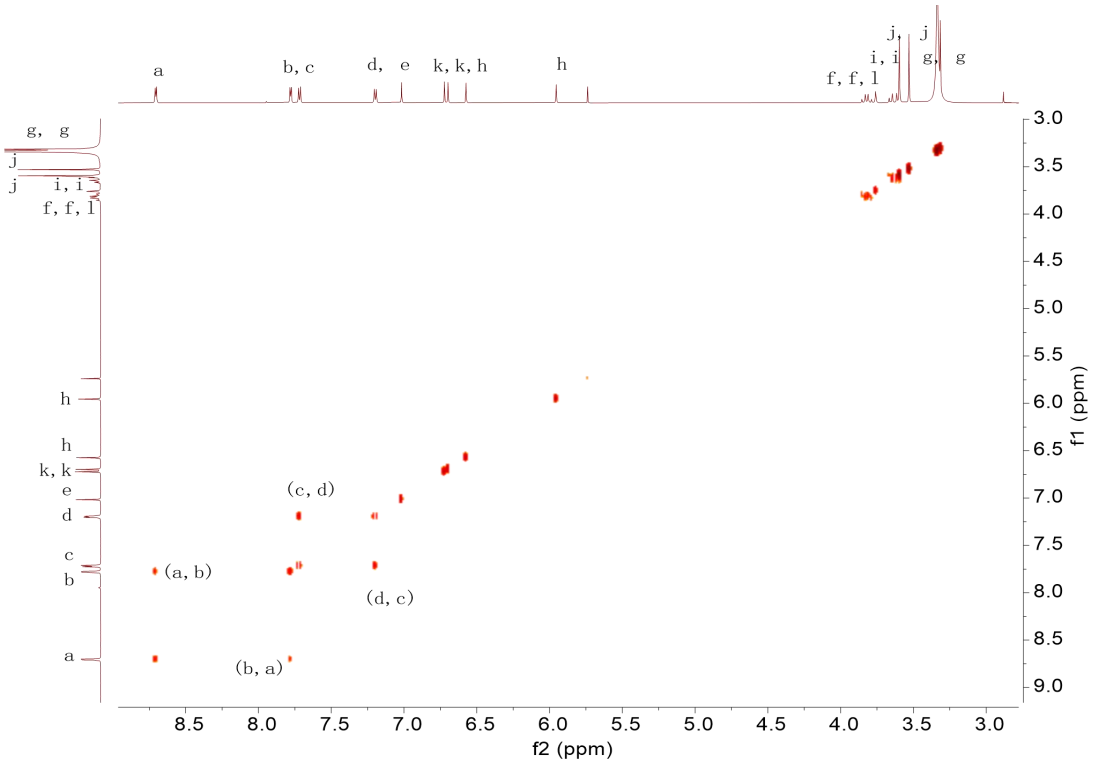

Figure S23. 2D ^{1}H–^{1}H COSY NMR spectrum (600 MHz, DMSO-D6, 298 K) of **P5PhPy2**.

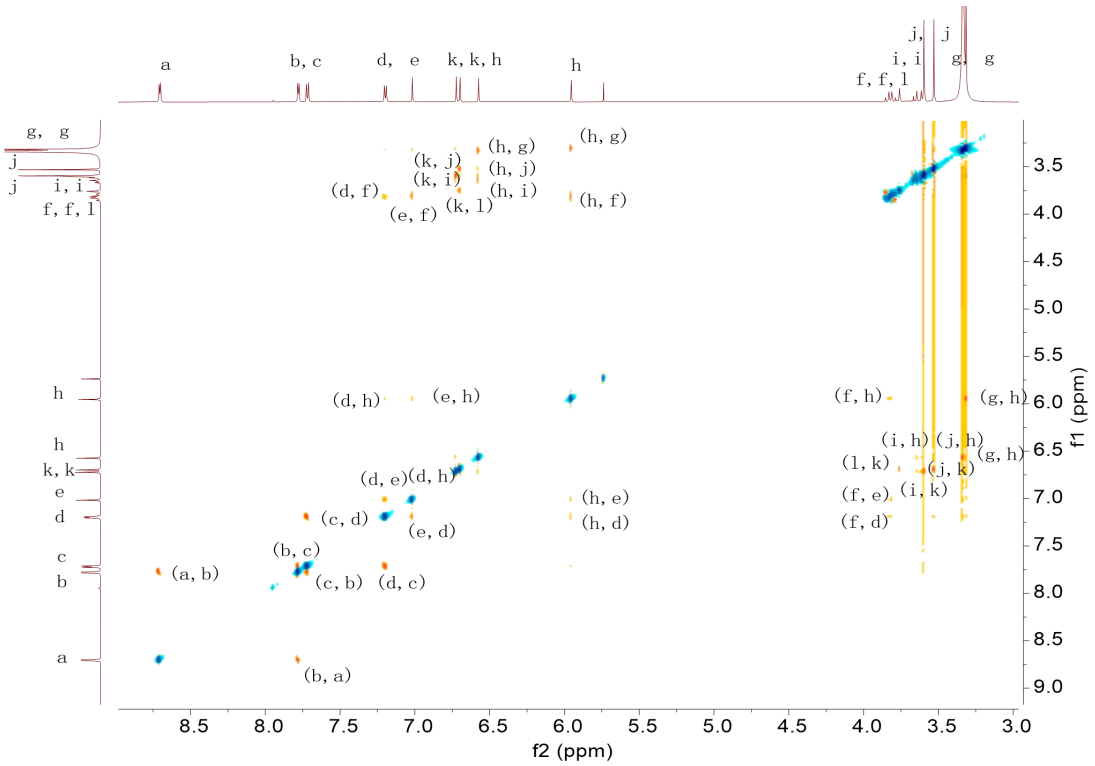

Figure S24. 2D ^{1}H–^{1}H NOESY NMR spectrum (600 MHz, DMSO-D6, 298 K) of **P5PhPy2**.

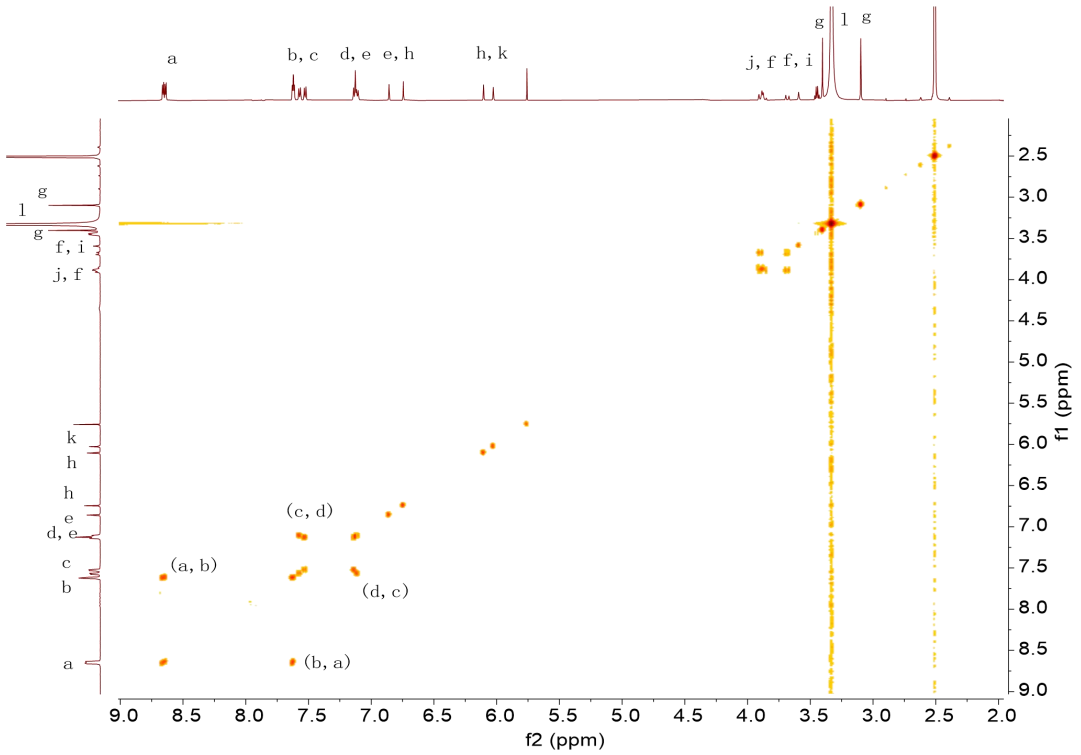

Figure S25. 2D ^{1}H–^{1}H COSY NMR spectrum (600 MHz, DMSO-D6, 298 K) of **P5PhPy4**.

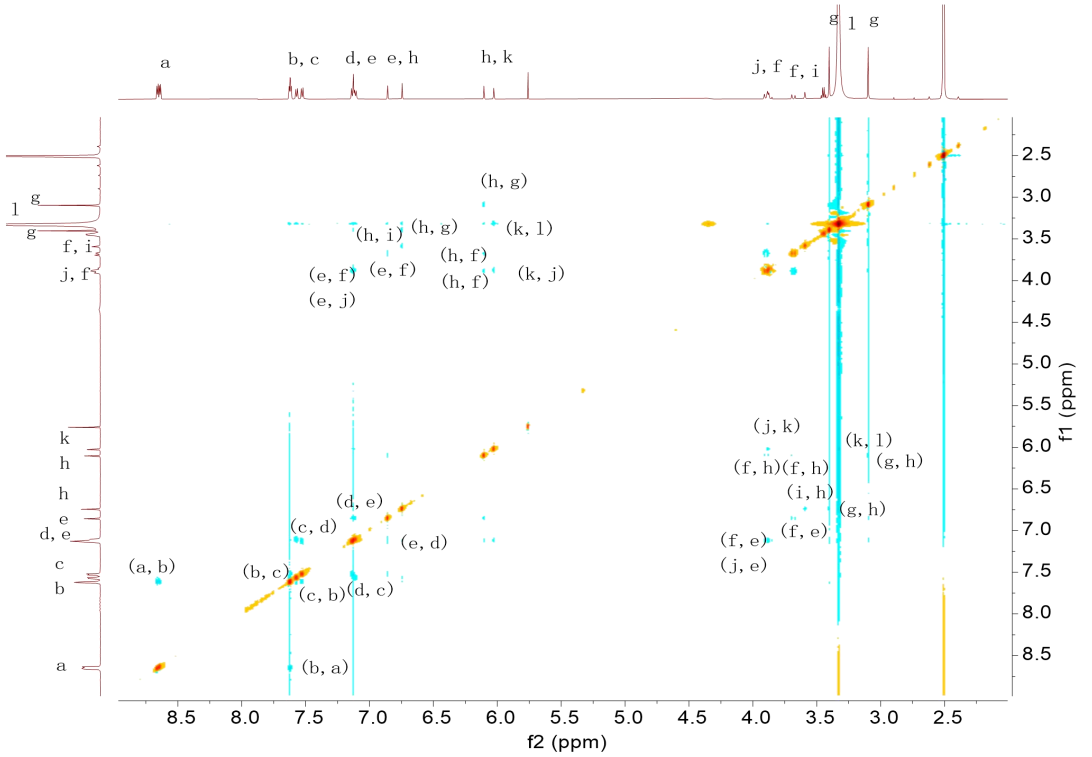

Figure S26. 2D ^{1}H–^{1}H COSY NMR spectrum (600 MHz, DMSO-D6, 298 K) of **P5PhPy4**.

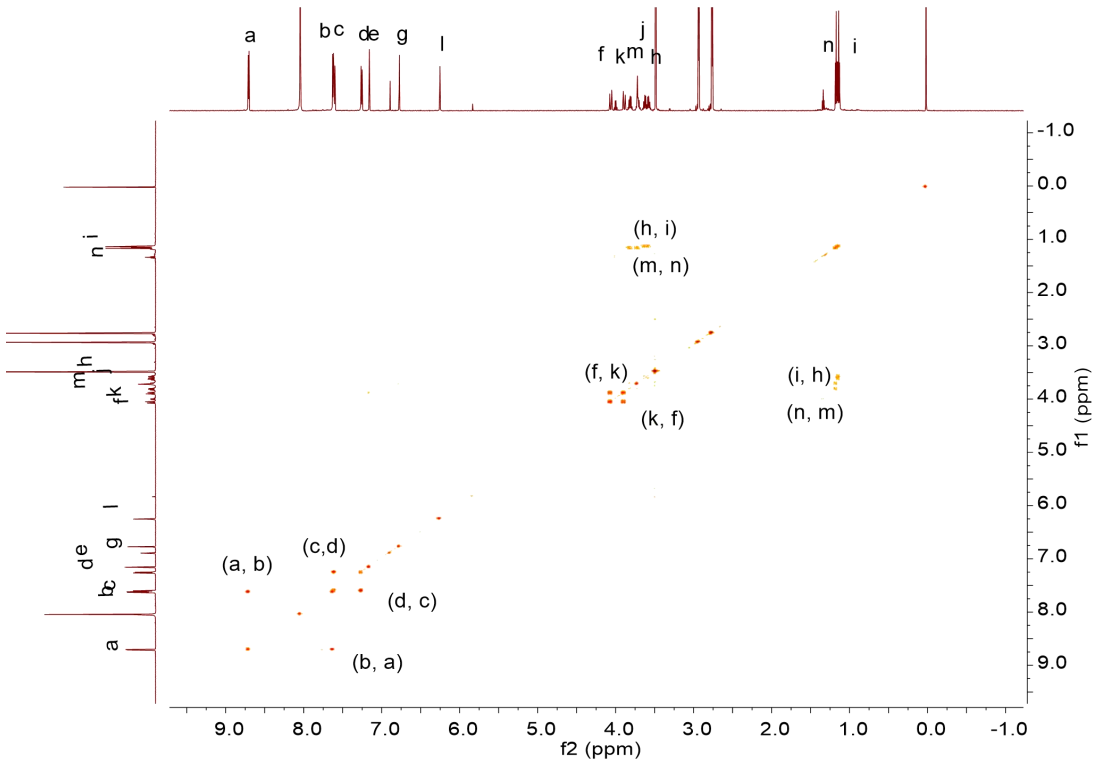

Figure S27. 2D ^{1}H–^{1}H COSY NMR spectrum (600 MHz, DMF-D7, 298 K) of **P6PhPy4**.

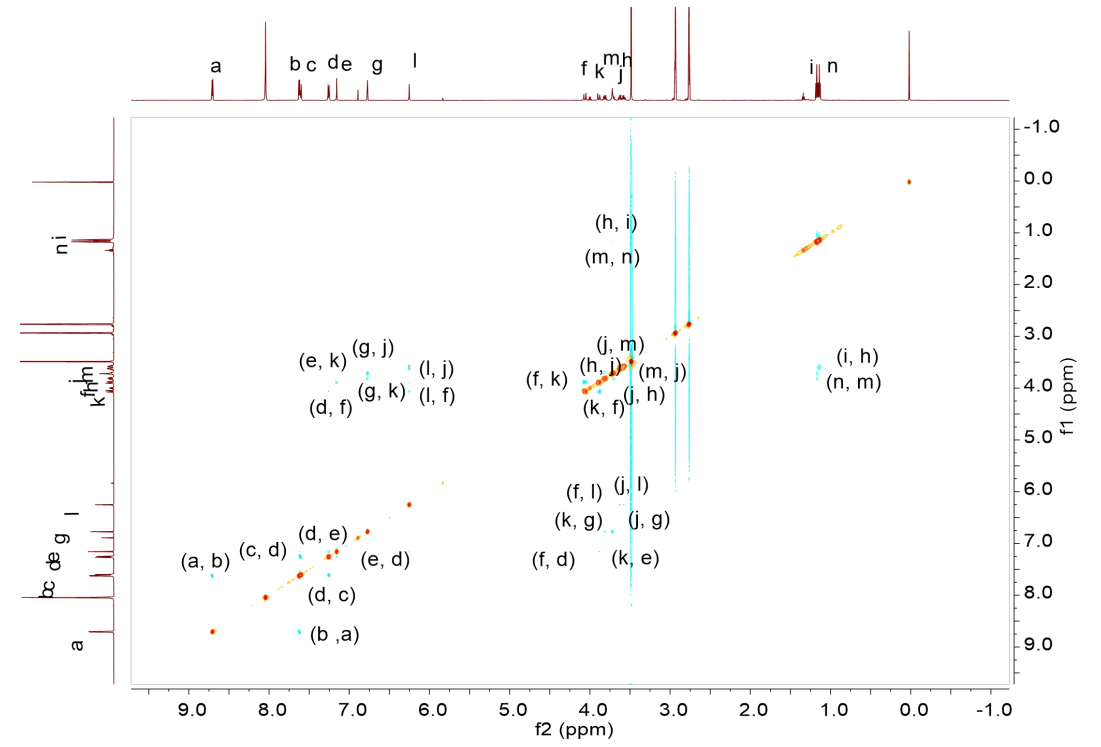

Figure S28. 2D ^{1}H–^{1}H COSY NMR spectrum (600 MHz, DMF-D7, 298 K) of **P6PhPy4**.

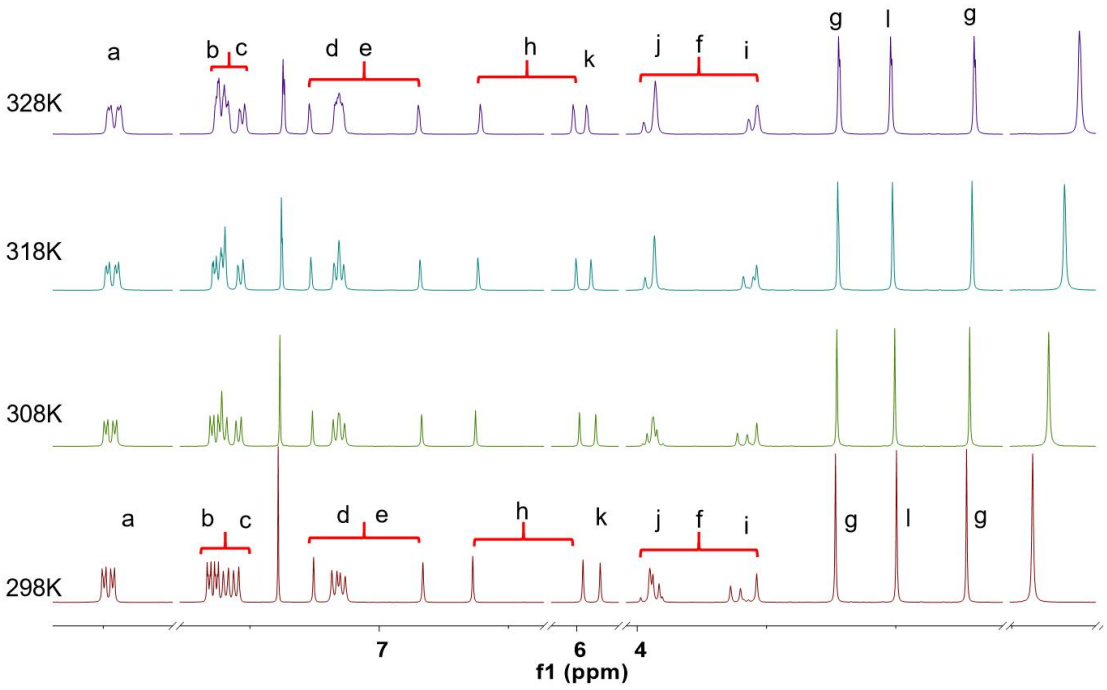

Figure S29. ^{1}H NMR variable-temperature experiments for **P5PhPy4** in $CDCl_3$ (600 MHz 298K to 328K).

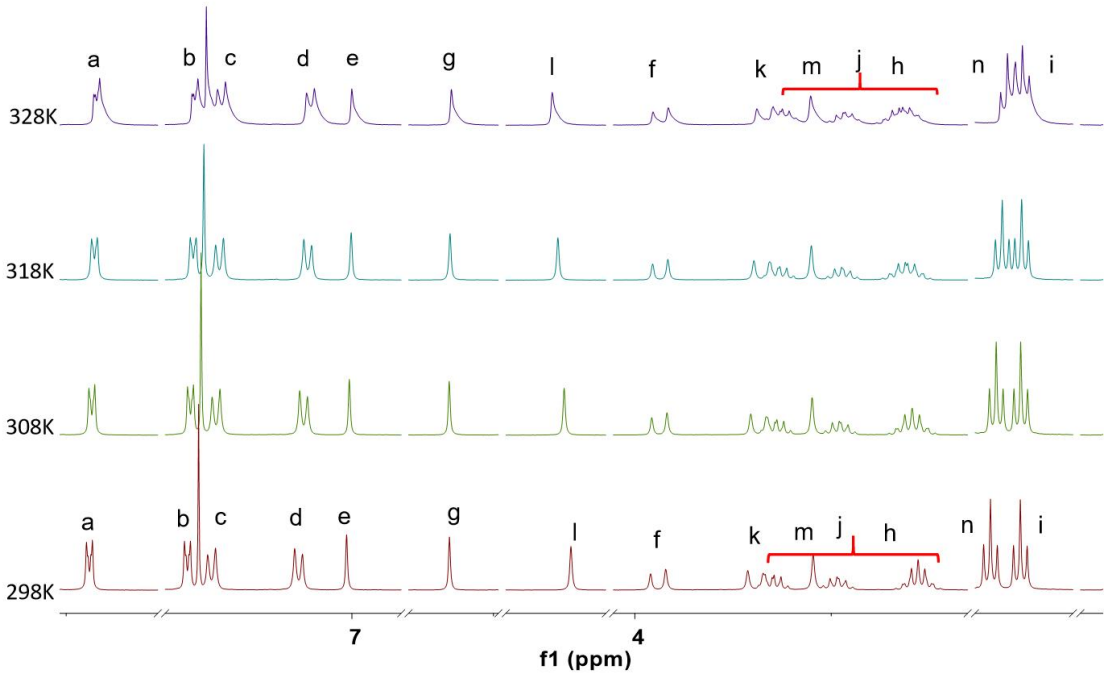

Figure S30. ^{1}H NMR variable-temperature experiments for **P6PhPy4** in $CDCl_3$ (600 MHz 298K to 328K).

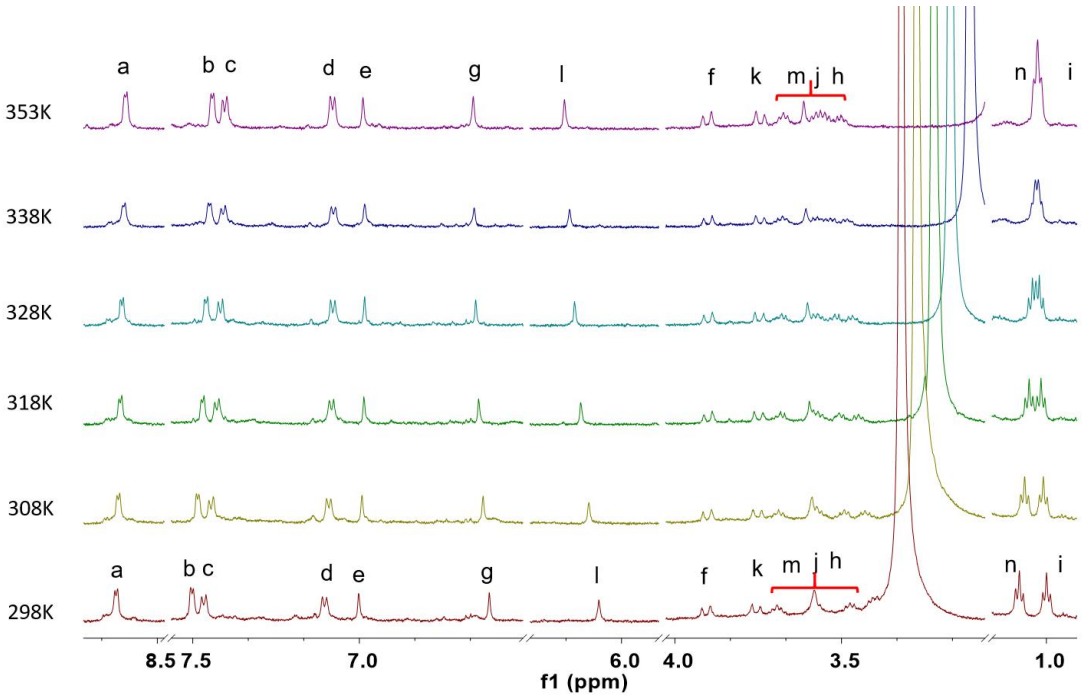

Figure S31. [1]H NMR variable-temperature experiments for **P6PhPy4** in DMSO-d6 (600 MHz 298K to 353K).

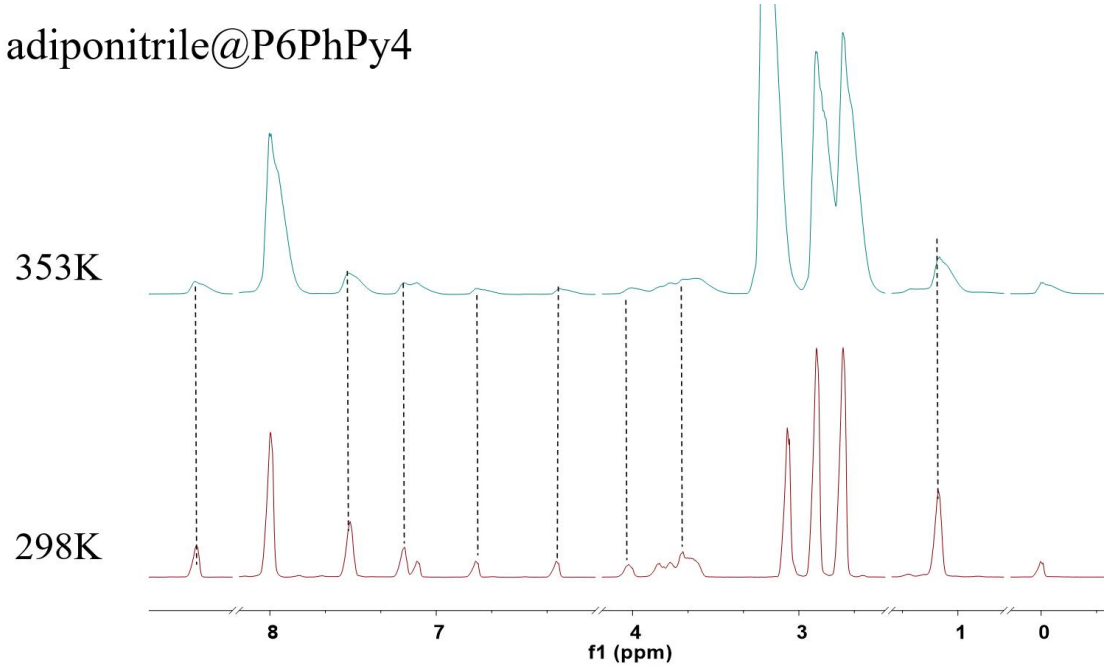

Figure S32. [1]H NMR experiments for adiponitrile@**P6PhPy4** in DMF-d7 (600 MHz) at room temperature and 80 °C.

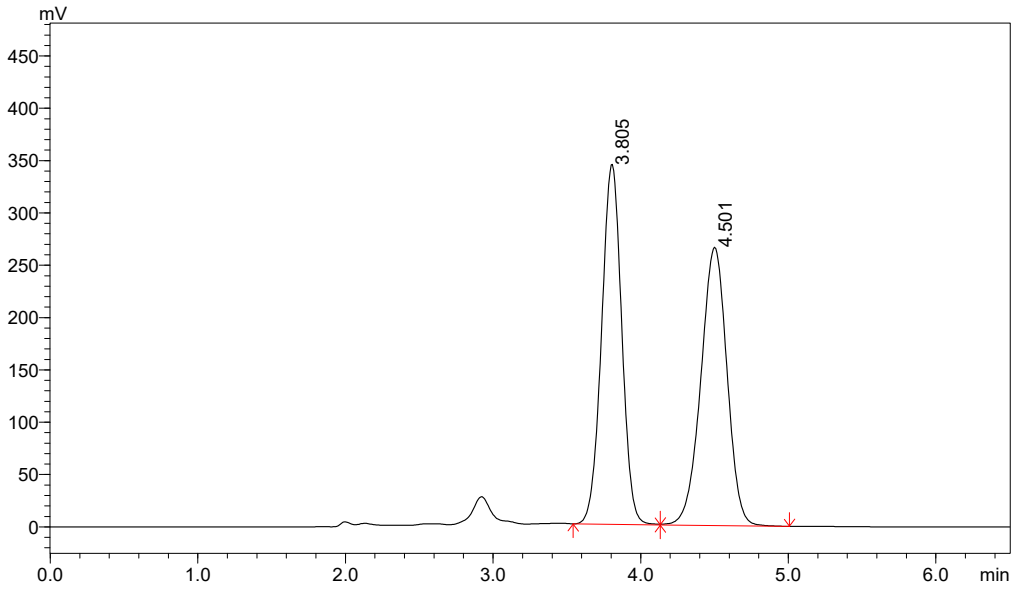

Peak#	Ret. Time	Area	Area%	T.Plate#	Tailing F.	Resolution
1	3.805	3260218	49.902	0.992	3460	43.347
2	4.501	3273010	50.098	0.954	2965	50.599

Figure S33. Resolution of the enantiomers of **P6PhPy4** by chiral HPLC.

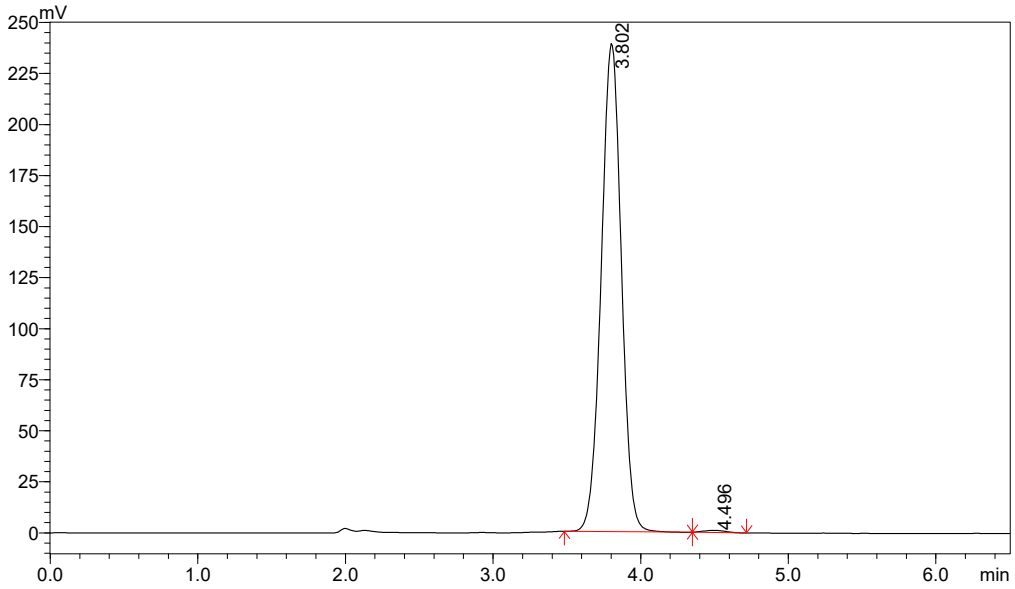

Peak#	Ret. Time	Area	Area%	T.Plate#	Tailing F.	Resolution
1	3.802	2266560	99.544	0.994	3465	43.290
2	4.496	10386	0.456	1.073	4003	37.476

Figure S34. Chromatograms of resolved ***pS*-P6**, confirmed by single crystal analysis.

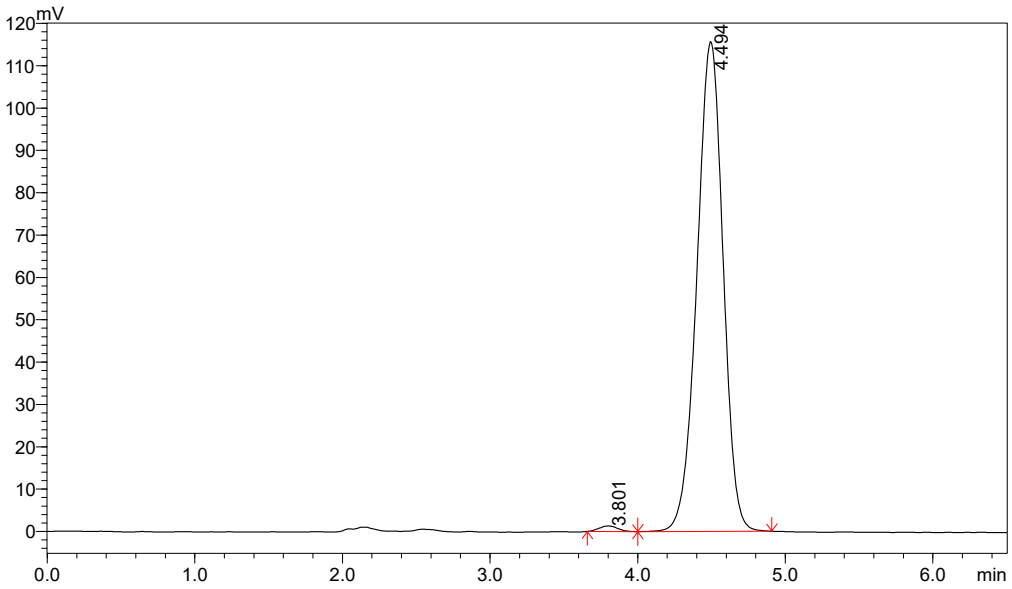

Peak#	Ret. Time	Area	Area%	T.Plate#	Tailing F.	Resolution
1	3.801	11409	0.796	1.043	3888	38.576
2	4.494	1422802	99.204	0.953	2959	50.689

Figure S35. Chromatograms of resolved ***pR*-P6**, confirmed by single crystal analysis.

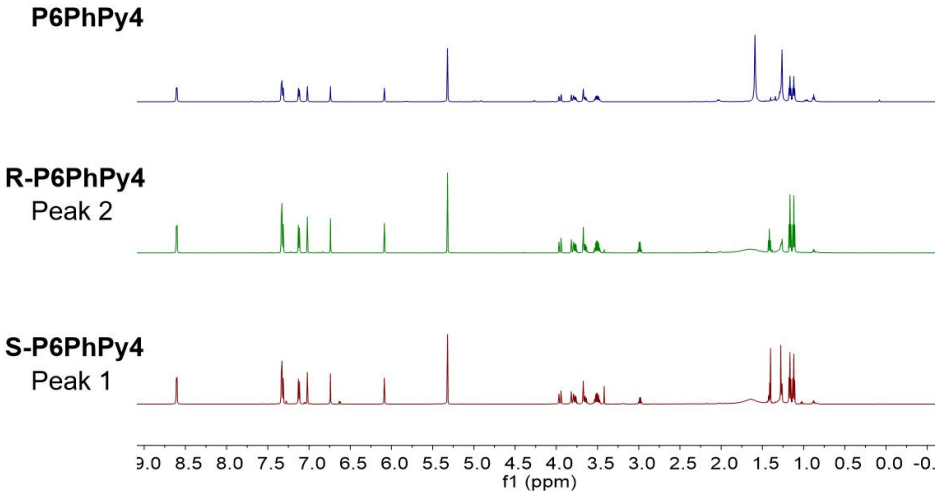

Figure S36. ^{1}H NMR spectrum (600 MHz) of compound **P6PhPy4** (blue line), ***S*-P6PhPy4** (red line) and ***R*-P6PhPy4** (green line) in CD_2Cl_2.

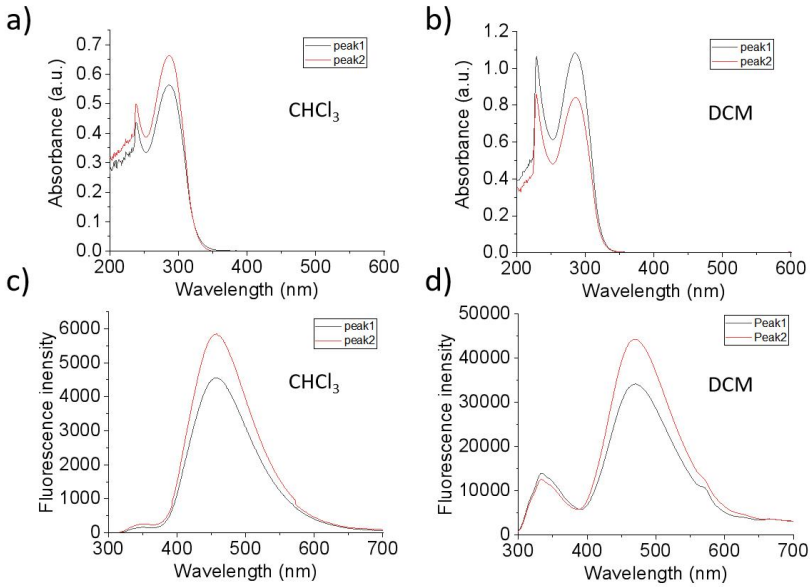

Figure S37. UV-vis spectra of ***S*-P6PhPy4** (black line) and ***R*-P6PhPy4** (red line) in $CHCl_3$ (a) and DCM (b), and fluorescence spectra of ***S*-P6PhPy4** (black line) and ***R*-P6PhPy4** (red line) in $CHCl_3$ (c) and DCM (d).

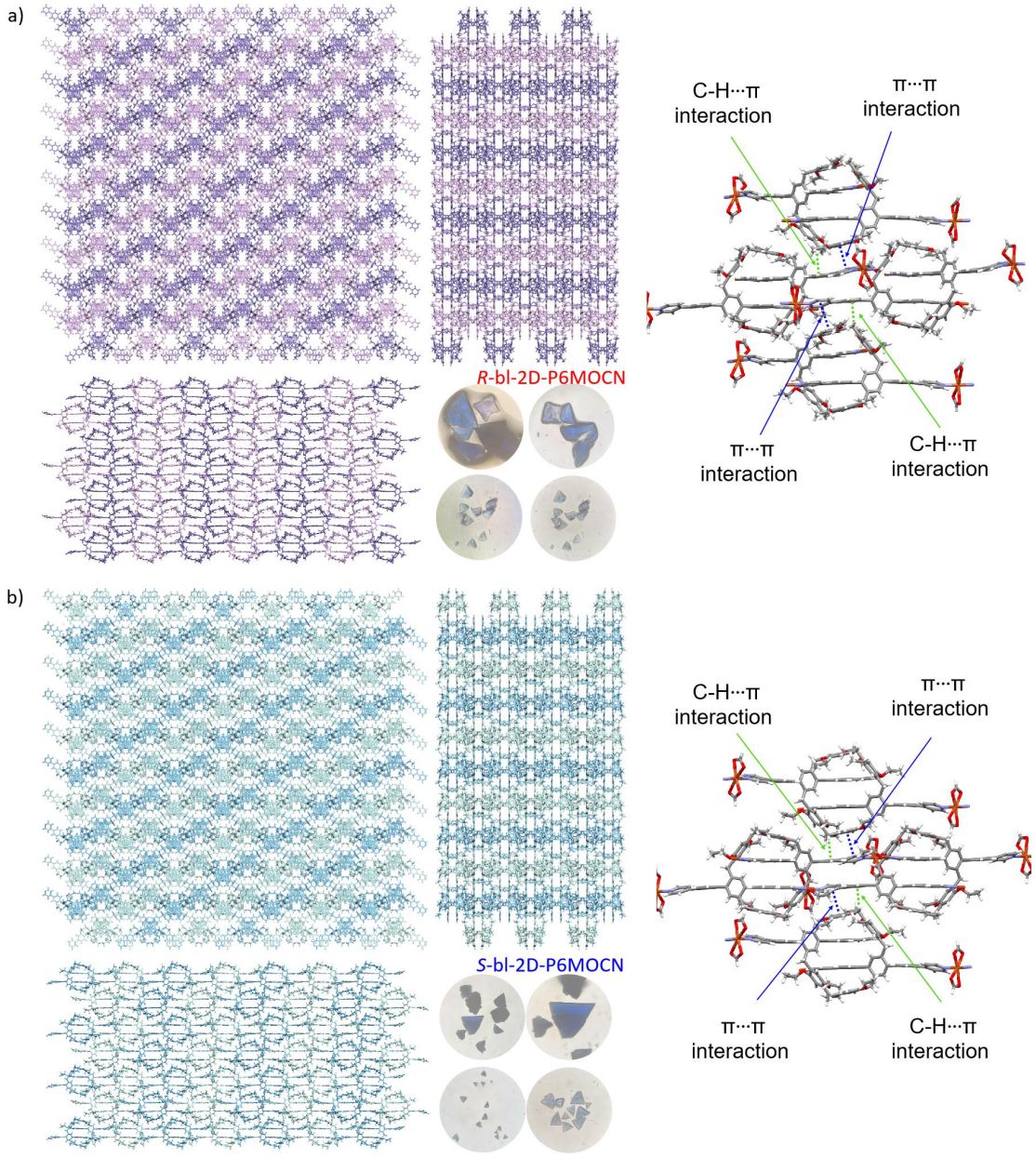

Figure S38. Microscope images of ***R*-bl-2D-P6MOCN** and the top and side view of the crystal structure ***R*-bl-2D-P6MOCN** (a) and microscope images of ***S*-bl-2D-P6MOCN** and the top and side view of the crystal structure ***S*-bl-2D-P6MOCN** (b) .

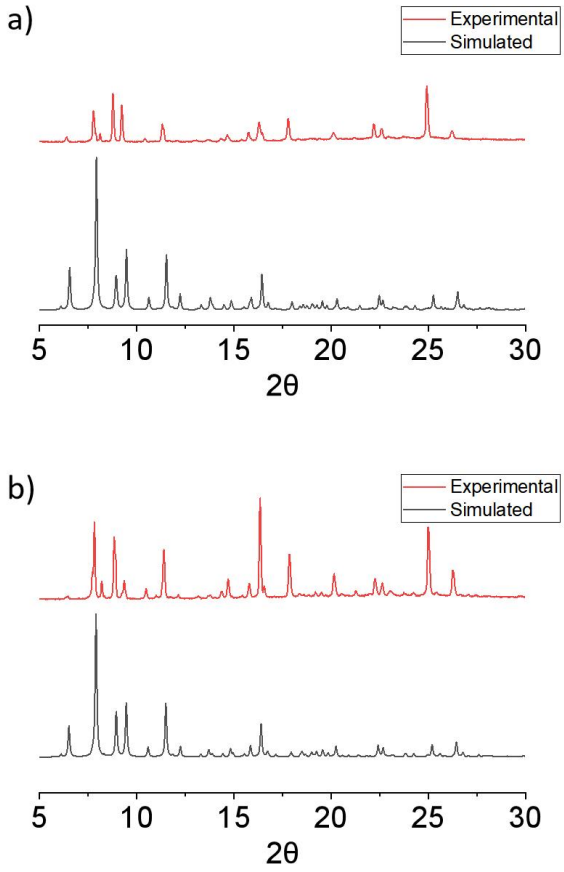

Figure S39. Experimental (red) and simulated (black) PXRD patterns of ***S*-bl-2D-P6MOCN** (a) and ***R*-bl-2D-P6MOCN** (b).

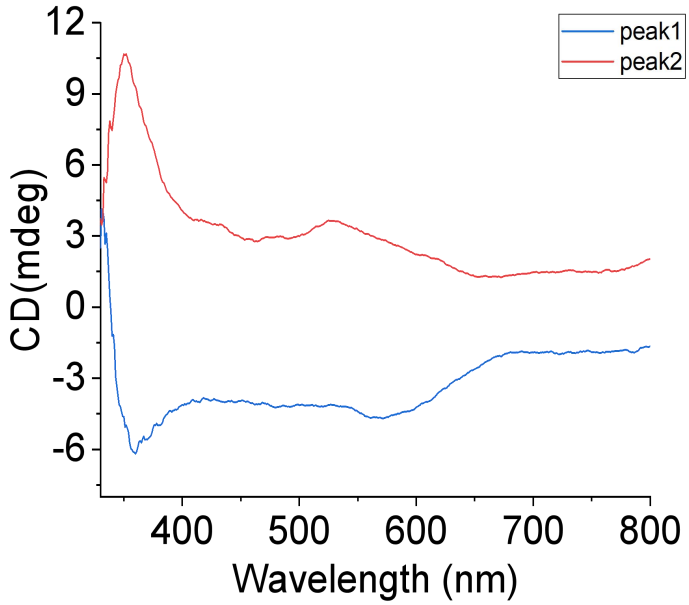

Figure S40. CD spectra of ***S*-bl-2D-P6MOCN** (blue line) and ***R*-bl-2D-P6MOCN** (red line) in solid state.

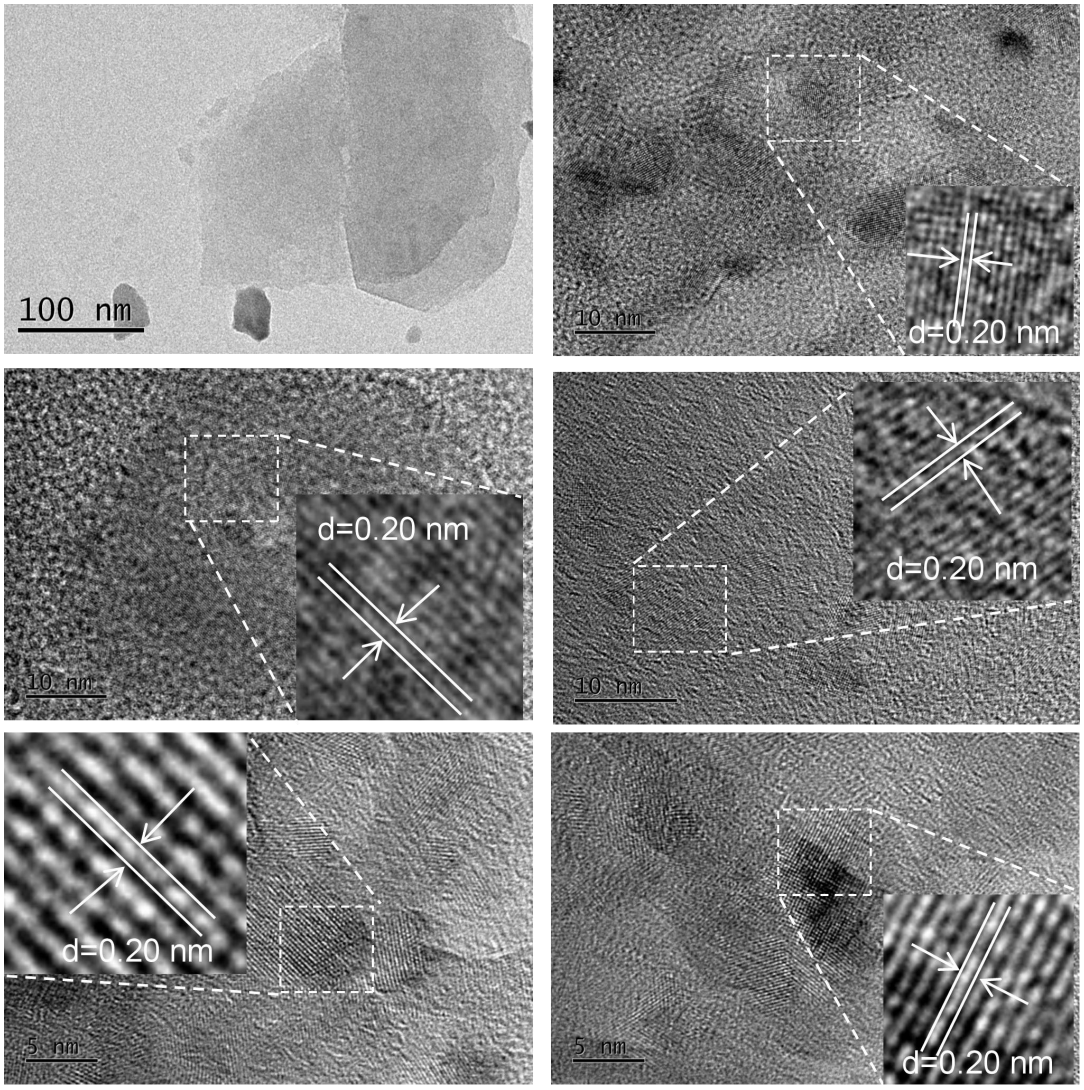

Figure S41. TEM images of **ml-2D-P5MOCN**.

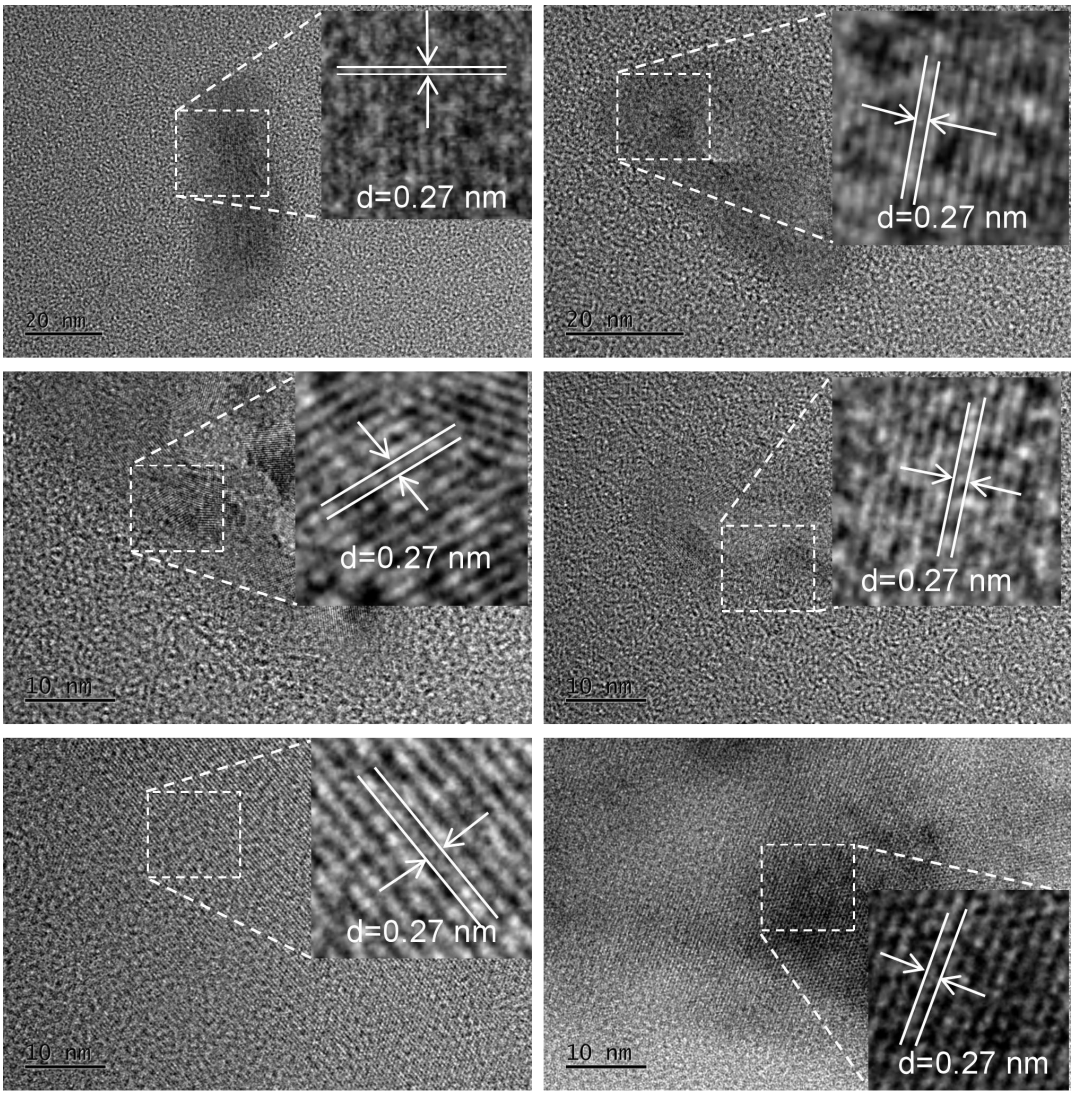

Figure S42. TEM images of **bl-2D-P5MOCN**.

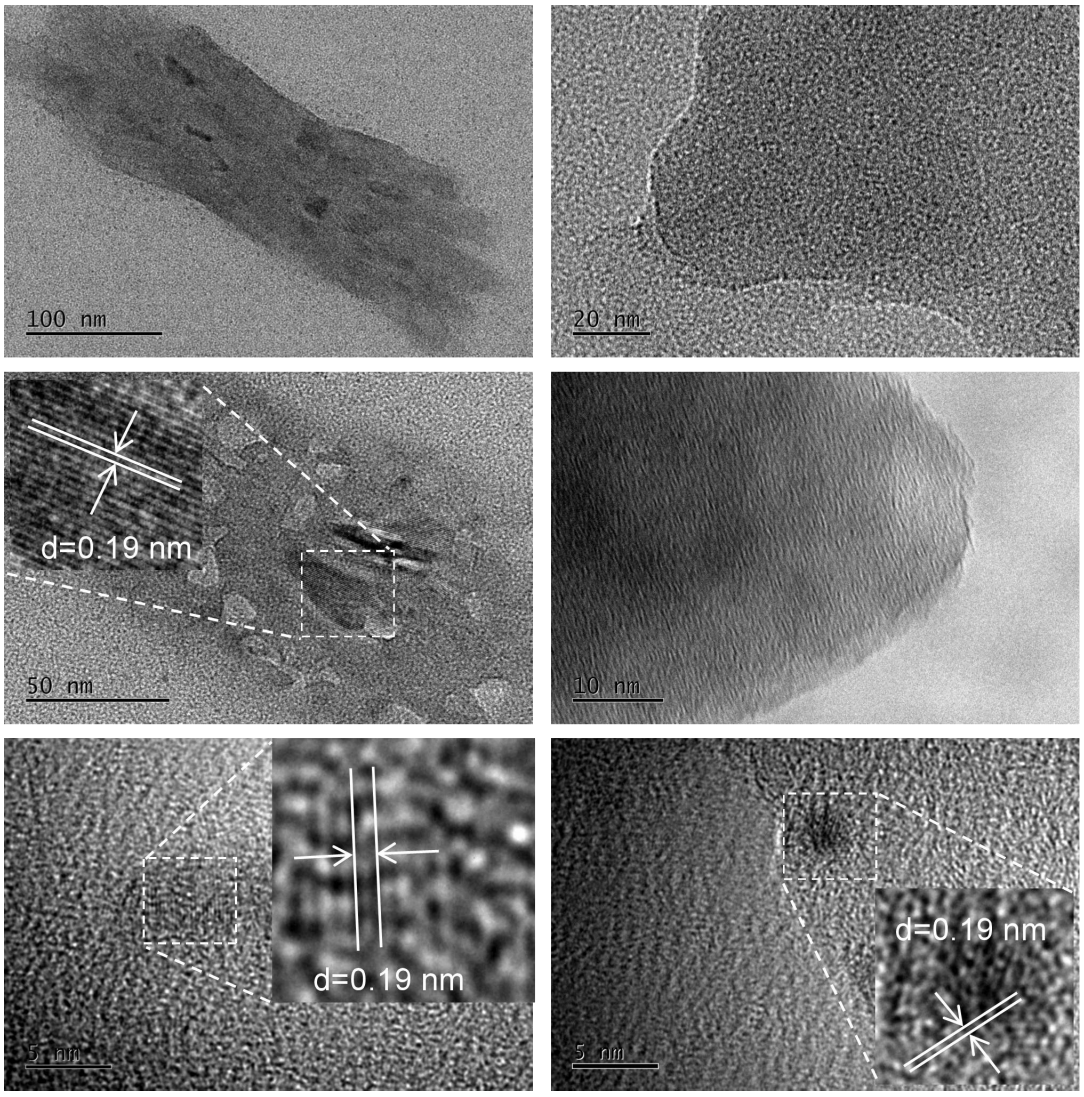

Figure S43. TEM images of **bl-2D-P6MOCN**.

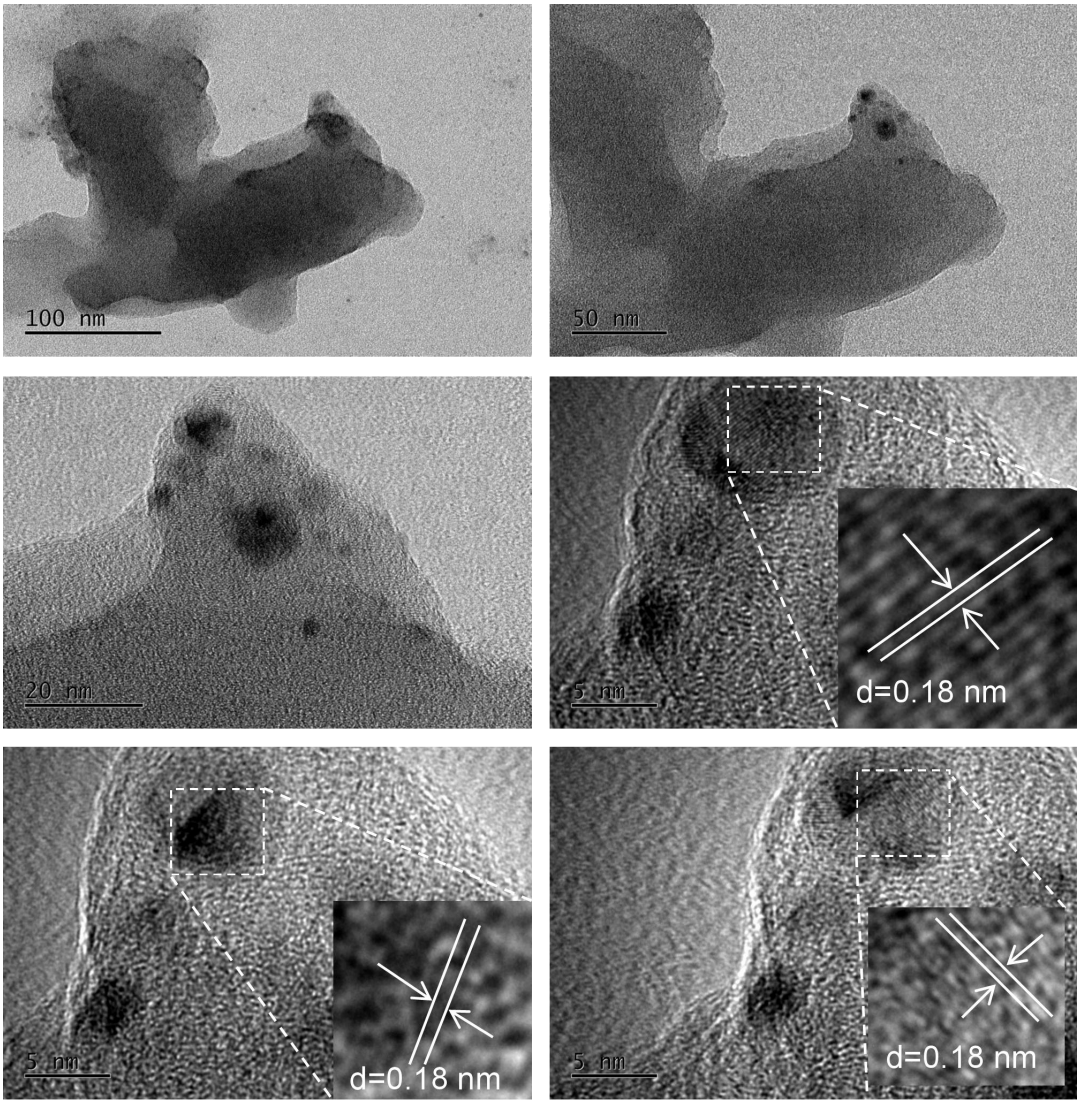

Figure S44. TEM images of **sbl-2D-P6MOCN**.

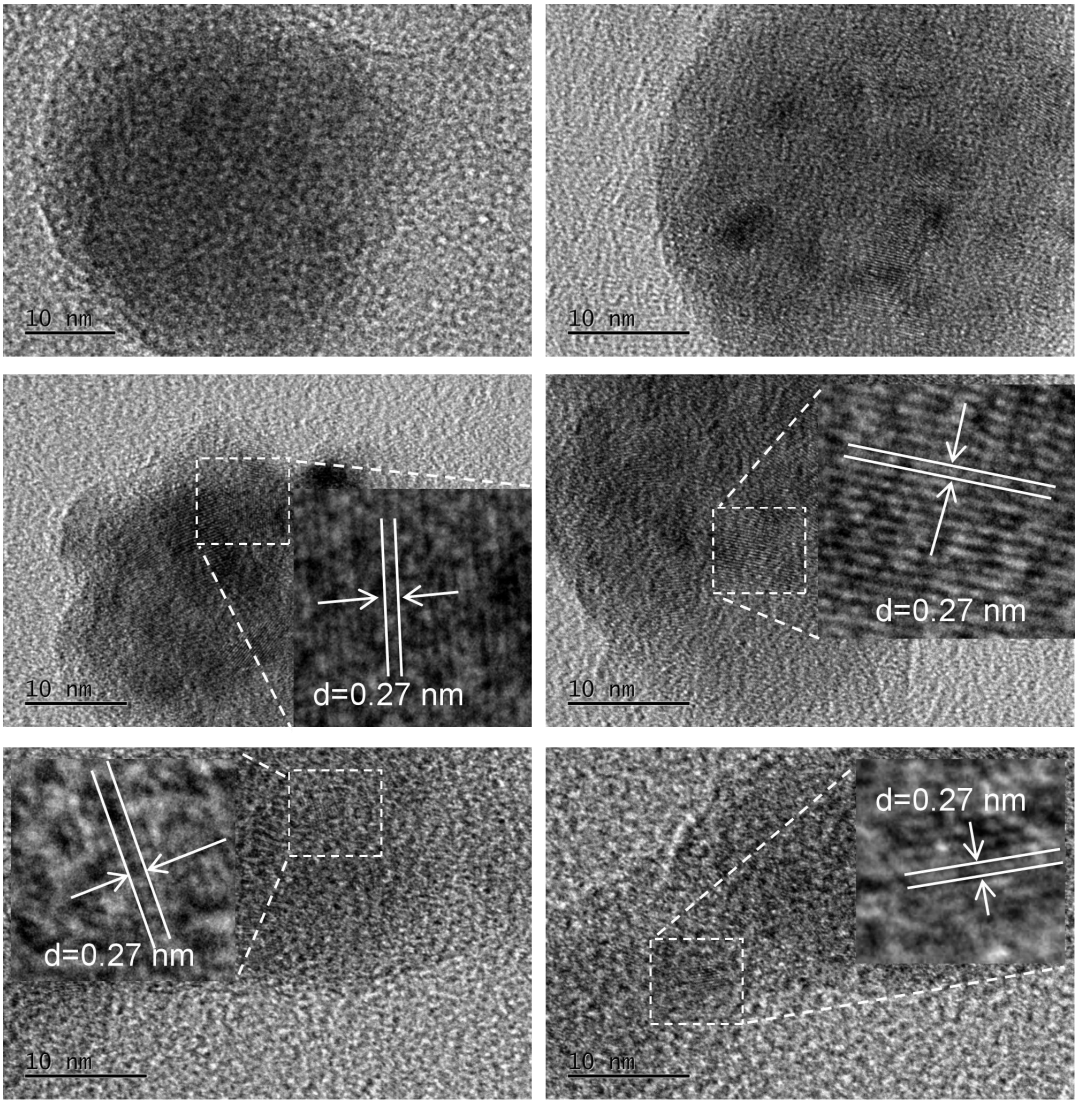

Figure S45. TEM images of **fl-2D-P6MOCN**.

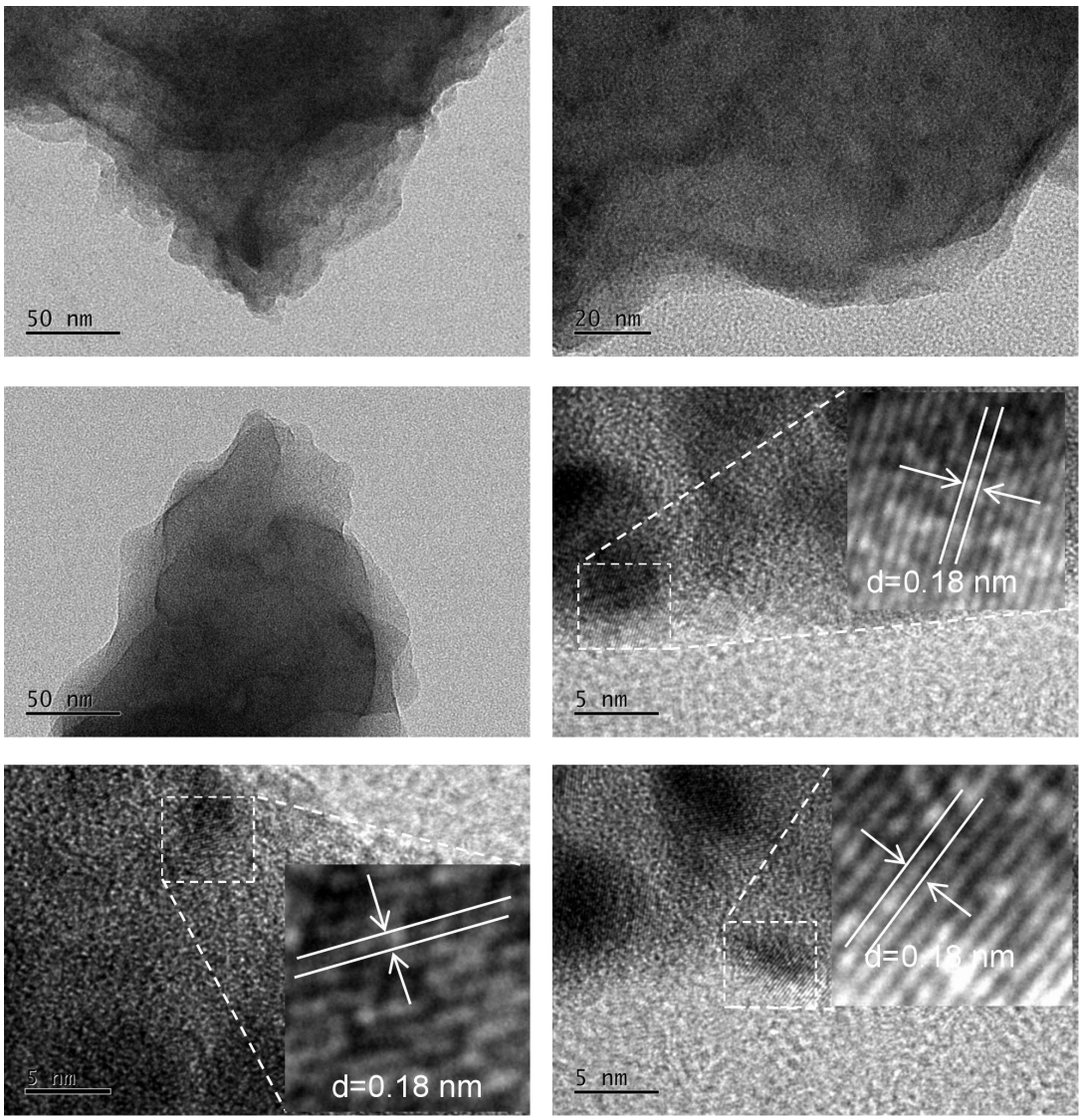

Figure S46. TEM images of **mtl-2D-P6MOCN**.

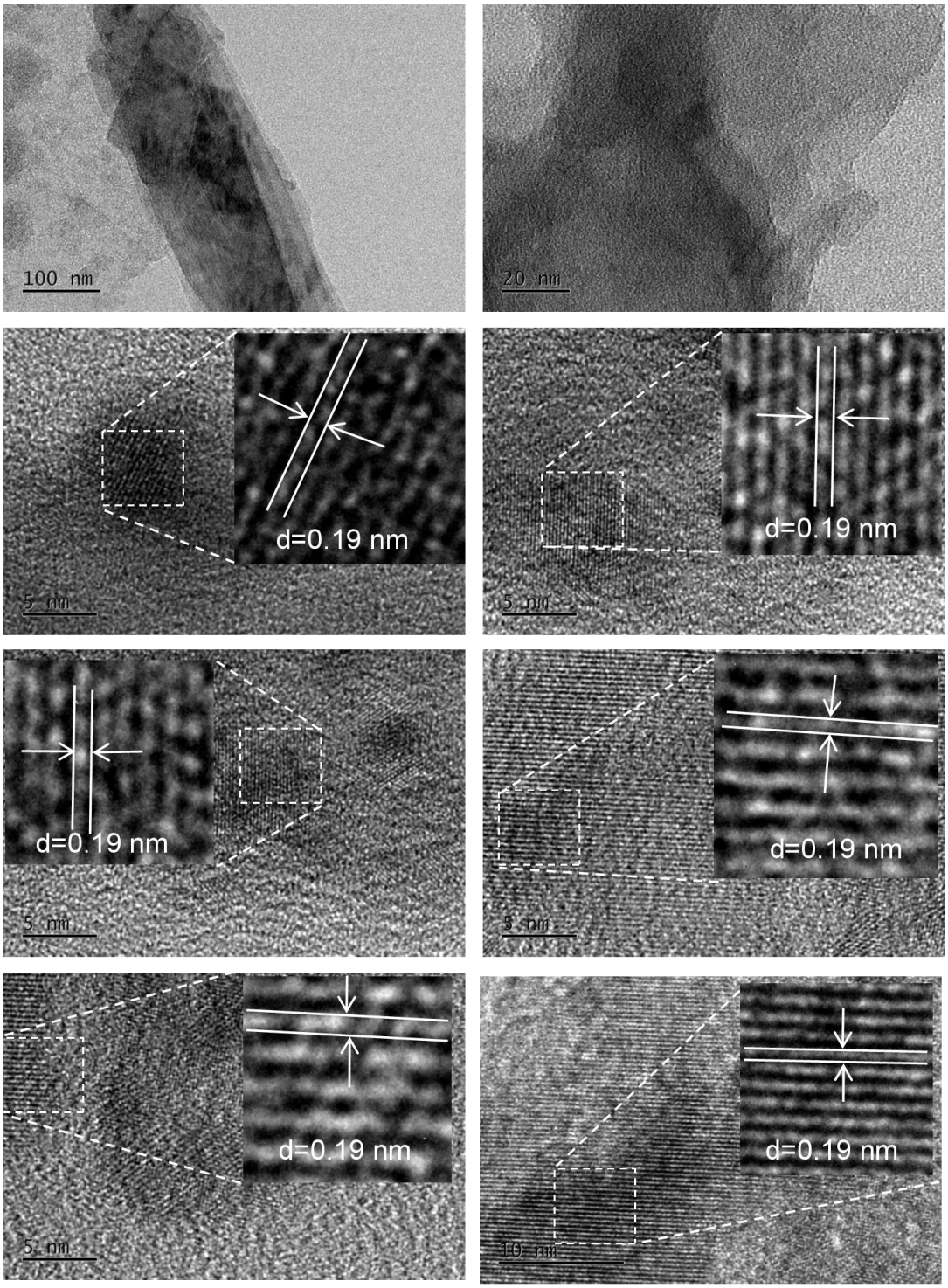

Figure S47. TEM images of **R-bl-2D-P6MOCN**.

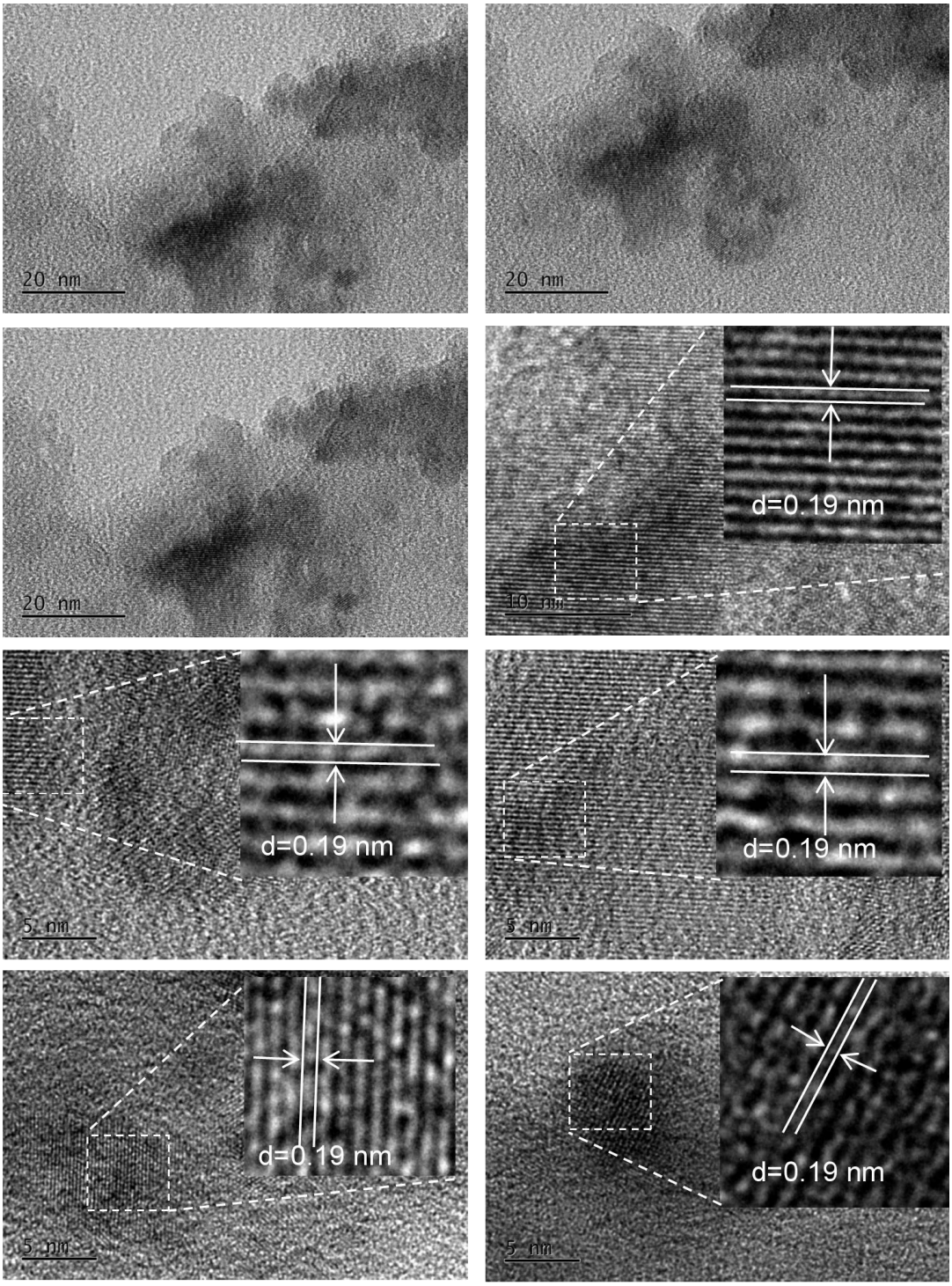

Figure S48. TEM images of **S-bl-2D-P6MOCN**.

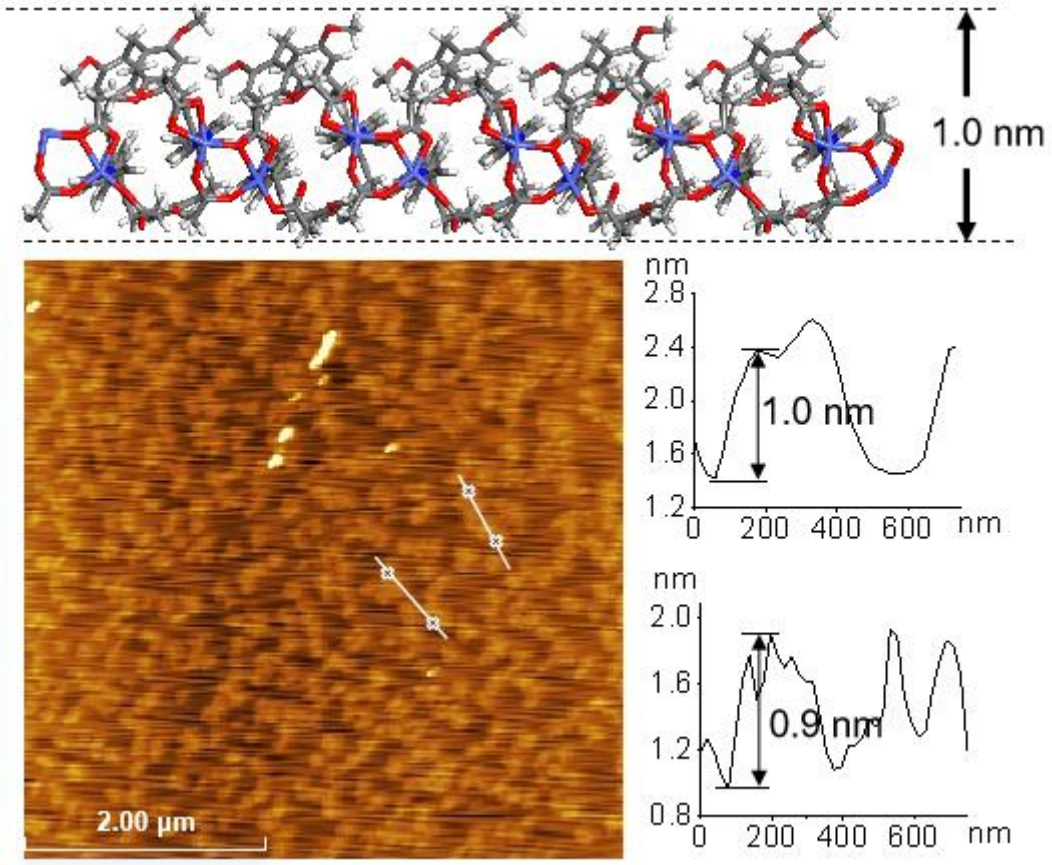

Figure S49. AFM images of **ml-2D-P5MOCN**.

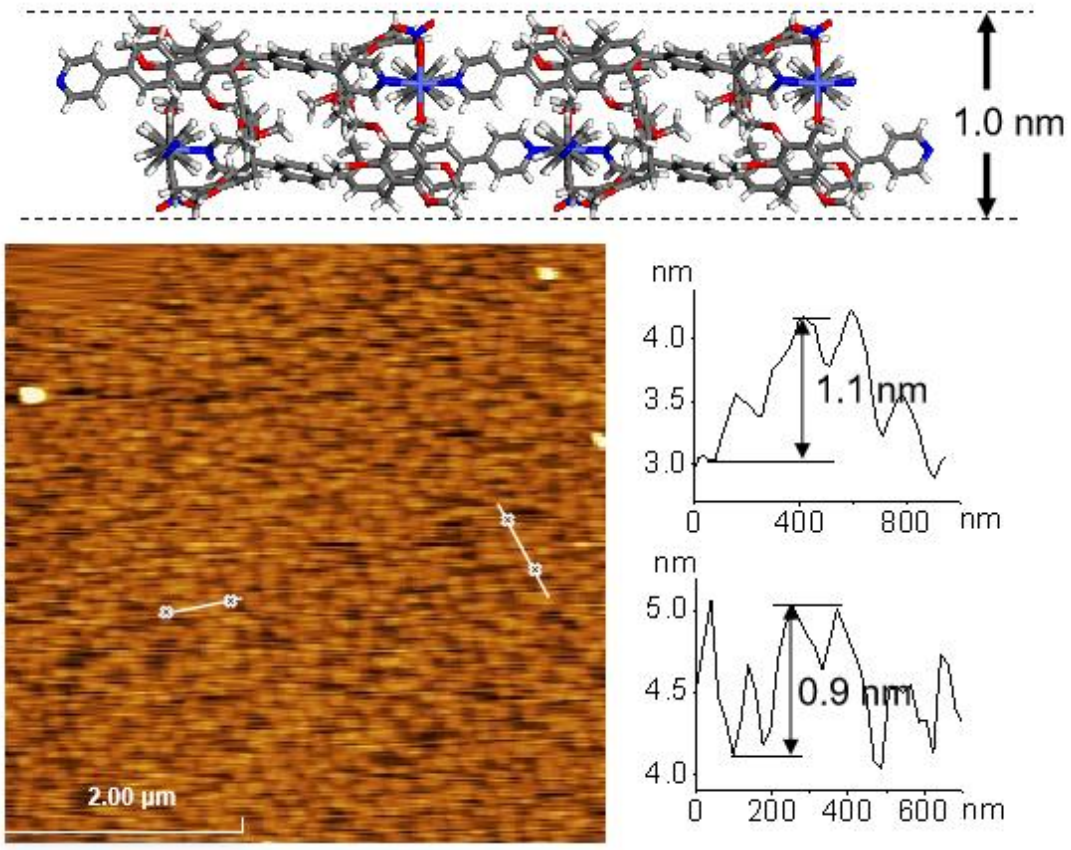

Figure S50. AFM images of **bl-2D-P5MOCN**.

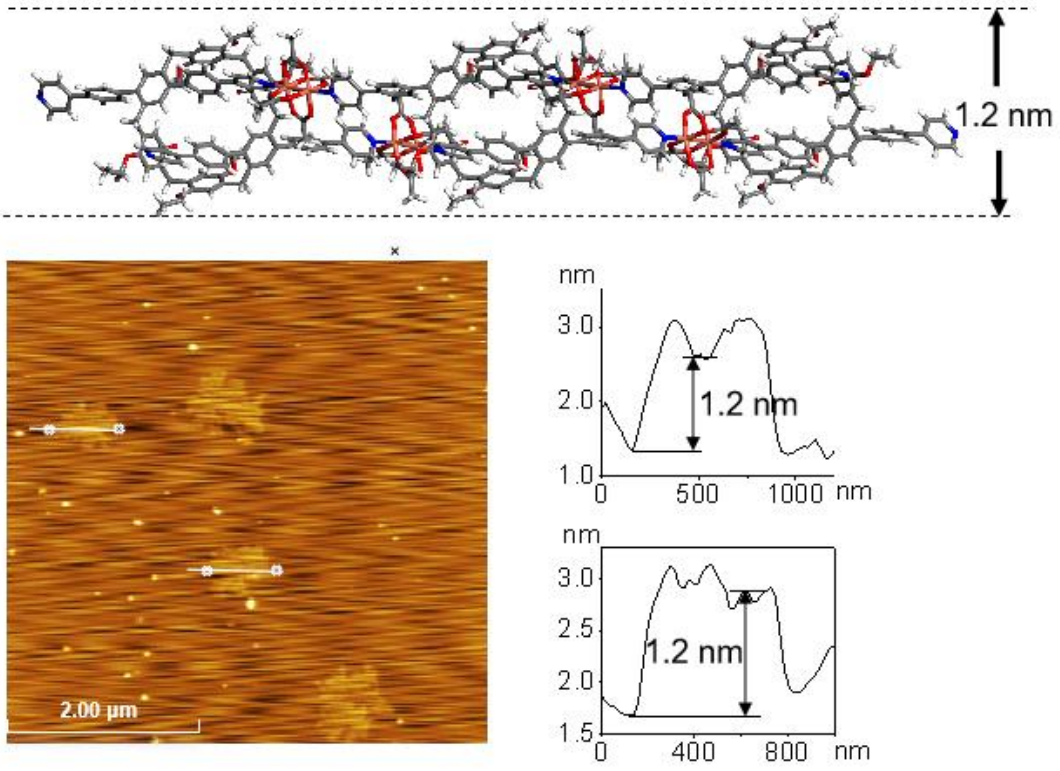

Figure S51. AFM images of **bl-2D-P6MOCN**.

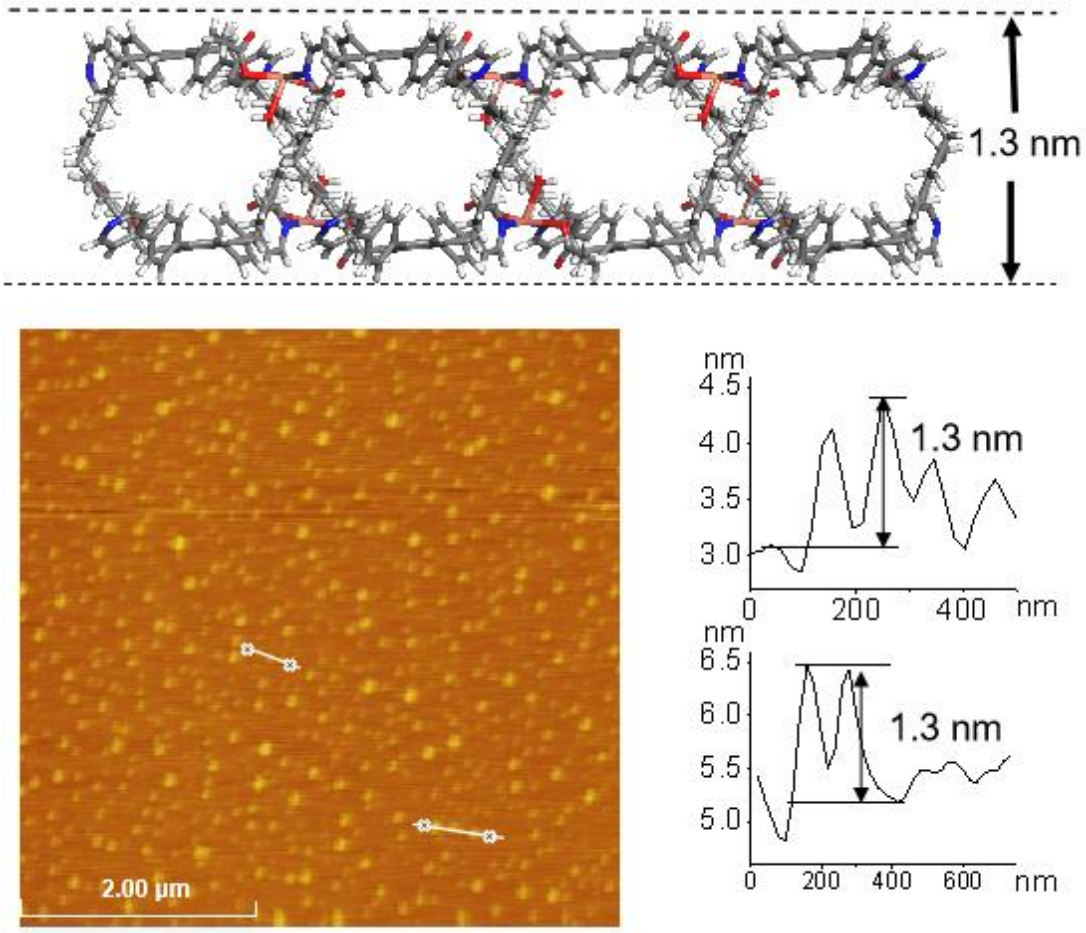

Figure S52. AFM images of **sbl-2D-P6MOCN**.

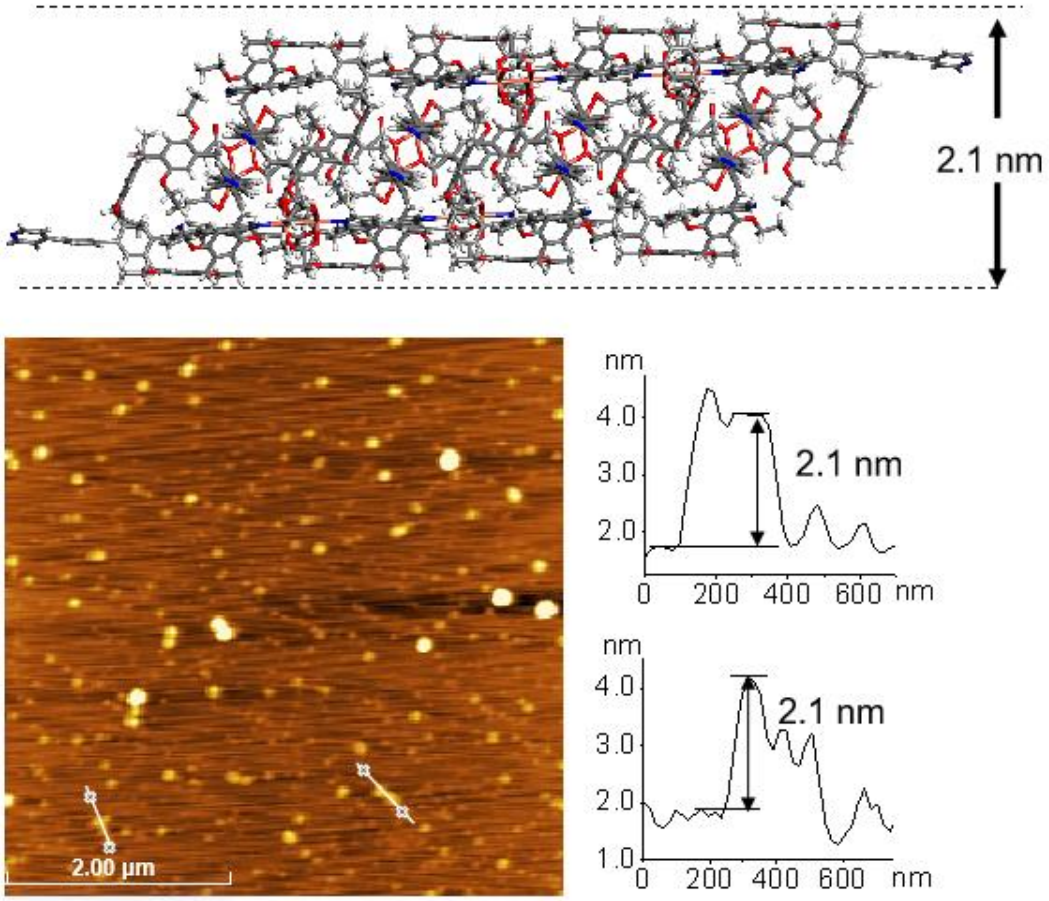

Figure S53. AFM images of **fl-2D-P6MOCN**.

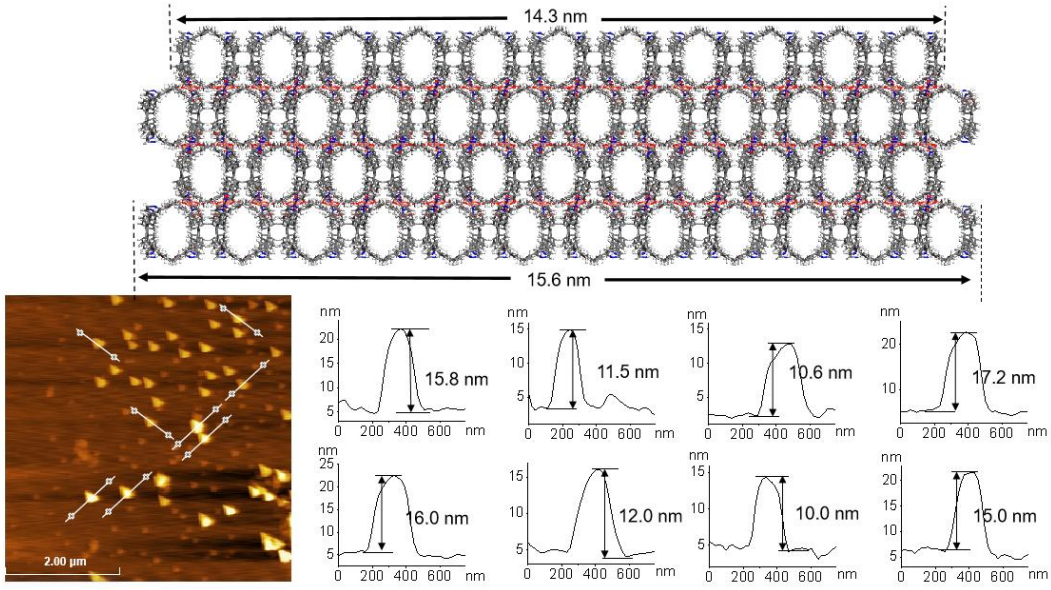

Figure S54. AFM images of **mtl-2D-P6MOCN**.

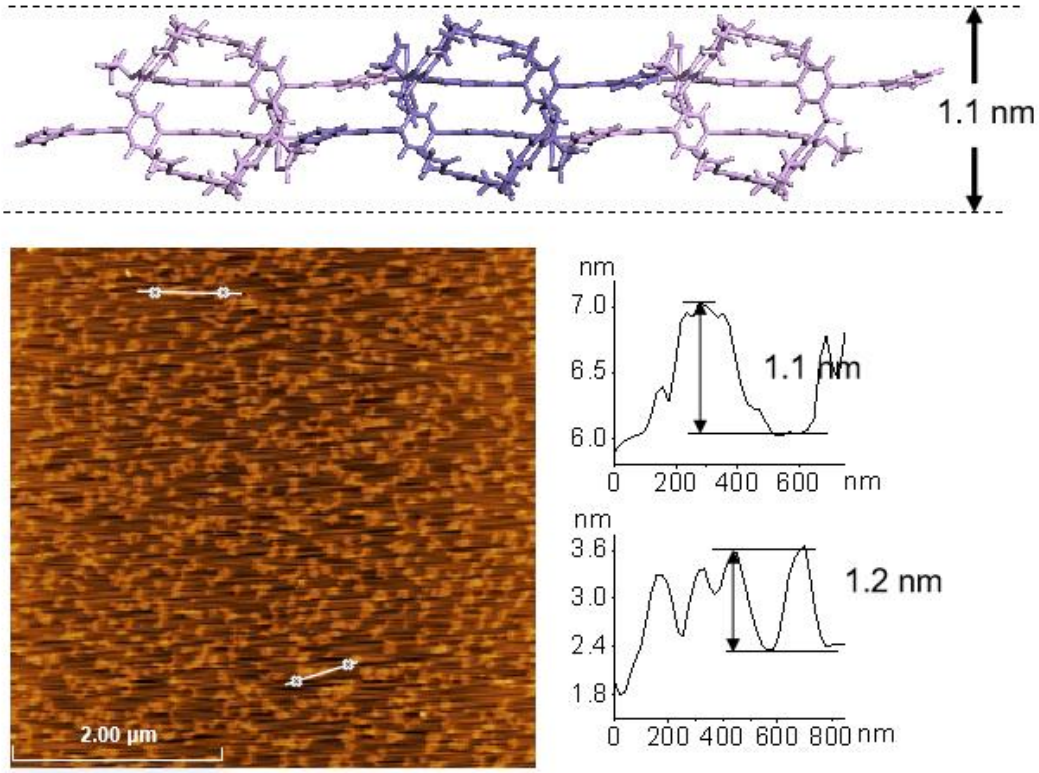

Figure S55. AFM images of **R-bl-2D-P6MOCN**.

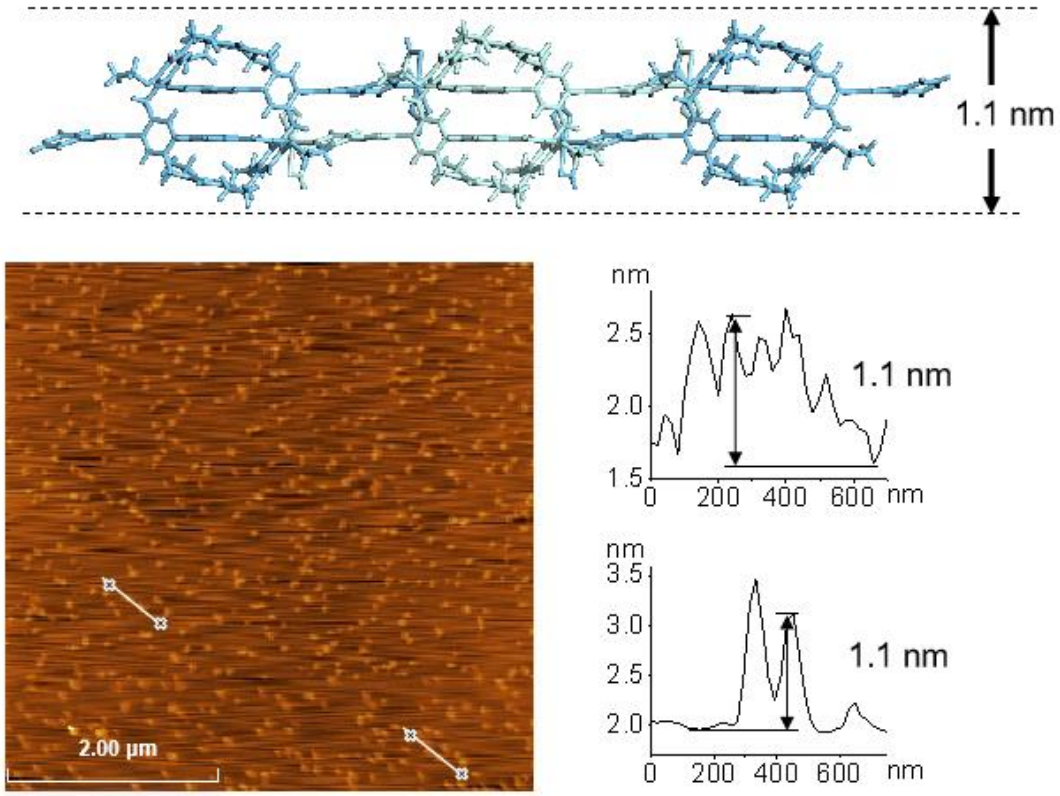

Figure S56. AFM images of **S-bl-2D-P6MOCN**.

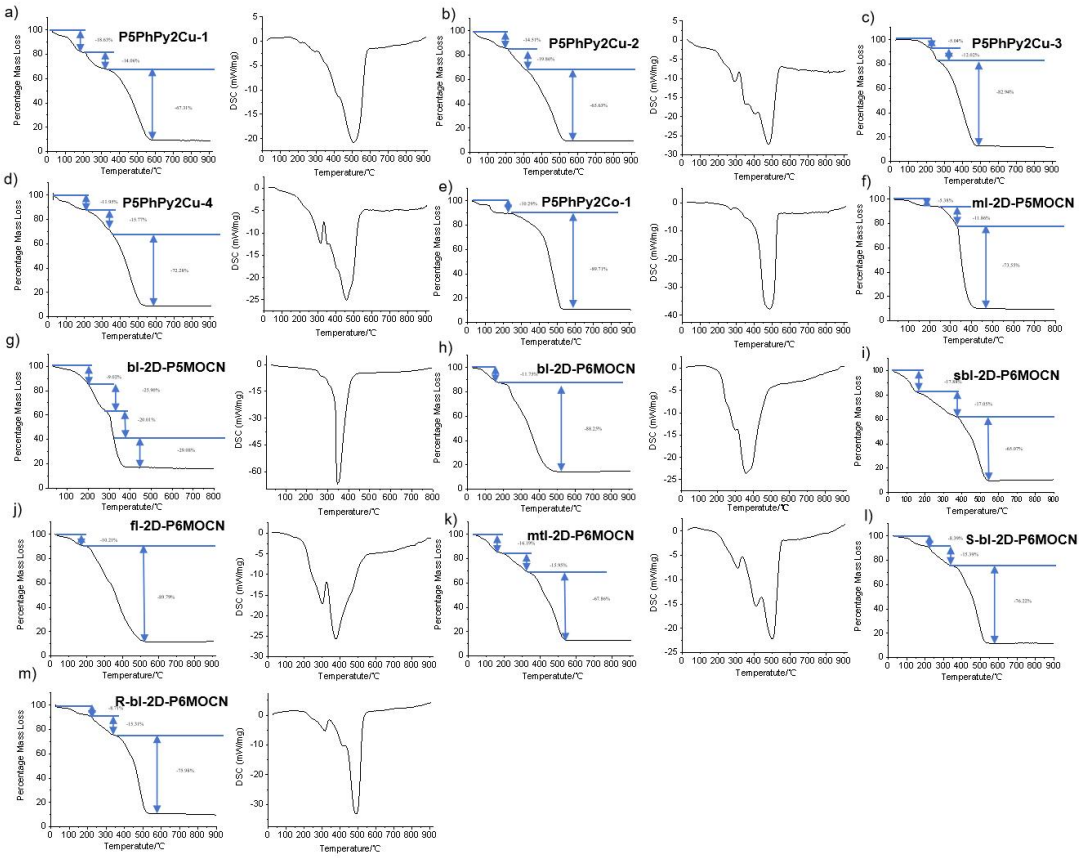

Figure S57. Tg and DSC spectra of **P5PhPy2Cu-1**(a), **P5PhPy2Cu-2**(b), **P5PhPy2Cu-3**(c), **P5PhPy2Cu-4**(d), **P5PhPy2Co-1**(e), **ml-2D-P5MOCN**(f), **bl-2D-P5MOCN**(g), **bl-2D-P6MOCN**(h), **sbl-2D-P6MOCN**(i), **fl-2D-P6MOCN**(j), **mtl-2D-P6MOCN**(k), **R-bl-2D-P6MOCN**(l), **S-bl-2D-P6MOCN**(m).

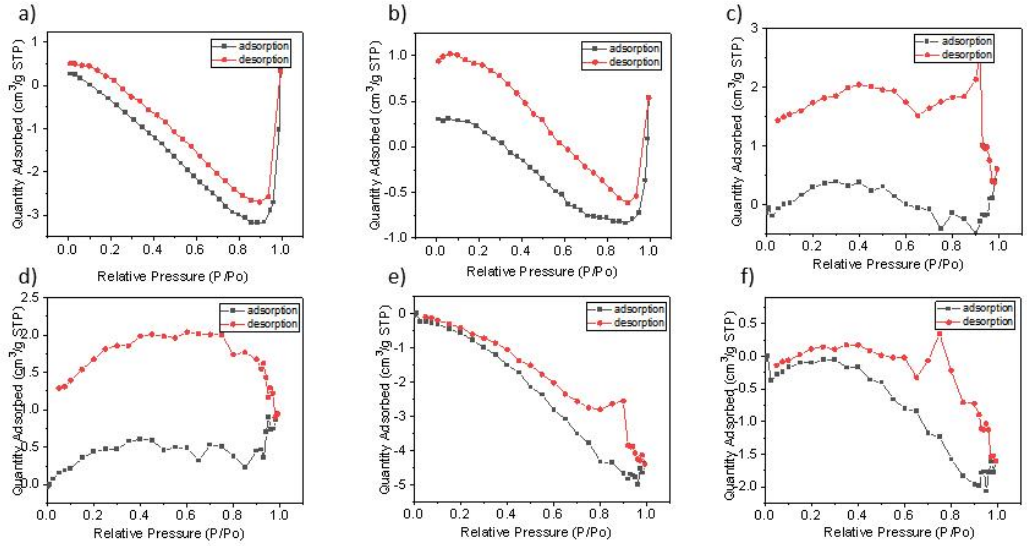

Figure S58. N_2 adsorption isotherms of **ml-2D-P5MOCN**(a), **bl-2D-P5MOCN** (b), **bl-2D-P6MOCN**(c), **sbl-2D-P6MOCN**(d), **fl-2D-P6MOCN**(e) **and mtl-2D-P6MOCN** (f).

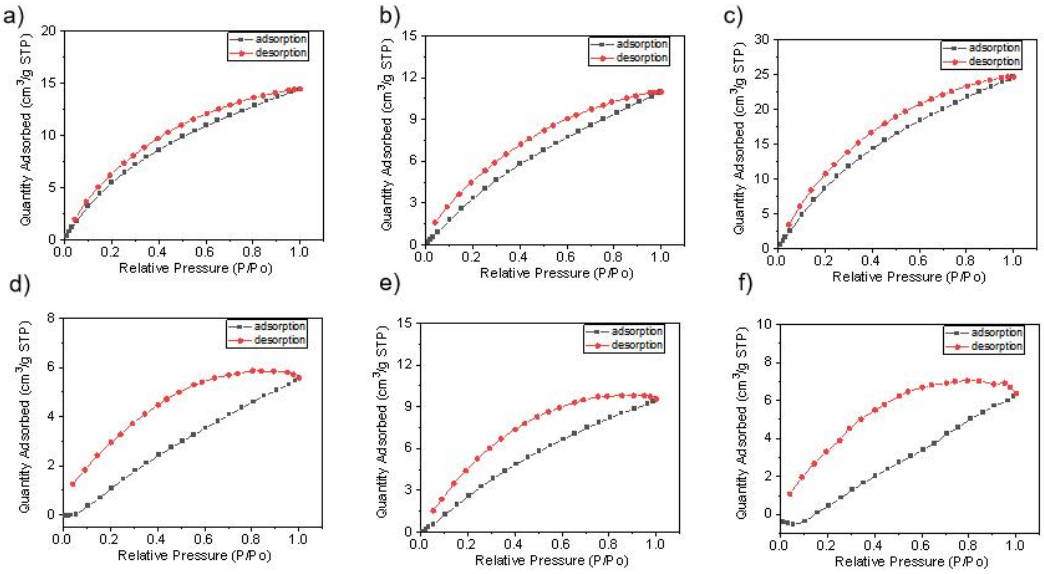

Figure S59. CO_2 adsorption (black) and desorption (red) isotherms of **ml-2D-P5MOCN** (a), **bl-2D-P5MOCN** (b), **bl-2D-P6MOCN** (c), **sbl-2D-P6MOCN** (d), **fl-2D-P6MOCN** (e) **and mtl-2D-P6MOCN** (f).

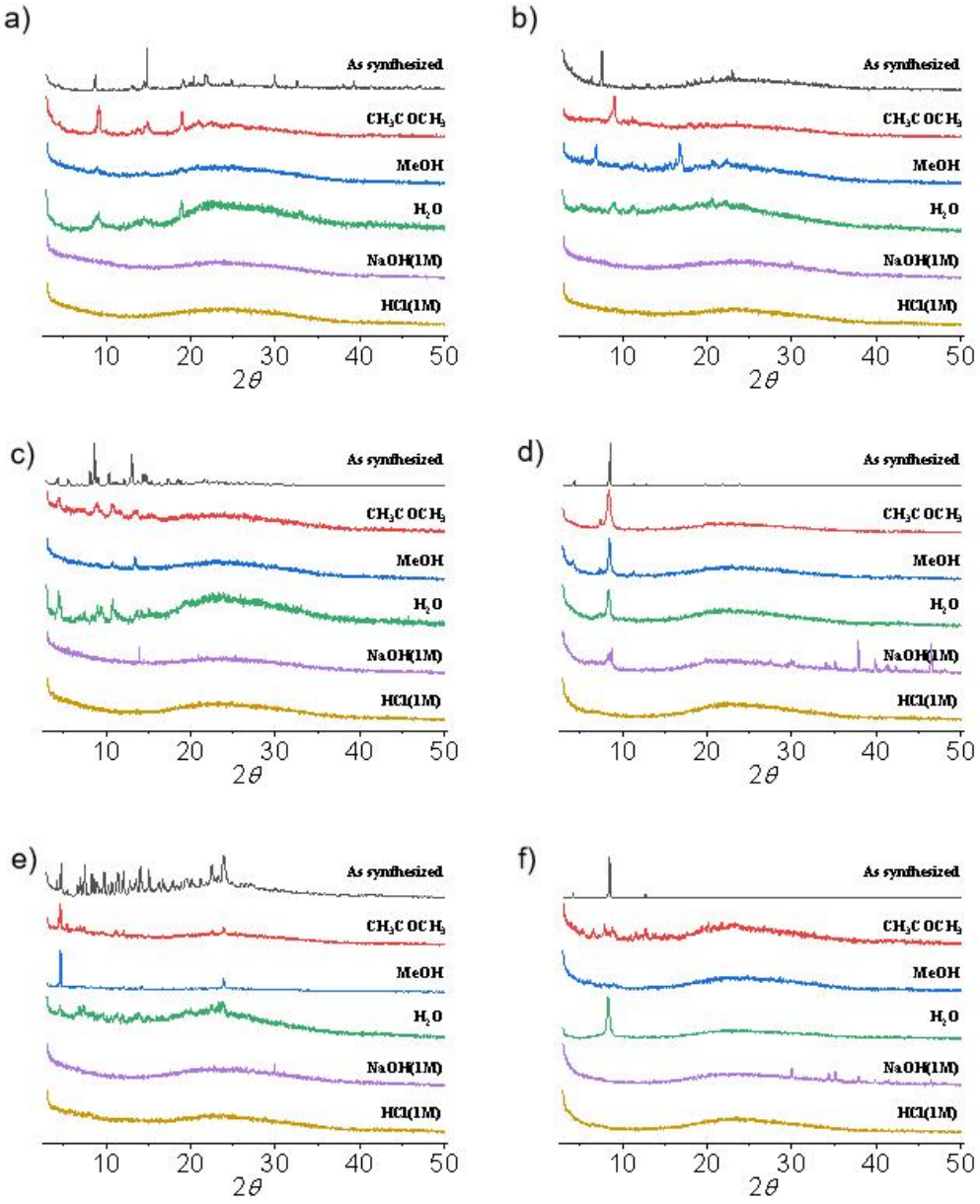

Figure S60. PXRD patterns of **ml-2D-P5MOCN** (a), **bl-2D-P5MOCN** (b), **bl-2D-P6MOCN** (c), **sbl-2D-P6MOCN** (d), **fl-2D-P6MOCN** (e) **and mtl-2D-P6MOCN** (f) after immersed in different solution for 12h.

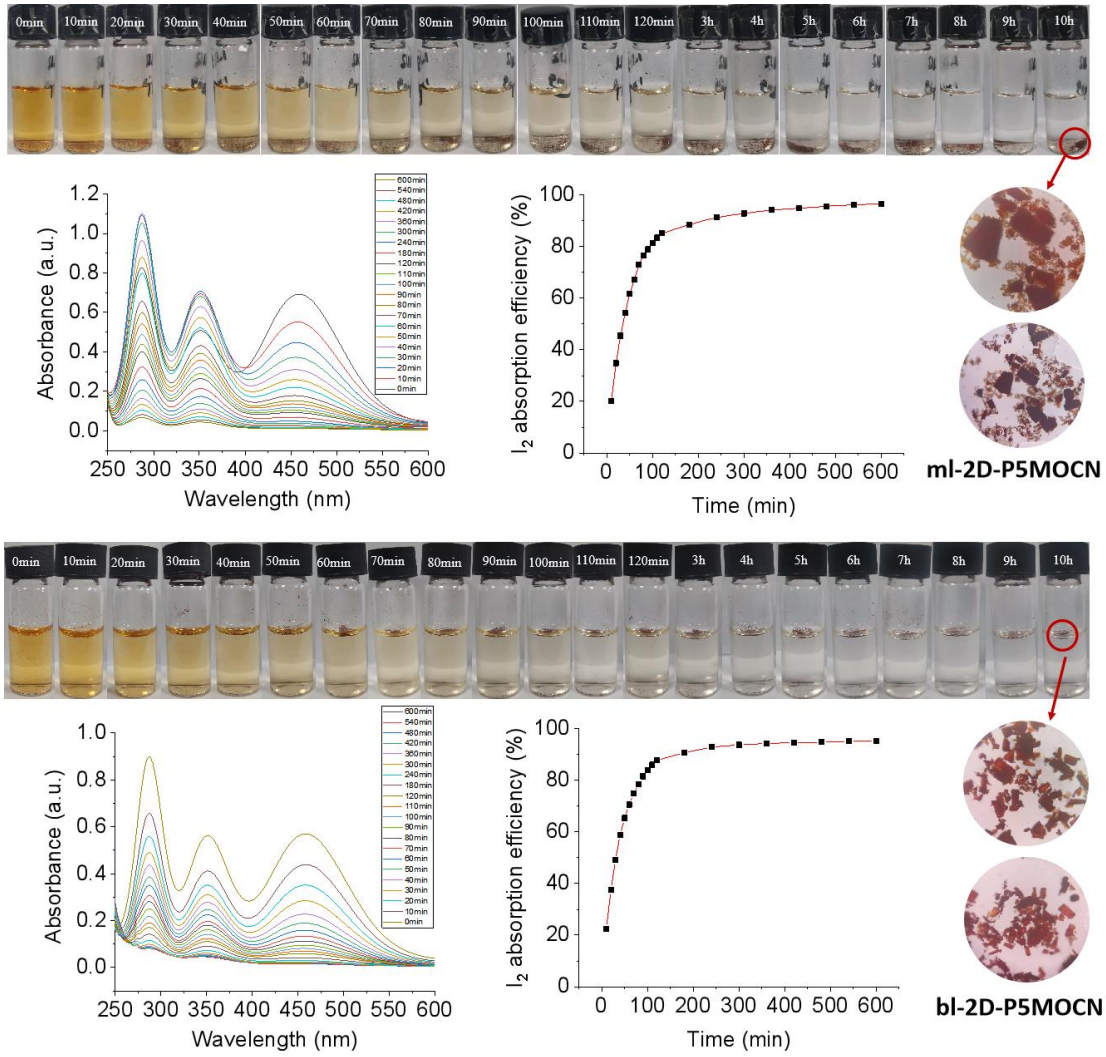

Figure S61. The I_2 adsorption experiments (1mM, 2.5 ml) of **ml-2D-P5MOCN** (1mg, up) and **bl-2D-P5MOCN** (1mg, down) in water.

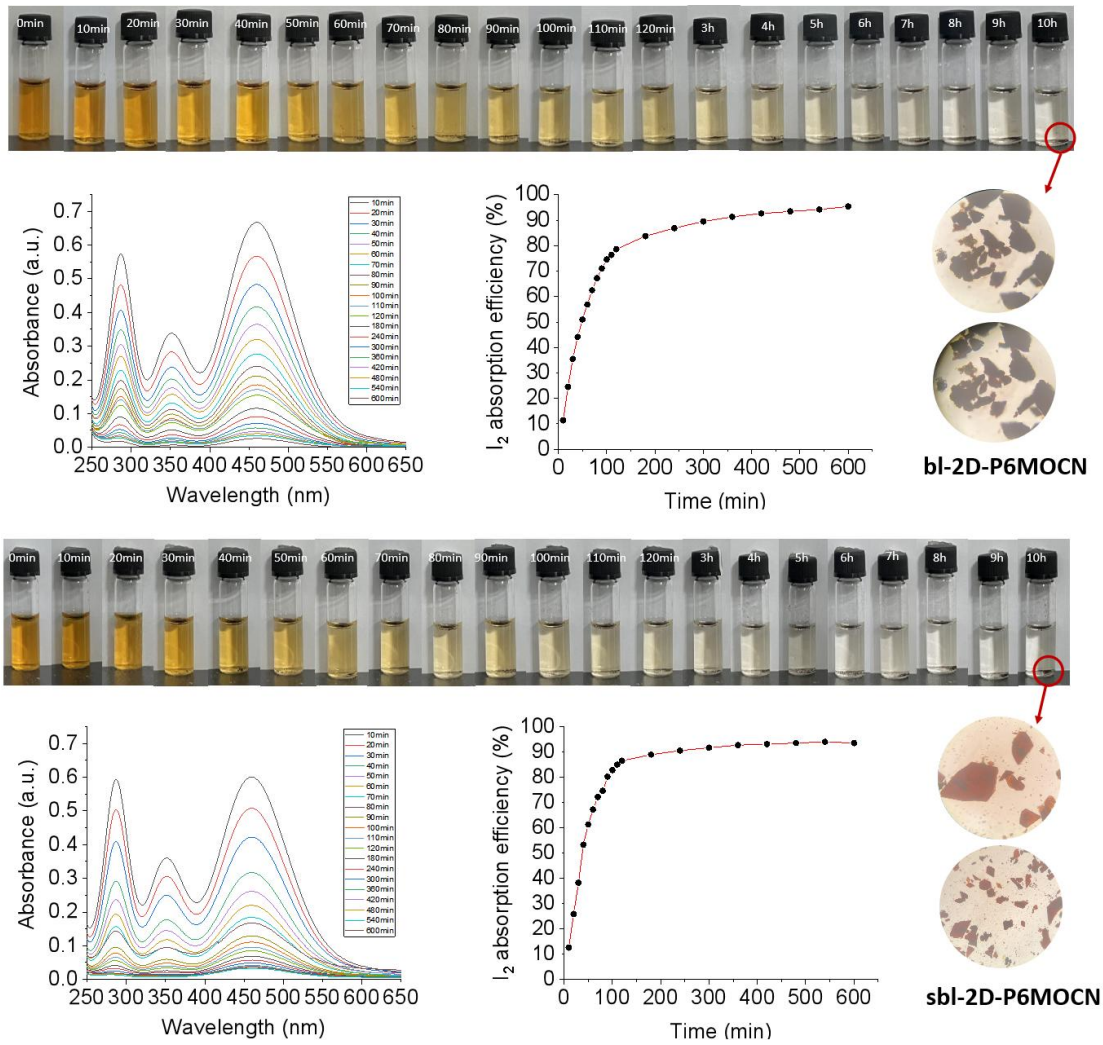

Figure S62. The I_2 adsorption experiments (1mM, 2.5 ml) of **bl-2D-P6MOCN** (1mg, up) and **sbl-2D-P6MOCN** (1mg, down) in water.

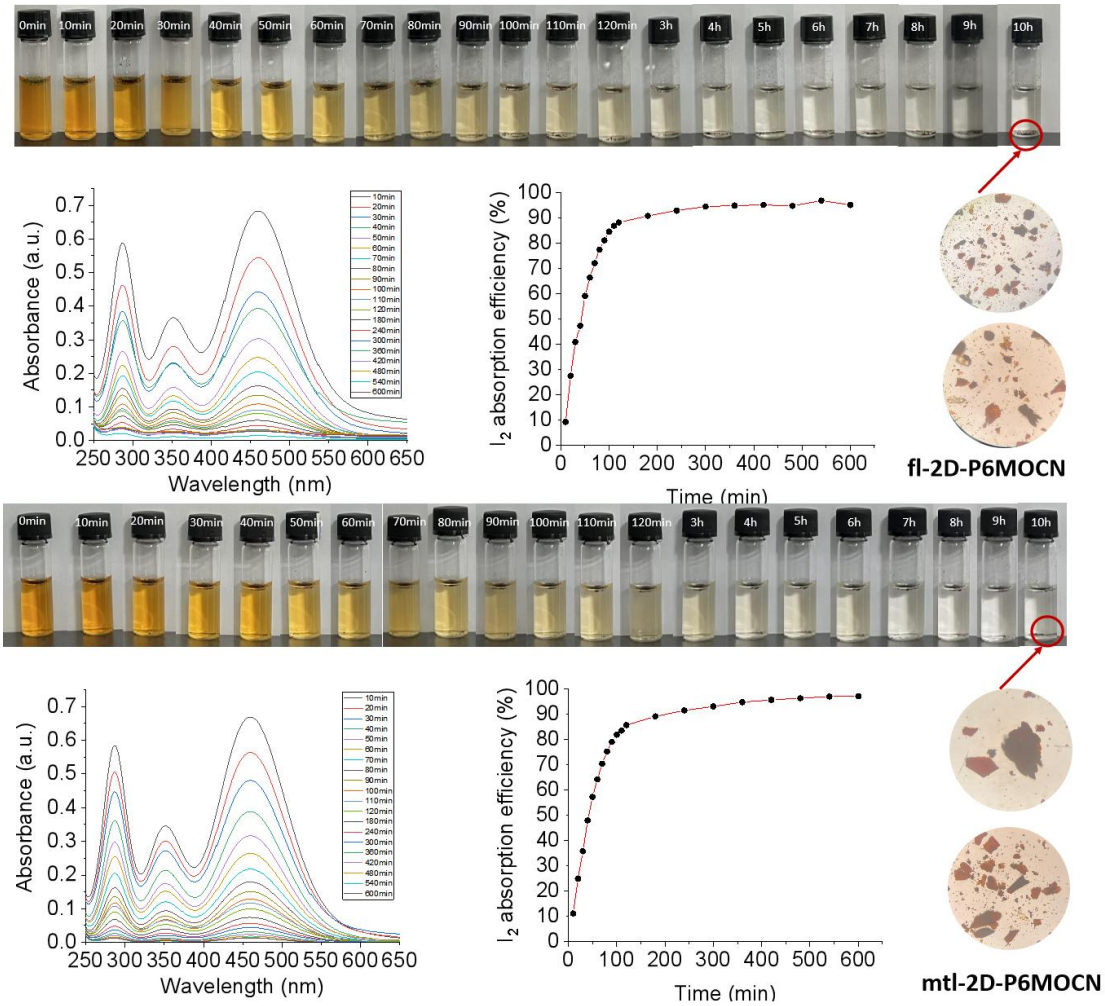

Figure S63. The I_2 adsorption experiments (1mM, 2.5 ml) of **fl-2D-P6MOCN** (1mg, up) and **mtl-2D-P6MOCN** (1mg, down) in water.

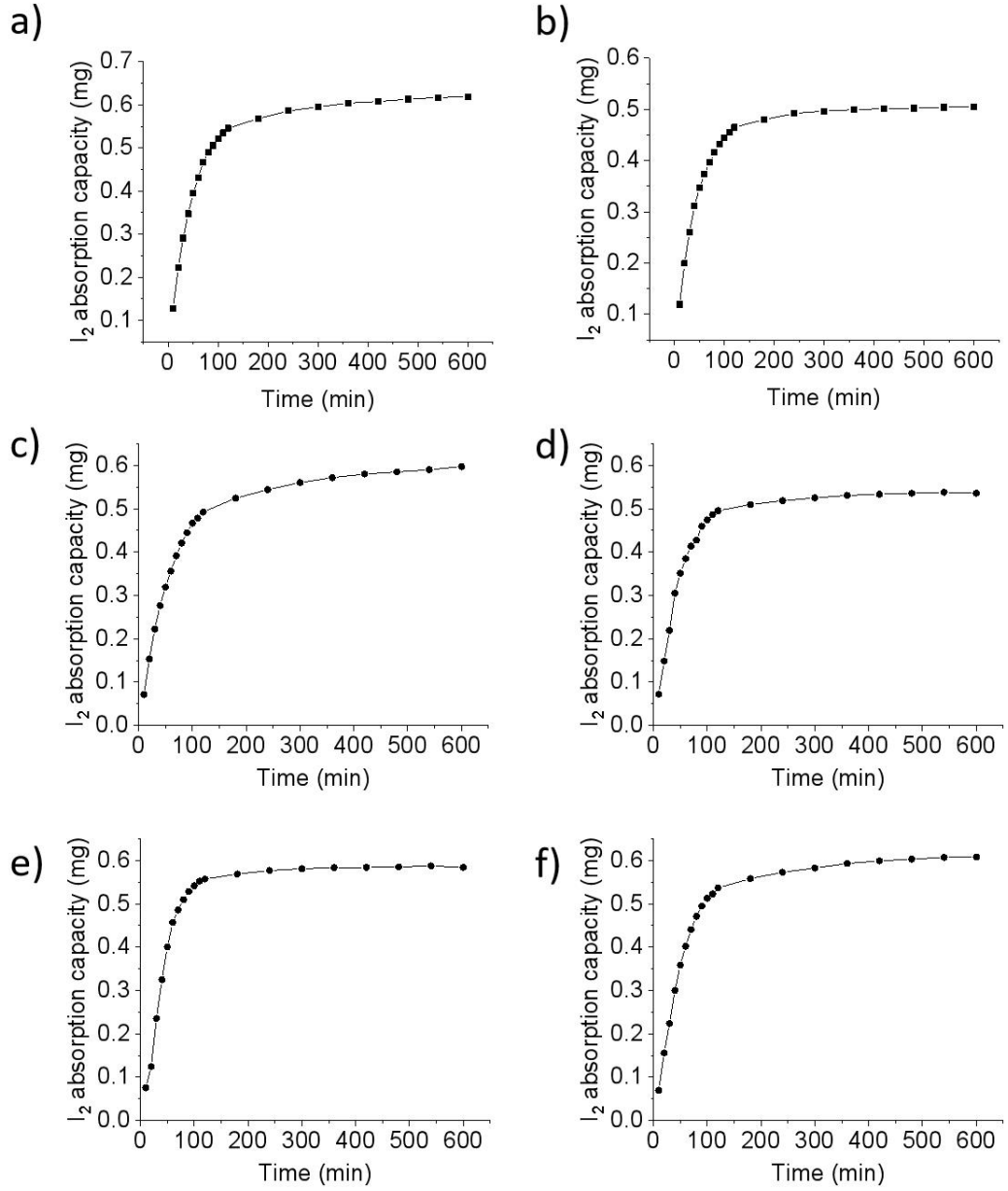

Figure S64. The I_2 adsorption experiments (1mM, 2.5 ml) of **ml-2D-P5MOCN** (1mg) (a), **bl-2D-P5MOCN** (1mg) (b), **bl-2D-P6MOCN** (1mg) (c), **sbl-2D-P6MOCN** (1mg) (d), **fl-2D-P6MOCN** (1mg) (e) and **mtl-2D-P6MOCN** (1mg) (f) in water.

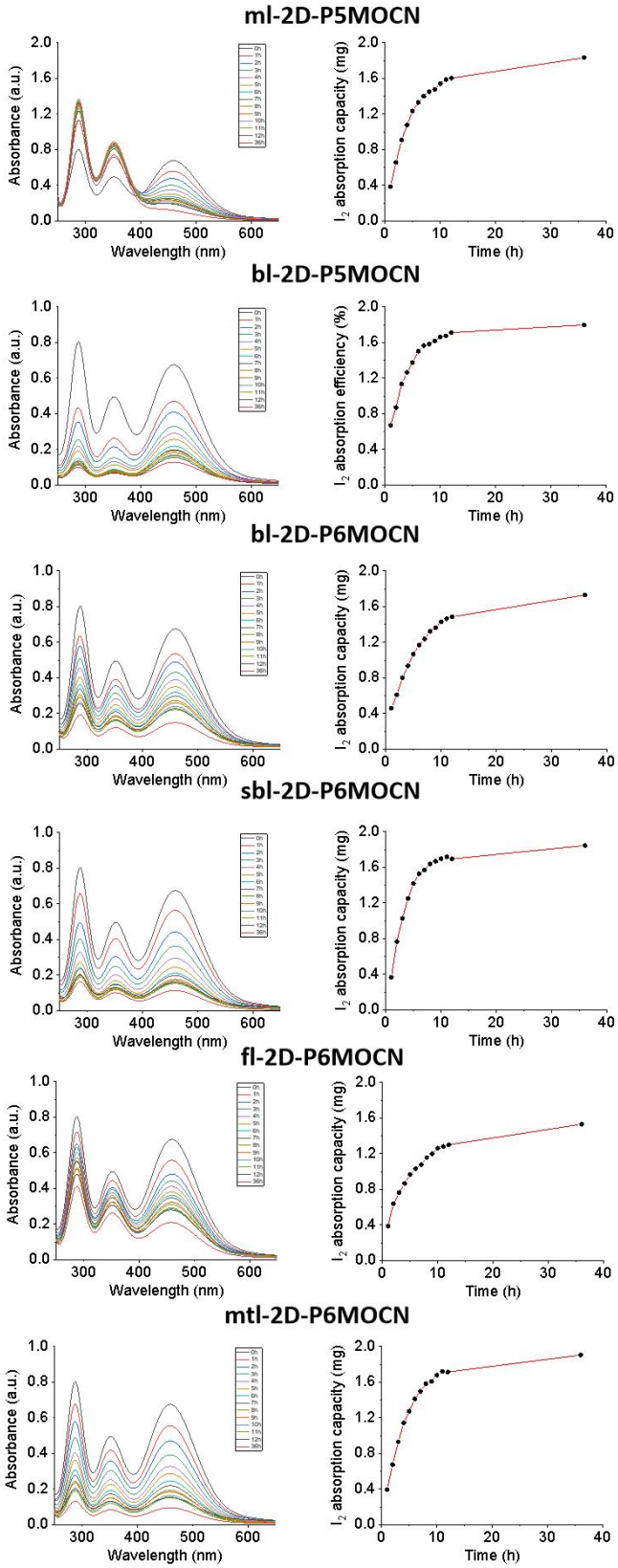

Figure S65. The I_2 final adsorption experiments (1mM, 10 ml) of **ml-2D-P5MOCN** (1.0 mg), **bl-2D-P5MOCN** (1.0 mg), **bl-2D-P6MOCN** (1.0 mg), **sbl-2D-P6MOCN** (1.0 mg), **fl-2D-P6MOCN** (1.0 mg) and **mtl-2D-P6MOCN** (1.0 mg) in water.

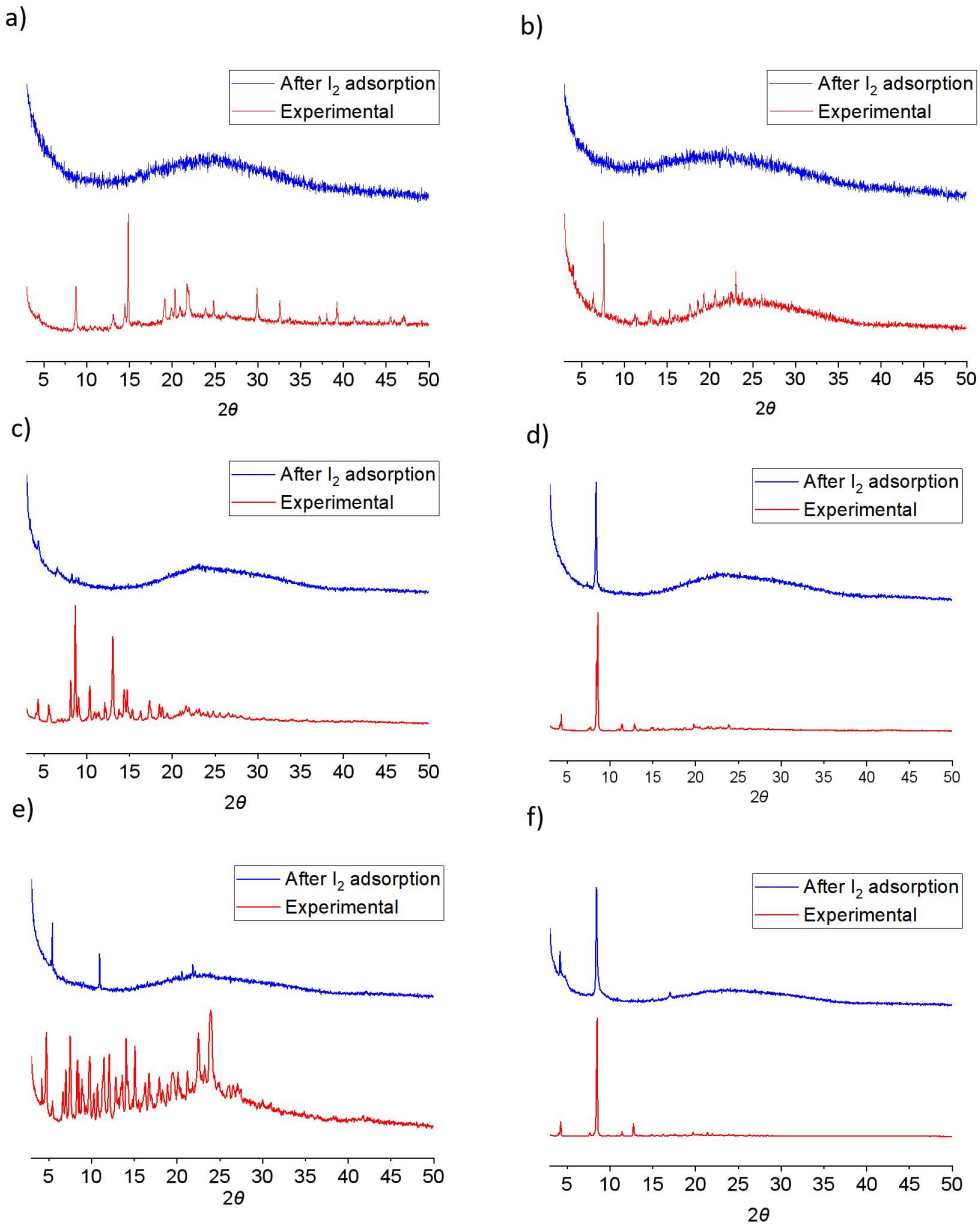

Figure S66. Experimental (red) and adsorbing iodine (blue) PXRD patterns of I_2⊂**ml-2D-P5MOCN** (a), I_2⊂**bl-2D-P5MOCN** (b), I_2⊂**bl-2D-P6MOCN** (c), I_2⊂**sbl-2D-P6MOCN** (d), I_2⊂**fl-2D-P6MOCN** (e) and I_2⊂**mtl-2D-P6MOCN** (f).

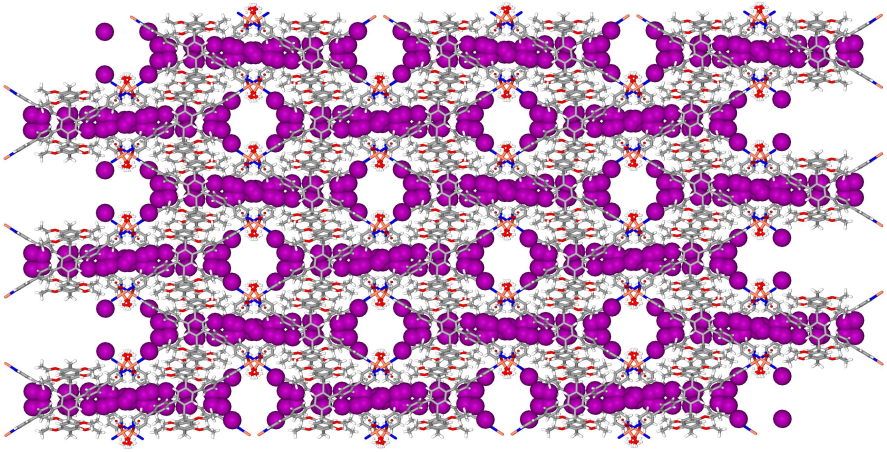

Figure S67. The side view of **mtl-2D-P6MOCN** after iodine adsorption experiment in water.

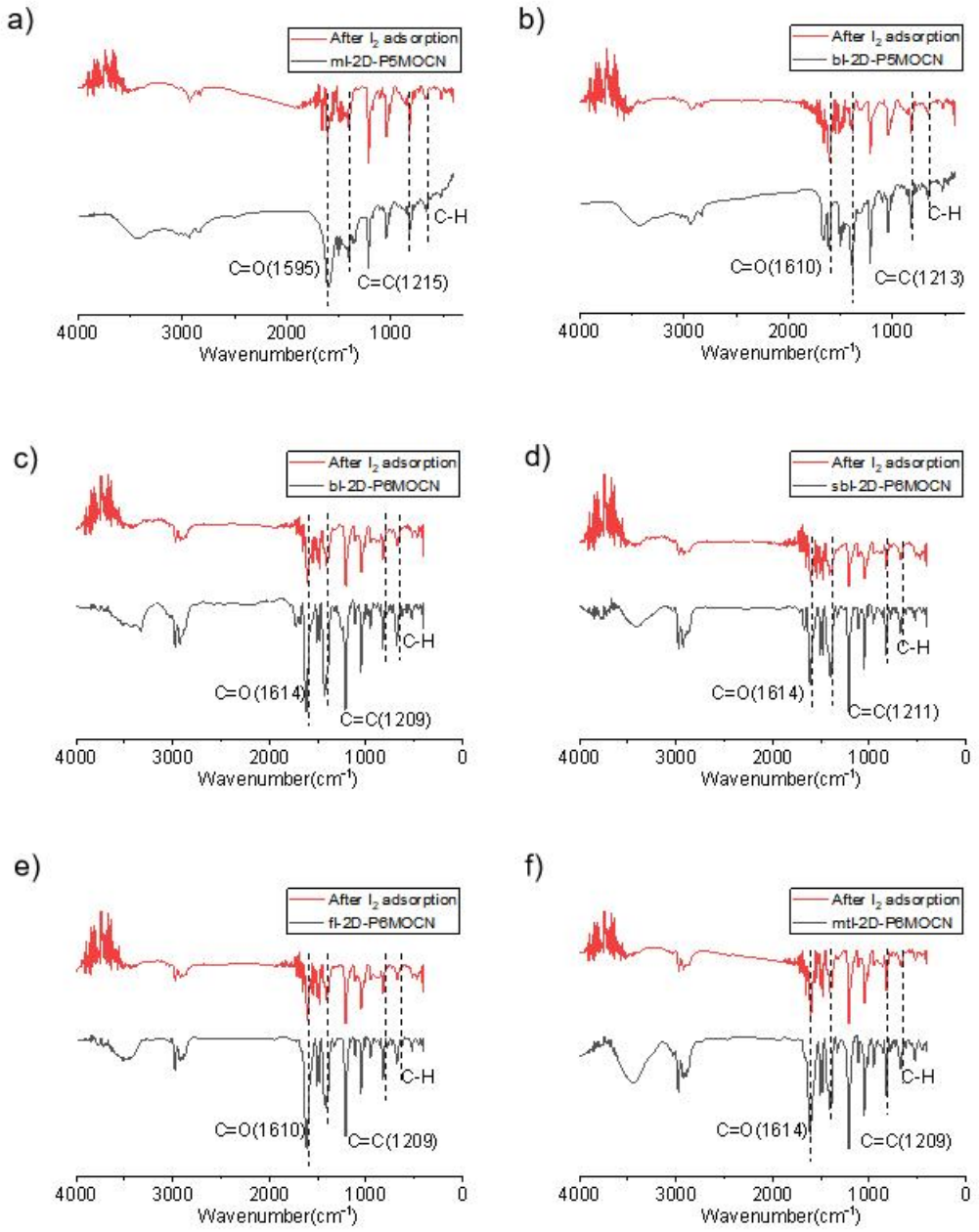

Figure S68. FT-IR spectra of **ml-2D-P5MOCN** (a), **bl-2D-P5MOCN** (b), **bl-2D-P6MOCN** (c), **sbl-2D-P6MOCN** (d), **fl-2D-P6MOCN** (e) and **mtl-2D-P6MOCN** (f) before (black) and after iodine adsorption (red).

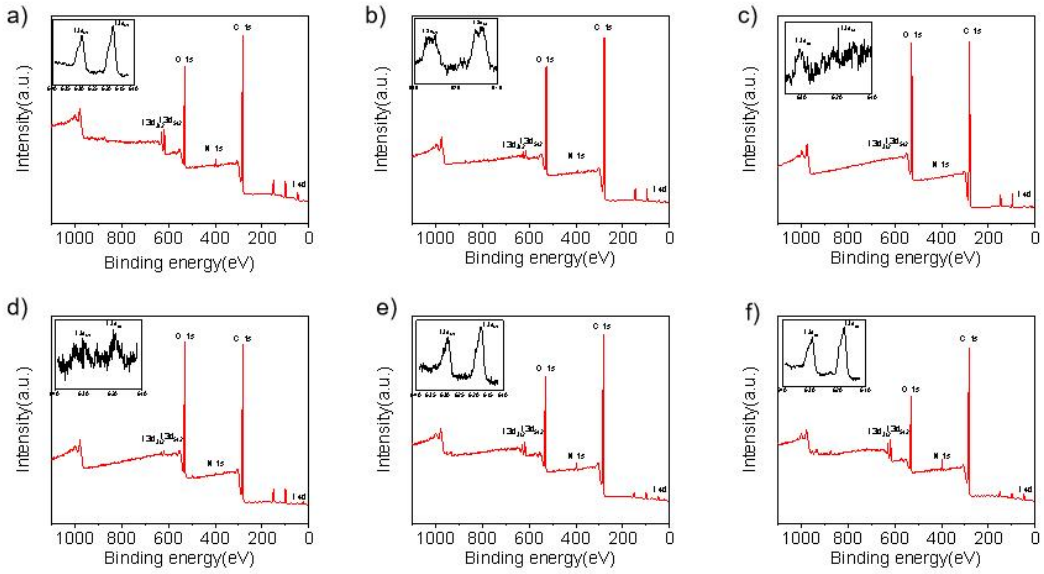

Figure S69. The XPS spectra of **ml-2D-P5MOCN** (a), **bl-2D-P5MOCN** (b), **bl-2D-P6MOCN** (c), **sbl-2D-P6MOCN** (d), **fl-2D-P6MOCN** (e) and **mtl-2D-P6MOCN** (f) after iodine adsorption.

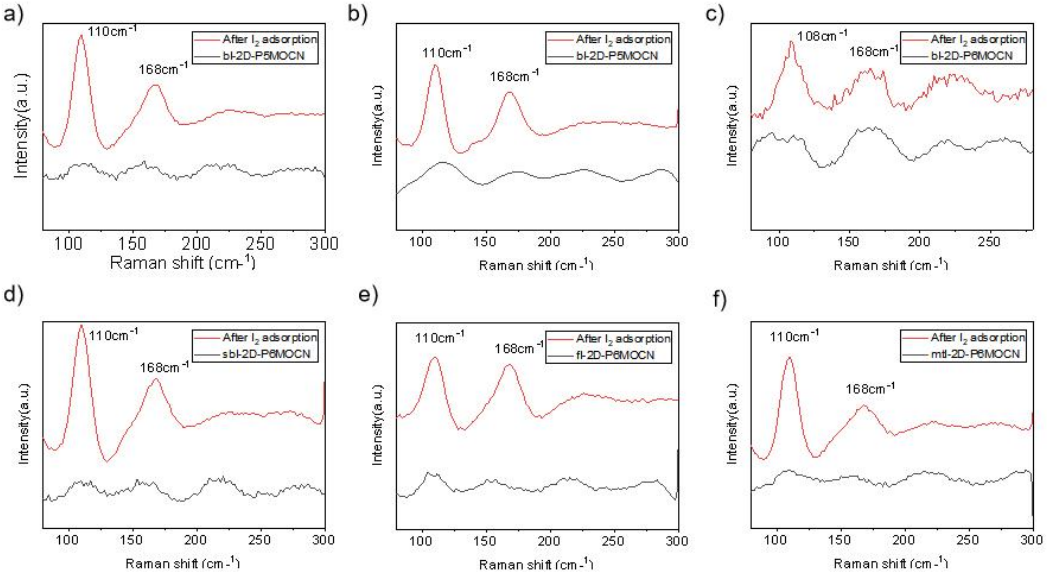

Figure S70. Raman spectra of **ml-2D-P5MOCN** (a), **bl-2D-P5MOCN** (b), **bl-2D-P6MOCN** (c), **sbl-2D-P6MOCN** (d), **fl-2D-P6MOCN** (e) and **mtl-2D-P6MOCN** (f) before (black) and after iodine adsorption (red).

Crystal data and structure refinement

Table S1. Crystal data and structure refinement for **P5PhPy2**, **P5PhPy4** and **P6PhPy4**.

Name	**P5PhPy2**	**P5PhPy4**	**P6PhPy4**
Identification code	2244321	2244320	2326170
Empirical formula	$C_{67}H_{66}Cu_{0.25}I_{0.25}N_7O_3$	$C_{89}H_{82}Cl_4N_4O_8$	$C_{102}H_{99}N_4O_{9.5}$
Formula weight	1064.87	1477.38	1532.85
Temperature/K	301(2)K	193	193.00
Crystal system	monoclinic	triclinic	monoclinic
Space group	P121/n1	P-1	$P2_1/n$
a/Å	12.6808(11)	12.9179(3)	10.3276(9)
b/Å	24.763(2)	17.0625(4)	32.363(2)
c/Å	18.6875(5)	17.3348(4)	25.149(2)
α/°	90	94.9090(10)	90
β/°	97.784(6)	97.0560(10)	95.279(3)
γ/°	90	91.9560(10)	90
Volume/Å^3	5814.1(9)	3774.09(15)	8370.0(12)
Z	4	2	4
ρ_{calc}g/cm^3	1.217	1.300	1.216
μ/mm^{-1}	1.702	1.259	0.078
F(000)	2246	1552.0	3260.0
Crystal size/mm^3	0.100 x 0.180 x 0.200	0.13 × 0.12 × 0.1	0.16× 0.15 × 0.08
Radiation	CuKα (λ = 1.54178)	GaKα (λ = 1.34139)	MoKα (λ = 0.71073)
2 Θ range for data collection/°	2.98 to 65.13°	4.488 to 107.806	3.488 to 50.976
Index ranges	-14<=h<=14, -28<=k<=29, -21<=l<=21	-15 ⩽ h ⩽ 15, -20 ⩽ k ⩽ 19, -20 ⩽ l ⩽ 20	-11 ≤ h ≤ 12, -39 ≤ k ≤ 38, -30 ≤ l ≤ 30
Reflections collected	57994	47111	64178
Independent reflections	9904 [R_{int} = 0.1226]	13808 [R_{int} = 0.0566, R_{sigma} = 0.0622]	15486 [R_{int} = 0.1325, R_{sigma} = 0.1314]
Data/restraints/parameters	9904 / 0 / 684	13808/19/967	15486/2/1045
Goodness-of-fit on F^2	1.013	1.038	1.096
Final R indexes [I>=2 σ (I)]	R_1 = 0.0643,wR_2 = 0.1578	R_1 = 0.0842, wR_2 = 0.2324	R_1 = 0.0982, wR_2 = 0.1608
Final R indexes [all data]	R_1 = 0.1047, wR_2 = 0.1868	R_1 = 0.1340, wR_2 = 0.2696	R_1 = 0.1995, wR_2 = 0.2024
Largest diff. peak/hole / e Å^{-3}	0.185/-0.213	1.11/-1.38	0.30/-0.26

Table S2. Crystal data and structure refinement for **P5PhPy2Cu-1-P5PhPy2Cu-4**.

Name	**P5PhPy2Cu-1**	**P5PhPy2Cu-2**	**P5PhPy2Cu-3**	**P5PhPy2Cu-4**
Identification code	2244322	2244323	2244324	2244325
Empirical formula	$C_{85}H_{102}Cu_2N_6O_{21}$	$C_{164}H202Cu_4N_4O_{46}$	$C_{76}H_{81}Cu_2N_3O_{18}$	$C_{75.69}H_{82.28}N_{4.5}O_{13.69}CuICl_{0.41}$
Formula weight	1670.80	3303.50	1451.51	1351.96
Temperature/K	292.00	193.00	150.00	153.15
Crystal system	monoclinic	monoclinic	triclinic	triclinic
Space group	$P2_1$	$P2_1$	P-1	P-1
a/Å	12.0846(19)	12.1284(9)	12.3580(3)	13.2377(3)
b/Å	21.322(4)	21.1102(19)	16.3529(4)	14.9966(3)
c/Å	19.015(3)	35.055(3)	17.9257(4)	20.4324(4)
α/°	90	90	97.3870(10)	81.365(2)
β/°	104.018(5)	96.044(4)	103.4240(10)	71.316(2)
γ/°	90	90	98.4550(10)	86.856(2)
Volume/Å^3	4753.7(14)	8925.4(13)	3435.12(14)	3798.83(14)
Z	2	2	2	2
ρ_{calc}g/cm^3	1.167	1.229	1.403	1.182
μ/mm^{-1}	0.513	2.951	0.694	1.042
F(000)	1760.0	3480.0	1520.0	1427.0
Crystal size/mm^3	0.13 × 0.12 × 0.1	0.13 × 0.12 × 0.1	0.2 ×0.16 × 0.13	0.16 × 0.1 × 0.02
Radiation	MoKα (λ = 0.71073)	GaKα (λ = 1.34139)	MoKα (λ = 0.71073)	CuKα (λ = 1.54178)
2 Θ range for data collection/°	3.964 to 43.934	4.258 to 107.812	2.554 to 52.872	5.96 to 149.532
Index ranges	-12 ⩽ h ⩽ 12, -22 ⩽ k ⩽ 22, -20 ⩽ l ⩽ 20	-14 ⩽ h ⩽ 14, -25 ⩽ k ⩽ 25, -42 ⩽ l ⩽ 42	-15 ⩽ h ⩽ 15, -19 ⩽ k ⩽ 20, -22 ⩽ l ⩽ 22	-16 ⩽ h ⩽ 16, -18 ⩽ k ⩽ 17, -25 ⩽ l ⩽ 25
Reflections collected	66475	54062	54142	102440
Independent reflections	11585[R_{int} = 0.0911, R_{sigma} = 0.0578]	29261 [R_{int} = 0.0530, R_{sigma} = 0.1150]	14051[R_{int}=0.0518, R_{sigma} = 0.0545]	15301[R_{int} = 0.0557, R_{sigma} = 0.0357]
Data/restraints/parameters	11585/1966/1088	29261/104/1720	14051/67/907	15301/1234/1037
Goodness-of-fit on F^2	1.039	1.001	1.063	1.029
Final R indexes [I>=2σ (I)]	R_1 = 0.0696, wR_2 = 0.1862	R_1 = 0.0678, wR_2 = 0.1710	R_1 = 0.0765, wR_2 = 0.2088	R_1 = 0.0779, wR_2 = 0.2378
Final R indexes [all data]	R_1 = 0.1012, wR_2 = 0.2079	R_1 = 0.1338, wR_2 = 0.1979	R_1 = 0.1013, wR_2 = 0.2213	R_1 = 0.0881, wR_2 = 0.2497
Largest diff. peak/hole/e Å^{-3}	0.48(3)	0.40/-0.50	1.02/-1.16	1.22/-0.64

Table S3. Crystal data and structure refinement for **P5PhPy2Co-1**, **ml-2D-P5MOCN** and **bl-2D-P5MOCN**.

Name	**P5PhPy2Co-1**	**ml-2D-P5MOCN**	**bl-2D-P5MOCN**
Identification code	2244326	2244327	2244328
Empirical formula	$C_{81}H_{102}CoN_6O_{20}$	$C_{409}H_{429}Co_8N_{29}O_{76.5}$	$C_{100}H_{109}CoN_{11}O_{19}$
Formula weight	1538.61	7446.23	1827.91
Temperature/K	193.00	193.00	193.00
Crystal system	triclinic	monoclinic	triclinic
Space group	P-1	$P2_1$	P-1
a/Å	13.9662(6)	18.5576(19)	13.9766(5)
b/Å	14.9970(6)	40.892(4)	18.8234(8)
c/Å	20.3479(8)	24.167(2)	24.3526(9)
α/°	94.792(2)	90	112.3290(10)
β/°	106.615(3)	90.150(6)	103.5880(10)
γ/°	92.619(3)	90	92.9400(10)
Volume/Å^3	4058.9(3)	18339(3)	5689.8(4)
Z	2	2	2
ρ_{calc}g/cm^3	1.259	1.348	1.067
μ/mm^{-1}	1.543	2.383	0.213
F(000)	1634.0	7828	1930.0
Crystal size/mm^3	0.13 × 0.12 × 0.1	0.12 × 0.1 × 0.08	0.13 × 0.12 × 0.1
Radiation	GaKα (λ = 1.34139)	GaK_α (λ=1.34139 Å)	MoKα (λ = 0.71073)
2Θ range for data collection/°	5.76 to 107.81	1.88 to 84.24	3.544 to 50.758
Index ranges	-16 ⩽ h ⩽ 16, -18 ⩽ k ⩽ 18, -24 ⩽ l ⩽ 19	-18 ⩽ h ⩽ 16, -34 ⩽ k ⩽ 40, -24 ⩽ l ⩽ 23	-16 ⩽ h ⩽ 16, -22 ⩽ k ⩽ 15, -29 ⩽ l ⩽ 29
Reflections collected	43239	84763	44378
Independent reflections	14819 [R_{int} = 0.0806, R_{sigma} = 0.1150]	35136 [R_{int} = 0.1246, R_{sigma} = 0.2317	20744 [R_{int} = 0.0667, R_{sigma} = 0.1122]
Data/restraints/parameters	14819/2324/1014	35136/7263/3865	20744/238/1134
Goodness-of-fit on F^2	1.017	1.156	1.022
Final R indexes [I>=2σ (I)]	R_1 = 0.1242, wR_2 = 0.2793	R_1 = 0.1129, wR_2 = 0.2609	R_1 = 0.0845, wR_2 = 0.2301
Final R indexes [all data]	R_1 = 0.2276, wR_2 = 0.3242	R_1 = 0.2205, wR_2 = 0.3069	R_1 = 0.1353, wR_2 = 0.2653
Largest diff. peak/hole / e Å^{-3}	0.60/-0.55	0.95/-0.75	0.94/-0.51

Table S4. Crystal data and structure refinement for **bl-2D-P6MOCN**, **sbl-2D-P6MOCN** and **fl-2D-P6MOCN**.

Name	**bl-2D-P6MOCN**	**sbl-2D-P6MOCN**(1)	**sbl-2D-P6MOCN**(2)	**fl-2D-P6MOCN**
Identification code	2326171	2342430	2326172	2326174
Empirical formula	$C_{124}H_{154}Cu_4N_6O_{36}$	$C_{122}H_{148}Cu_2N_8O_{26}$	$C_{117}H_{146}Cu_2N_7O_{30}$	$C_{126}H_{148}Cu_3N8O_{27}$
Formula weight	2558.68	2269.56	2257.48	2397.14
Temperature/K	193.00	193.00	193.00	193.00
Crystal system	monoclinic	monoclinic	monoclinic	triclinic
Space group	C2/c	$P2_1/n$	C2/c	P-1
a/Å	30.2976(8)	13.7491(7)	22.8584(7)	16.692(2)
b/Å	30.0377(8)	41.664(2)	41.6812(12)	19.198(3)
c/Å	15.6700(4)	22.7927(13)	13.7257(5)	20.104(3)
α/°	90	90	90	69.195(4)
β/°	91.5770(10)	91.860(3)	92.088(2)	81.270(4)
γ/°	90	90	90	83.209(3)
Volume/Å^3	14255.4(6)	13049.9(12)	13068.7(7)	5938.0(14)
Z	4	4	4	2
ρ_{calc}g/cm^3	1.192	1.155	1.147	1.341
μ/mm^{-1}	1.266	2.117	0.976	0.610
F(000)	5376.0	4088.0	4780.0	2526.0
Crystal size/mm^3	0.13 × 0.1 × 0.1	0.14 × 0.11 × 0.09	0.14 × 0.11 × 0.08	0.14 ×0.11 × 0.08
Radiation	CuKα (λ = 1.54178)	GaKα (λ = 1.34139)	CuKα (λ = 1.54178)	MoKα (λ= 0.71073)
2 Θ range for data collection/°	4.142 to 159.45	3.846 to 107.814	4.41 to 136.492	4.318 to 40
Index ranges	-38 ≤ h ≤ 38, -37 ≤ k ≤ 37, -18 ≤ l ≤ 19	-16 ⩽ h ⩽ 13, -50 ⩽ k ⩽ 50, -24 ⩽ l ⩽ 27	-27 ≤ h ≤ 27, -46 ≤ k ≤ 50, -16 ≤ l ≤ 16	-15 ≤ h ≤ 16, -18 ≤ k ≤ 18, -16 ≤ l ≤ 19
Reflections collected	102073	87570	66435	22942
Independent reflections	15264 [R_{int} = 0.0504, R_{sigma} = 0.0305]	23828 [R_{int} = 0.0899, R_{sigma} = 0.1157]	11944 [R_{int} = 0.0569, R_{sigma} = 0.0597]	10964 [R_{int} = 0.0441, R_{sigma} = 0.0792]
Data/restraints/parameters	15264/136/800	23828/1597/1530	11944/328/756	10964/975/1283
Goodness-of-fit on F^2	1.024	1.080	1.029	1.045
Final R indexes [I>=2σ (I)]	R_1 = 0.0616, wR_2 = 0.1833	R_1 = 0.1124, wR_2 = 0.2949	R_1 = 0.0992, wR_2 = 0.2673	R_1 = 0.1238, wR_2 = 0.3054
Final R indexes [all data]	R1 = 0.0690, wR2 = 0.1893	R_1 = 0.1896, wR_2 = 0.3365	R_1 = 0.1173, wR_2 = 0.2841	R_1 = 0.1664, wR_2 = 0.3325
Largest diff. peak/hole / e Å^{-3}	0.65/-0.60	0.77/-0.57	0.64/-0.39	1.27/-0.79

Table S5. Crystal data and structure refinement for **mtl-2D-P6MOCN**, I_2⊂**mtl-2D-P6MOCN**, ***R*-bl-2D-P6MOCN** and ***S*-bl-2D-P6MOCN**.

Name	**mtl-2D-P6MOCN**	I_2⊂**mtl-2D-P6MOCN**	***R*-bl-2D-P6MOCN**	***S*-bl-2D-P6MOCN**
Identification code	2326175	2326165	2326166	2326167
Empirical formula	$C_{110}H_{120.5}Cu_2N_4O_{22.25}$	$C_{114}H_{136}Cu_2I_4N8O_{18}$	$C_{112}H_{114}Cu_2N_6O_{18}$	$C_{112}H_{122}Cu_2N_6O_{22}$
Formula weight	1981.68	2540.98	1959.17	2031.23
Temperature/K	193.00	193.00	193.00	193.00
Crystal system	orthorhombic	orthorhombic	orthorhombic	orthorhombic
Space group	Pnnn	Pnnn	$P2_12_12$	$P2_12_12$
a/Å	13.8537(8)	13.7025(3)	19.721(5)	19.800(3)
b/Å	22.6927(15)	22.6702(5)	21.191(5)	21.138(4)
c/Å	41.561(3)	41.6085(10)	13.551(3)	13.471(3)
α/°	90	90	90	90
β/°	90	90	90	90
γ/°	90	90	90	90
Volume/Å^3	13066.0(14)	12925.2(5)	5663(2)	5638.1(17)
Z	4	4	2	2
ρ_{calc}g/cm^3	1.007	1.136	1.149	1.196
μ/mm^{-1}	2.058	8.385	0.439	0.445
F(000)	4178	5160.0	2060.0	2140.0
Crystal size/mm^3	0.13 × 0.12 × 0.1	0.12 × 0.1 × 0.09	0.14 × 0.11 × 0.09	0.13 × 0.1 × 0.09
Radiation	GaKα (λ = 1.34139)	CuKα (λ = 1.54178)	MoKα (λ = 0.71073)	MoKα (λ = 0.71073)
2Θ range for data collection/°	5.85 to 107.796	4.438 to 137.088	3.844 to 50.696	4.368 to 50.698
Index ranges	-16 ≤ h ≤ 15, -26 ≤ k ≤ 27, -50 ≤ l ≤ 46	-16 ≤ h ≤ 13, -27 ≤ k ≤ 26, -50 ≤ l ≤ 46	-23 ≤ h ≤ 23, -25 ≤ k ≤ 25, -16 ≤ l ≤ 16	-21 ≤ h ≤ 23, -25 ≤ k ≤ 25, -16 ≤ l ≤ 16
Reflections collected	96701	88773	65274	69588
Independent reflections	11951 [R_{int} = 0.0836, R_{sigma} = 0.0677]	11909 [R_{int} = 0.1172, R_{sigma} = 0.0900]	10366 [R_{int} = 0.1624, R_{sigma} = 0.1199]	10335 [R_{int} = 0.1009, R_{sigma} = 0.0737]
Data/restraints/parameters	11951/223/728	11909/274/690	10366/160/625	10335/547/636
Goodness-of-fit on F^2	0.974	1.137	0.965	1.002
Final R indexes [I>=2σ (I)]	R_1 = 0.1380, wR_2 = 0.3019	R_1 = 0.1319, wR_2 = 0.3146	R_1 = 0.0886, wR_2 = 0.2338	R_1 = 0.0874, wR_2 = 0.2426
Final R indexes [all data]	R_1 = 0.2090, wR_2 = 0.3428	R_1 = 0.1716, wR_2 = 0.3384	R_1 = 0.1475, wR_2 = 0.2811	R_1 = 0.1204, wR_2 = 0.2803
Largest diff. peak/hole / e Å^{-3}	1.48/-1.22	1.29/-0.72	0.36/-0.42	0.48/-0.39

^{1}H NMR and ^{13}C NMR spectrum

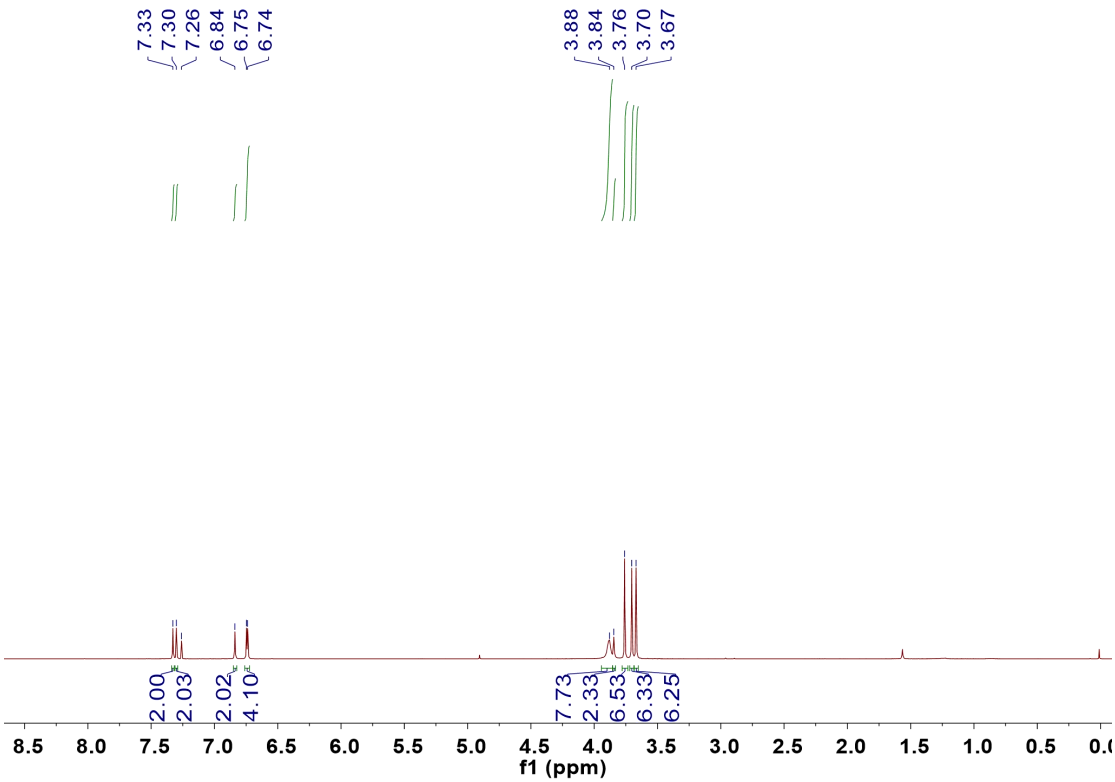

Figure S71. ^{1}H NMR spectrum (400 MHz) of compound **3** in $CDCl_3$.

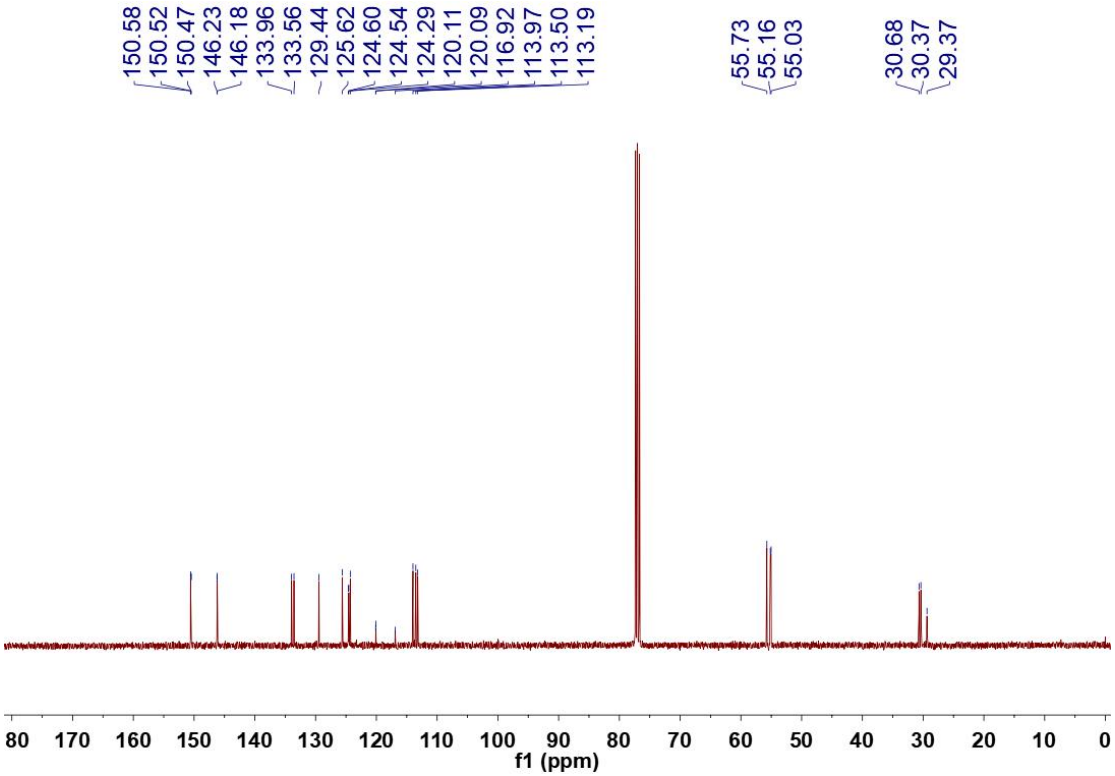

Figure S72. ^{13}C NMR spectrum (100 MHz) of compound **3** in $CDCl_3$.

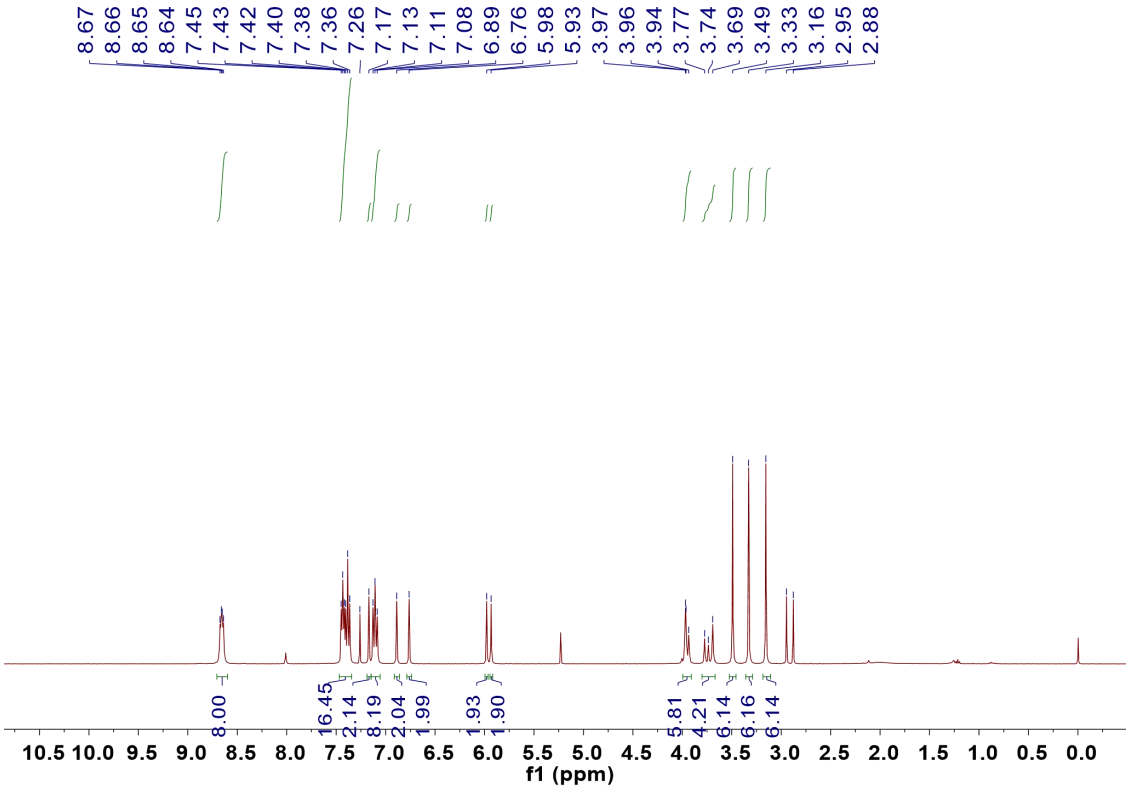

Figure S73. ^{1}H NMR spectrum (400 MHz) of compound **P5PhPy4** in $CDCl_3$.

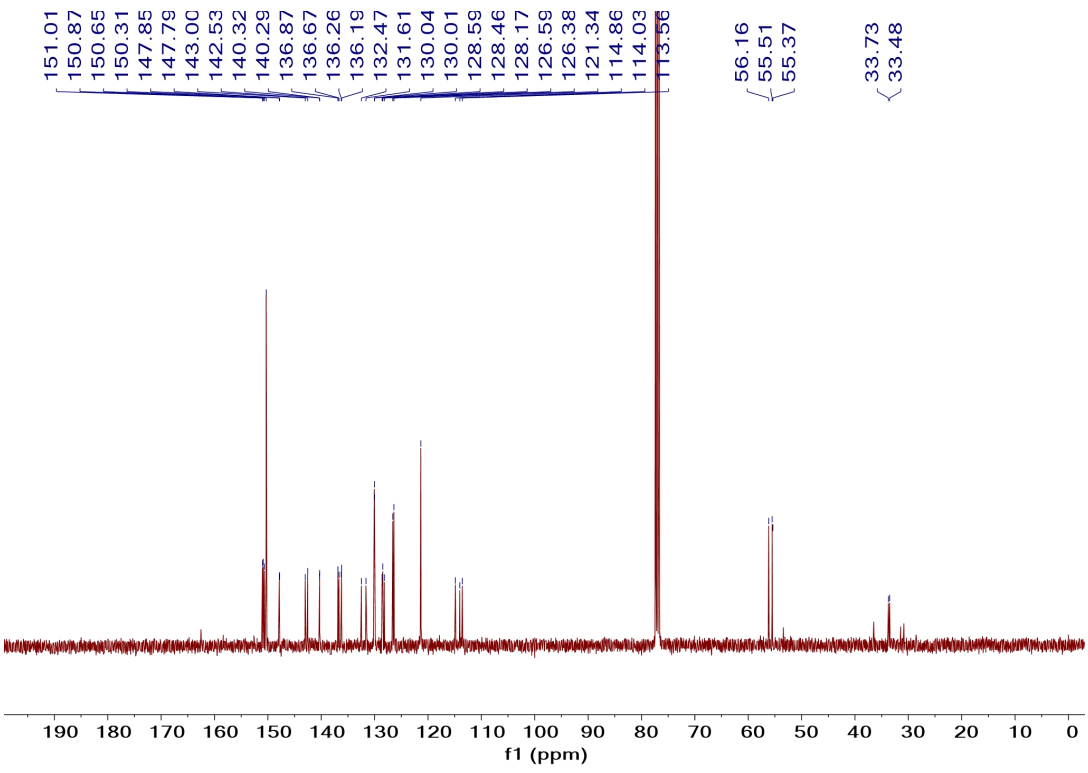

Figure S74. ^{13}C NMR spectrum (100 MHz) of compound **P5PhPy4** in $CDCl_3$.

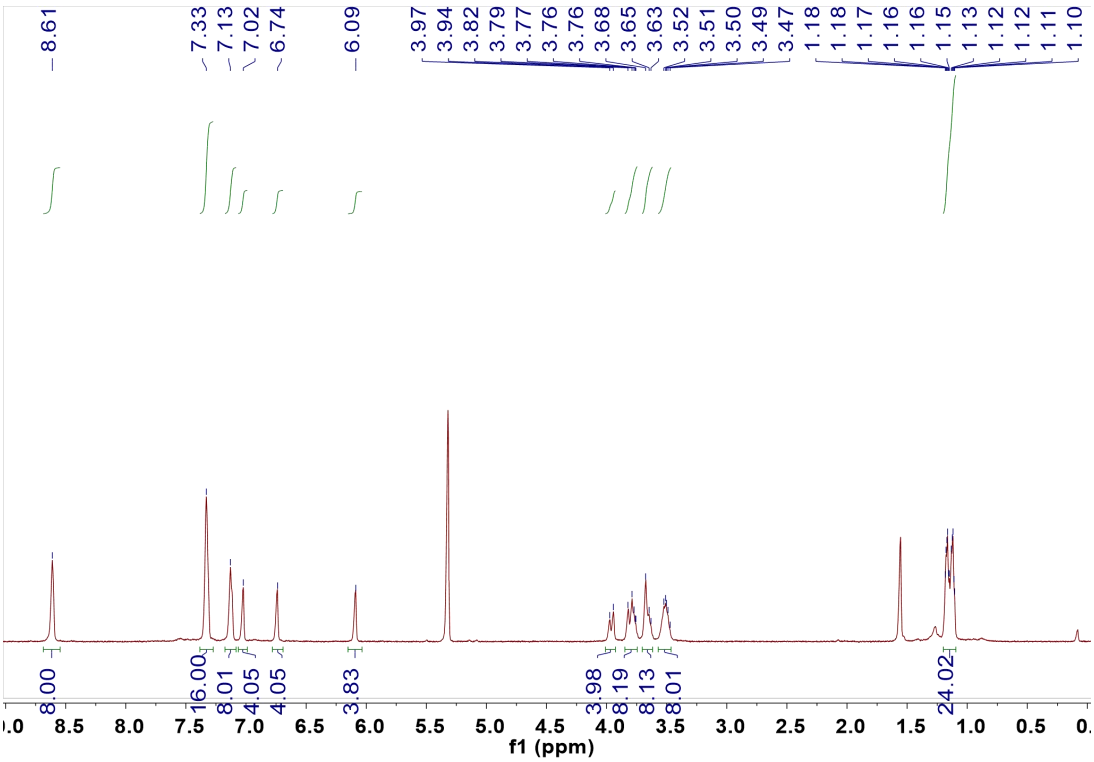

Figure S75. ^{1}H NMR spectrum (500 MHz) of compound **P6PhPy4** in CD_2Cl_2.

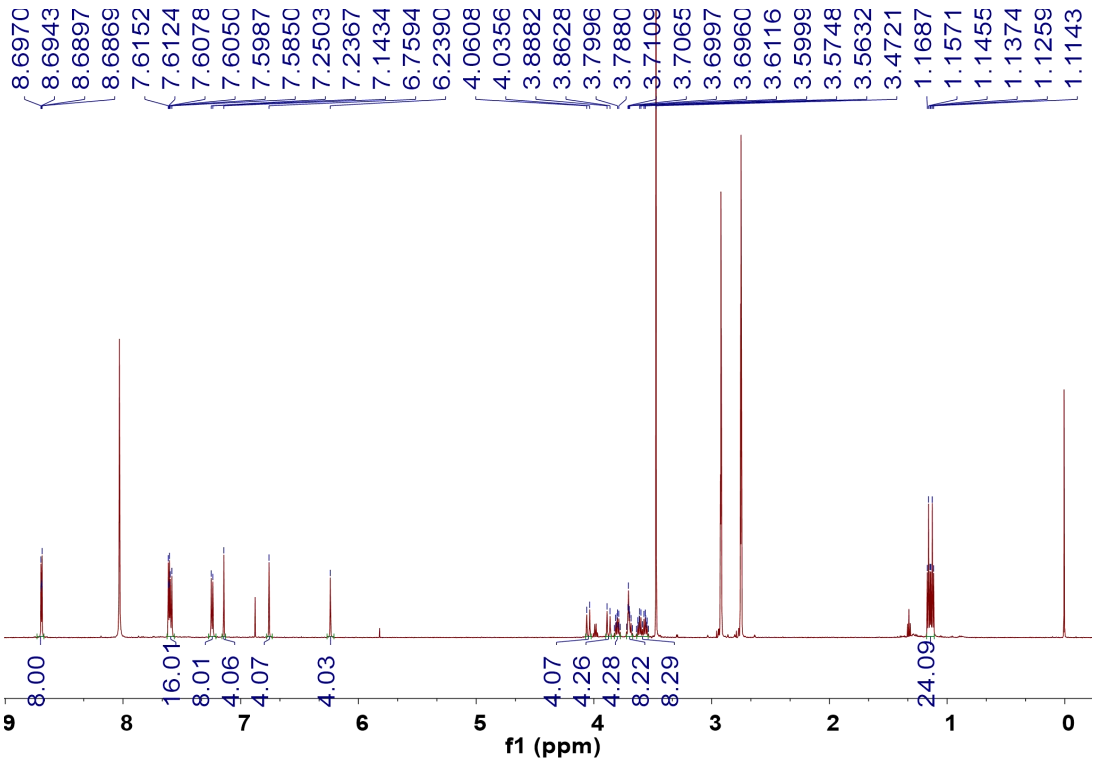

Figure S76. ^{1}H NMR spectrum (600 MHz) of compound **P6PhPy4** in DMF-D7.

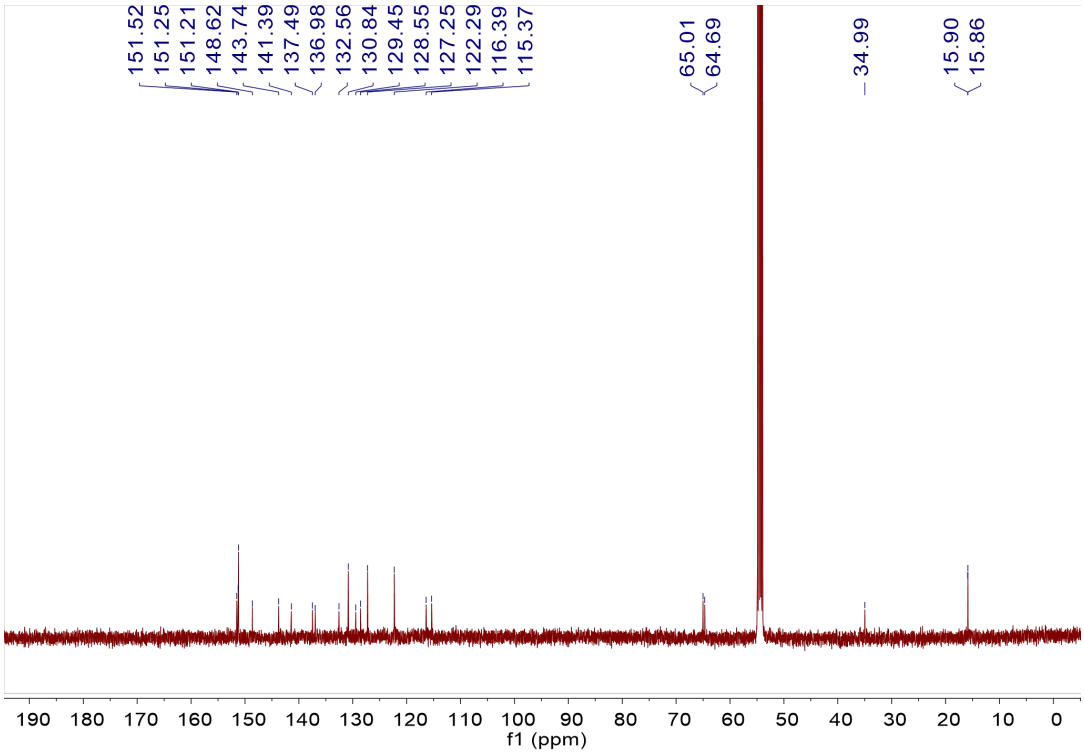

Figure S77. ^{13}C NMR spectrum (126 MHz) of compound **P6PhPy4** in CD_2Cl_2.

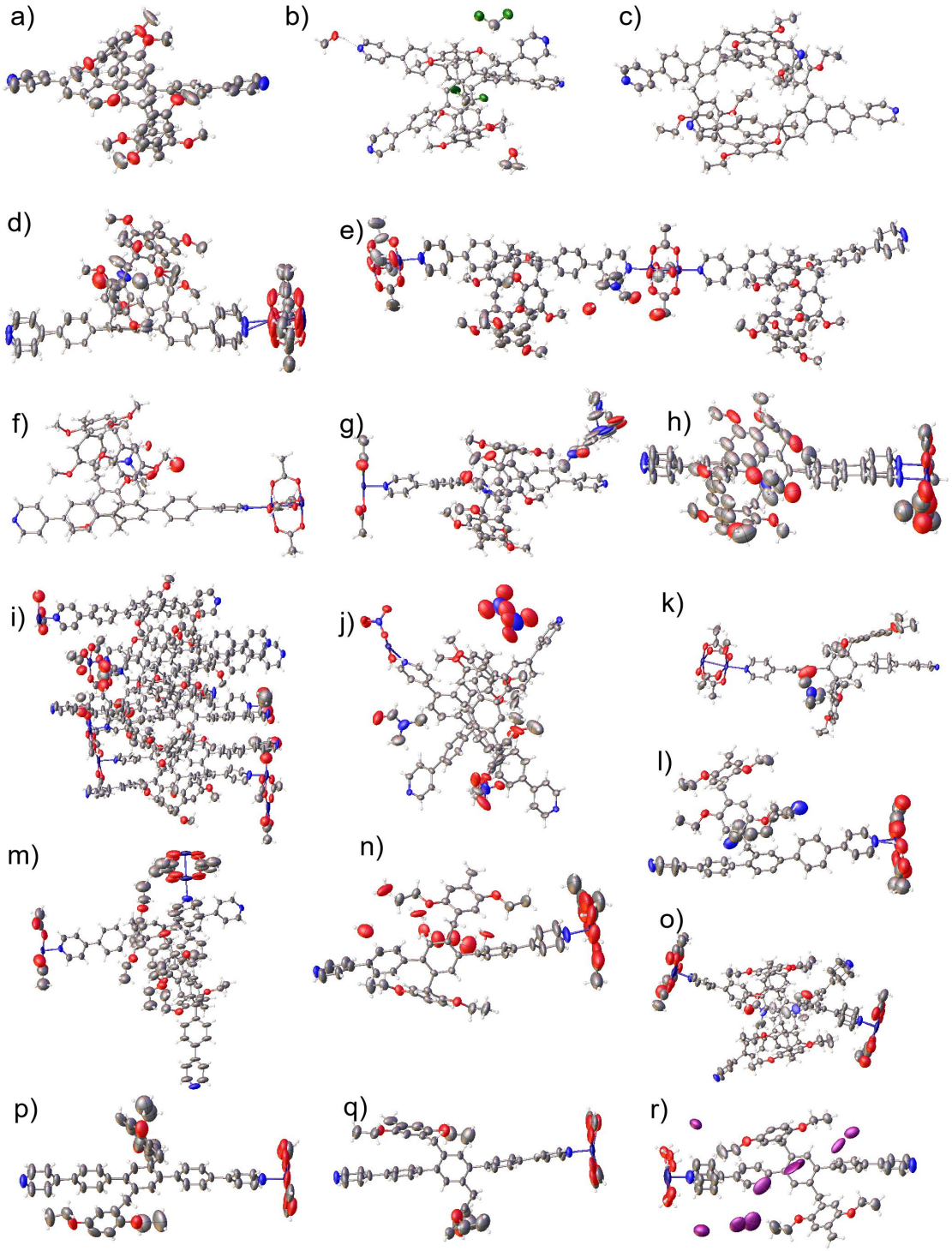

Figure S78. ADPs of **P5PhPy2**(a), **P5PhPy4**(b), **P6PhPy4**(c), **P5PhPy2Cu-1**(d), **P5PhPy2Cu-2**(e), **P5PhPy2Cu-3**(f), **P5PhPy2Cu-4**(g), **P5PhPy2Co-1**(h), **ml-2D-P5MOCN**(i), **bl-2D-P5MOCN**(j), **bl-2D-P6MOCN**(k), **sbl-2D-P6MOCN**(1)(l), **fl-2D-P6MOCN**(m), **mtl-2D-P6MOCN**(n), **sbl-2D-P6MOCN**(2)(o), **R-bl-2D-P6MOCN**(p), **S-bl-2D-P6MOCN**(q) **and I2@mtl-2D-P6MOCN(r)**.

Reference

1. T. Ogoshi, T. Aoki, K. Kitajima, S. Fujinami, T. A. Yamagishi, Nakamoto, Y. *J. Org. Chem.* 2011, **76**, 328-331.

2. M. Pan, M. Xue, *Eur. J. Org. Chem.* 2013, 4787-4793.

3. X. Y. Lou, N. Song, Y. W. Yang, *Natl. Sci. Rev.* 2021, **8**, nwaa281.

4. H. Zhu, Q. Li, B. Shi, H. Xing, Y. Sun, S. Lu, L. Shangguan, X. Li, F. Huang, P. J. Stang, *J. Am. Chem. Soc.* 2020, **142**, 17340-17345.

5. H. Zeng, P. Liu, H. Xing, F. Huang, *Angew. Chem. Int. Ed.* 2022, **61**, e202115823.